Syntheses and uses of modified polyelectrolytes for therapeutic hydrogels and films with controlled and selective protein adsorption

Johanna Davila Ramos

UNIVERSITÉ DE STRASBOURG

ÉCOLE DOCTORALE DES SCIENCES CHIMIQUES

[Institut Charles Sadron]

THÈSE

présentée par

Johanna Davila

soutenue le **13 Avril 2012**

pour obtenir le grade de

Docteur de l'Université de Strasbourg

Discipline/ Spécialité : Chimie-Physique

Syntheses and uses of modified polyelectrolytes for therapeutic hydrogels and films with controlled and selective protein adsorption

THÈSE dirigée par :

M. MESINI Philippe Directeur de recherche, Université de Strasbourg

---

MEMBRES DU JURY :

M. HOLL Yves	Professeur, Université de Strasbourg et Président de jury
M. DURAND Alain	Professeur, Université de Lorraine, Nancy-LCPM
M. ROUCOULES Vincent	Maître de Conférences, Université de Haute Alsace, Mulhouse-IS2M

Acknowledgements

After all this year's this thesis would not have been possible without the support of many people:

I would like to express my gratitude towards Philippe Mesini for giving me the opportunity to be a member in his research group, also for suggesting this interesting and challenging topic. Thanks to his valuable advices, encouragement and interest I was able to successfully complete my work.

I would like to extend my gratitude to Loïc Jierry for his scientific and personal advices, guidance, interesting and productive discussions during our meetings that helped me improve this work.

I would also like to thank to Alain Durand and Vicent Roucoules for having accepted to be part of the board of examiners and for providing interesting suggestions in my work. I am also grateful to Yves Holl for his participation as president of the advisory committee.

I would like to convoy my sincere thanks to Joseph Selb for the great help in rheological measurements analysis and the fruitful discussions for the interpretation of the results. Also thanks to Fouzia Boulmedais for working together and for all the help in the QCM measurements.

Many thanks to Francoise Hoegy and Armelle Chassepot who contributed to this work by completing the biological measurements. Thanks to Johan Longo, Camille Heid, Adrien Alibert and especially to Eric Gonthier for performing numerous experiments.

To my friends whom I had the fortune to meet, thanks for the discussions and the fun during lunch, coffee breaks and outside the lab. Without them it would have never been the same. I would like to especially thank to Andru the best labmate for always listening to me, Diana and Rebecca for their support and confidence and for teaching me a lot of things during all this time, Cesar for always making me laugh. I would like also to extend my warm gratitude to Patty who started this adventure with me a long time ago, thanks for all your moral support and for listening to me without complain, the next one will be you. "Vamos ya falta poco"

I would like to thank to my colleagues who accompanied me during all this time. Thanks to Rahul, Martin, Akkiz, Anna, Mirela, Tam, Christophe, Franck and to some of them that even far away supported me in someway Almeira, Maria, Gaby, Francine, Dominique, Edgar, Ivan for their huge support during the tough periods of my stay.

My deep thanks to my family. Without their constant support and advice I would not have been who I am today. Thanks for rekindling my dreams. Los amo.

With all my heart to my husband David who helped, supported, and always has faith in my abilities. Many thanks for all your love, patience and being beside me during my PhD work.

Table of Contents

Abbreviations

FTIR	Fourier transforms infrared spectroscopy
GR	grafting ratio
NMR	nuclear magnetic resonance spectroscopy
PC	phosphorylcholine or phosphorylcholine group
QCM	quartz crystal microbalance
SEC	size exclusion chromatography
AIBN	azobisisobutyronitrile
Boc_2O	di-*tert*-butyl dicarbonate
CH_2Cl_2	dichloromethane
DMF	*N*, *N*-dimethylformamide
EtOAc	ethyl acetate
EDCI	N-Ethyl-N'-(3-dimethylaminopropyl)carbodiimide hydrochloride
Et_3N	triethylamine
HCl	hydrochloric acid
HOBt	1-hydroxybenzotriazole hydrate
Hz	hertz
$MgSO_4$	magnesium sulfate
NHS	*N*-hydroxysuccinimide
NaN_3	sodium azide
Ph_3P	triphenylphosphine
PAA	poly(acrylic acid)
PAH	poly(allyl amine hydrochloride)
PEI	poly(ethyleneimine)
PSS	poly(sodium-4-styrenesulfonate)
Tris	tris(hydroxymethyl)aminomethane (buffer)
TsCl	tosyl chloride
THF	tetrahydrofuran
TBAI	tetra-butylammonium iodide

TLC	thin layer chromathography
TBM	*tert*-butyl methacrylate

Introduction

During the past decades the development of new materials for biomedical applications has involved more and more polymers.[1] This has been exemplified by the design of therapeutic macromolecules to increase the efficiency and the control in drug delivery. For instance, the efficiency of anticancer agents has been improved by using polymer-drug conjugates able to deliver them selectively in the targeted tissues.[2-7] Polymeric systems have also allowed considerable progress in implants such as prostheses or temporary implants, especially those used for regenerative medicine and tissue engineering and involved polymeric systems have experienced a throbbing interest.[8-10]

Many of these materials can accomplish very precise and complex functions, thanks to a careful design and refined modification and functionalization. The functionality of these materials can be programmed, by changing their intrinsic properties and architecture, but cannot be modulated according external conditions. For instance a polymeric drug system can be designed to deliver insulin in a given duration, but it is more difficult to make the system deliver only in case of hyperglycemia. That's why further work tends to obtain materials responsive to an external stimulus, for instance evolved polymers able to release drugs only on demands in a given stimulus. These stimuli can be simple physicochemical parameters such as temperature or pH. They can correspond to a biological situation: increase of temperature in case of fever, pH variation corresponding to the variation of pH along the digestive tract (acid in stomach, basic in duodenum) or to the acidic medium of lysosomes to release the drug only in the cell. More recent efforts try to elaborate materials able to respond to more sophisticated stimuli. For example recently magnetic field sensitive carriers have been developed to deliver drugs on demand or on a given spot of the organism.[11, 12]

The doctorate research presented here contributes to the elaboration of stimuli responsive materials based on modified polyelectrolytes.

In the first chapter we provide background information about the major elements required for the modification of surfaces with polyelectrolyte multilayer films.

In the second chapter, we have developed polyelectrolyte multilayers to design surfaces able to bind a given protein very selectively and repelling all other. This property is sought to form biosensors. One has also taken advantage to design surfaces that respond to mechanical

stretch. The expected response is to trigger cell adhesion under stretch, while under rest the same surface is anti-adhesive. The results of these studies are presented and discussed in chapter 3.

Subsequently we have presented a detailed study of the structure of associating polymers and the changes of their properties under the influence of different parameters. We have mentioned the applications as drug delivery systems that result from their properties.

The chapter 5 describes our efforts to obtain a polymeric gel with a rheological response when exposed to pathogen bacteria. The stimulus is constituted by microbial exoproteins that signal the presence of bacteria. The sought response is the viscosity decrease and resolubilization of the gel. Such polymer could be used as a drug carrier able to store high antibiotic doses and release them only in the case of infections.

CHAPTER 1:

Modification of polyelectrolytes to the buildup of films for biosensor and mechanoresponsive surfaces

First this study is related to the modification of polyelectrolyte to be used in the buildup of films. During my work we prepared poly(acrylic acid) PAA with two bioactive molecules, RGD and biotin. This functionalizations endows the films, incorporating the modified polymer with new properties necessary to form:

- Biosensor surfaces
- Mechanoresponsives multilayer films

This bibliographical part will first describe the key elements for the buildup of polyelectrolyte multilayer films (PEM) will be briefly described in this chapter. Then the applications of PEM will be gathered dedicated to biosensing surfaces and mechanoresponsive materials.

1.1 Introduction of polyelectrolyte multilayer films (PEM)

The multilayer systems were introduced in the 1930s by Irving Langmuir and Katherine Blodgett describing nanostructured films called "Langmuir-Blodgett" (LB) films.[13, 14] This technique consists in the construction of a monolayer of amphiphilic molecules at the air-water interface. This film is then transferred onto a solid support. The process can be repeated several times to obtain multilayer films. Yet the LB technique presents several limitations and inconveniencies, the films are not stable, they cannot be formed on substrates and have limited sizes. In the 1980s new systems were developed as an alternative to LB films, by self-assembled monolayers (SAMs) on silane-SiO_2 or by covalent[15] and coordinate[16] chemistry. However, these systems cannot produce high-quality multilayer films.

The development of nanostructured films based on electrostatic interactions was carried out by Iller.[17] The construction of multilayer films required colloida anionic and cationic particles, but this method was never proved. This technique relies on the electrostatic attraction between oppositely charged molecules seemed to be a good candidate with good driving forces for multilayer build-up. At the end of the 1980s this concept was applied in some studies on adsorption of proteins[18] and metallic's colloids.[19]

It was in the 1990s that Decher[20] demonstrated the possibility to build up films by the alternating physisorption of oppositely charged polyelectrolytes, so called layer-by-layer method

(LbL). This kind of construction allows the deposition of many organic and inorganic substances and organic as DNA[21], on any substrate from gold to silicon, through a simple stepwise process. Later the LbL was extended to other interactions than simple electrostatic, and some films have been successfully made via hydrophobic,[22] hydrogen bonds[23] or covalent bonds.[24]

Here we review only the PEM built from electrostatic interactions. We focus on the understanding of the properties of PEMs necessary to guide the functionalization of the polyelectrolytes with bioactive molecules.

1.1.1 Principle of the preparation of polyelectrolyte multilayer films

The technique is based on the electrostatic interactions between cationic and anionic species and the entropic release of coutenrions. The substrate is brought into contact with dipped in a solution of polyion, followed by a rinsing step to eliminate the excess or the weakly adhering polyelectrolyte chains.[20, 25, 26] Then the substrate is brought in contact with a solution of oppositely charged polyelectrolytes and rinsed again. A representation of the buildup of a multilayer film is displayed in Figure 1. 1. These steps are then repeated until the desired film thickness is obtained.

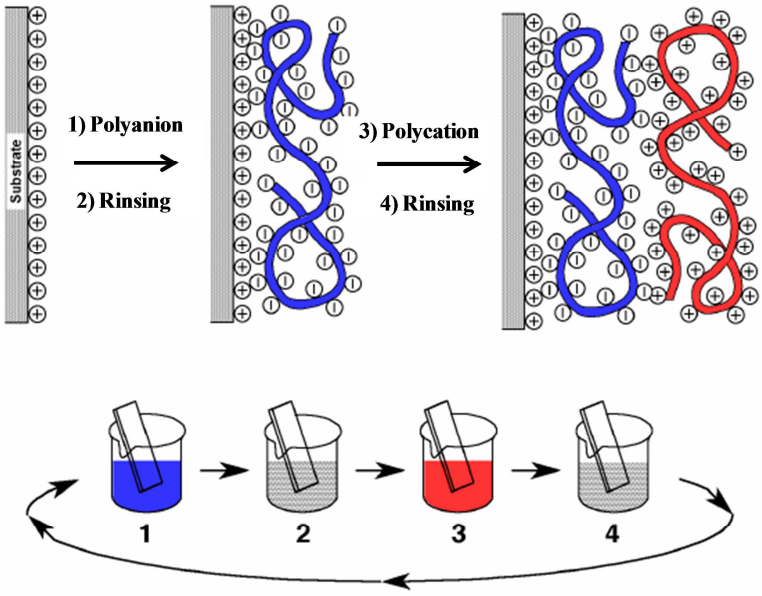

Figure 1. 1. Principle of the construction of polyelectrolyte multilayer films by dipping. Steps 1 and 3 represent the adsorption of polyanion and polycation, respectively. Followed by rising steps 2 and 4.[20]

The PEM can be obtained by different deposition techniques:

The dipping method is represented in Figure 1. 1. This is historically the first method and it is still the most widely used. The deposition requires between 5 and 20 minutes for each polycation/polyanion deposition cycle including the rinsing step. [20, 27] This technique can be coupled to measurements by quartz crystal microbalance (QCM) and optical waveguide lightmode spectroscopy (OWLS), by replacing the dipping steps by letting the different solutions flow through to measurement cells.

The spraying method consists in spraying the solutions horizontally on the surface held vertically. This technique considerably speeds up the process.[28] Porcel et *al*.[29] demonstrated that it is possible to produce films by simultaneously spraying both polyelectrolytes which reduces even more the time of film construction. The layer thicknesses obtained by spray Layer by Layer (LbL) are usually less than those obtained by dipping.[30, 31](Figure 1. 12(a))

Spin coating can also be used to build up PEM**.**[32, 33] It can produce more homogenous films, Figure 1. 12(b).

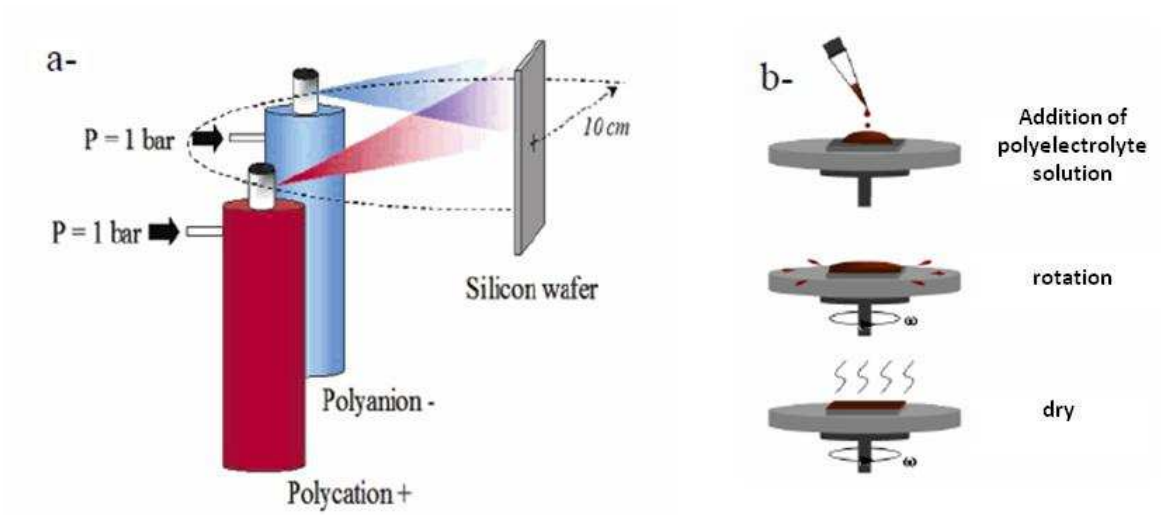

Figure 1. 2. Schematics representation of LbL deposition techniques on substrates. a) spray LbL. b) spin coating. The process is repeating several times until desired layer number is obtained.

When constructing PEM's by the LbL method both the mass and thickness of the film increase with the number of deposition steps. There are two types of film growth, linear and exponential, which will be reviewed in the following section.

1.1.2 Mode of growth on polyelectrolyte multilayer films

The two types of growth regimes are represented in Figure 1.3, where the variation of thickness with the number of the deposited layers is shown.

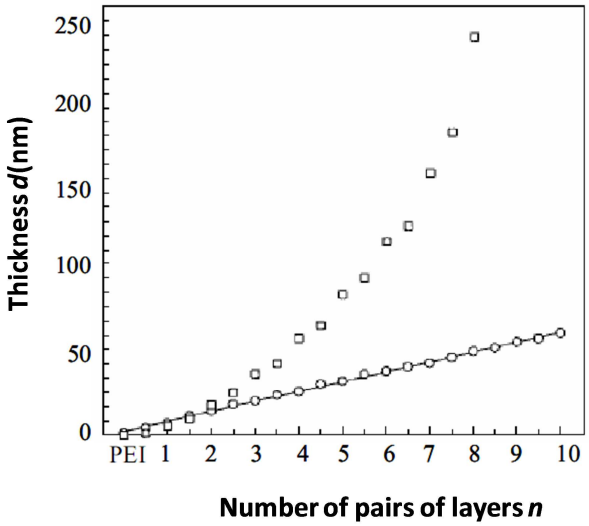

Figure 1. 3. Evolution of the polyelectrolyte thickness. Linear versus exponential growth. (□) PEI(PGA/PLL)$_n$ and (○) PEI(PSS/PAH)$_n$ as a function of the numbers of added layer pairs.[34]

In the linear growth regime, the thickness increment of the multilayers is constant with the number of alternative steps of deposition of polycation and polyanion. In this case, polyelectrolytes from the solution interact exclusively with the outer layer of the film without diffusing into the architecture. This is observed for the poly(styrene sulfonate (PSS)) and poly(allylamine hydrochloride (PAH)) (PSS/PAH)[34], for (PAH/PAA)[35] or poly(diallyldimethylammonium (PDADMA)) (PDADMA/PSS)[36] films.

If the film thickness and the amount of adsorbed polyelectrolytes increase with the number of deposition steps, the film shows an exponential growth. This behavior is displayed for example by (PGA/PLL)[34] and (PLL/HA).[34, 37] In those PEM's, part of the polyelectrolyte can diffuse freely throughout the thickness of the film. So the proposed model for the exponential growth is as follows: an amount of polyelectrolyte is adsorbed on the top of the film. This amount is limited by the charge compensation of the previous layer. But an additional amount migrates inside the film and freely diffuse throughout the thickness of the film. In the next step, when the oppositely charged polymer is brought into contact of the film, the free previous polyelectrolyte migrates back to the top and increases the amount of polymers that can be

compensated. This leads to a thickness increment proportional to the thickness of the multilayer and hence to an exponential growth.

1.1.3 Nature of the substrate

There are many substrates for the construction of polyelectrolyte multilayers. The surfaces can be flat or spherical. In this thesis we have worked with flat surfaces. Some types of surfaces are mineral (glass slide[20], quartz[38]), metal (sintered titanium[39]), silicon[40] and organic (polyethylene[41]).

In this work polydimethylsiloxane (PDMS) has been used as substrate in order to stretch the. This polymer is of particular interest because of its elastic properties, low toxicity, chemical inertness and biocompatibility. This property have been exploited in the domain of medical implants., especially in vascular grafts and breast implants.[42] Moreover it has been used to control and enhance cell adhesion.[43, 44]

It is not easy to build PEMs on PDMS: the surface is not charged. So the adsorption of the first layer of polyelectrolyte is quite delicate and relies exclusively on Van der Waals interactions. The adhesion to the silicon depends on the choice of polyelectrolytes. The films based on (PSS/PAH) are easily deposited on silicon surfaces[45], while (PAA/PAH) films shows a high surface roughness.[46]

1.2 Multilayer films responsive to mechanical stimuli

During the last years much research has been dedicated to materials with responsive surfaces. The design of materials that are sensitive to external stimuli such as pH[47], temperature[48], and light[49] has been widely investigated. However, less attention has been given to films that respond to mechanical stimuli.[50]

Genzer and coworkers[51] have stretched silicone sheets, modified them by attaching perfluoroalkane chains and relaxed them after modification. In this way, they were able to develop “mechanically assembled monolayers” which significantly decrease water contact angle upon relaxation. The final hydrophobicity strongly depends on the degree of stretching before chemical treatment.

One of the first examples of adaptative multilayer films has been reported by the group of P. Schaaf.[52] Nafion (Naf), a hydrophobic polyelectrolyte, was used to build the following film on PDMS substrates: $(PAH/Naf)_4$-$(PAH/PAA)_2$. At rest the film has a water contact angle of 45°. When the film is stretched to 220 % the contact angle increases to 100°. This property is attributed to the exposition of hydrophobic Naf layers at the surface when the film is stretched. (Figure 1.4)

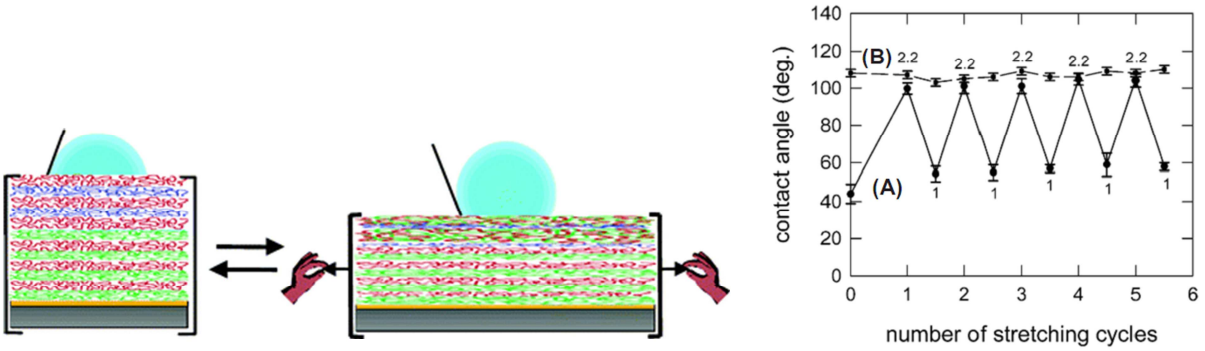

Figure 1. 4. *left*: schematic representation of the film that exhibits a reversible hydrophobic/hydrophilic transition upon stretching; *right*: evolution of the contact angle of $PEI(Naf/PAH)_4Naf(PAH/PAA)_2$ multilayer. The angle variations are observed for films ending with a hydrophilic layer (PAH/PAA) (A) deposited on top of a hydrophobic one whereas no changes in the contact angle are observed when the hydrophobic film (PAH/Naf) (B) is deposited on top of hydrophilic one.[52]

This system proved to be reversible and reproducible over successive stretching and relaxation cycles. The authors have hence achieved a system that responds to a mechanical stimulus by reversibly switching from hydrophilic to hydrophobic.

Another mechanosensitive system was recently reported by Möhwald and coworkers.[53] It is based on polyelectrolyte multilayer films from polystyrene sulfonate modified with pyrene (PSS-PY) and poly(diallyldimethylammonium)chloride (PDADMA) on PDMS. When the film is stretched, pyrene fluorescence at 457 nm decreases. This fluorescence corresponds to the emission of the excimer. When the film is stretched, the ratio of associated pyrenes diminishes because the polymer chain are forced into an uncoiled state. (Figure 1.5)

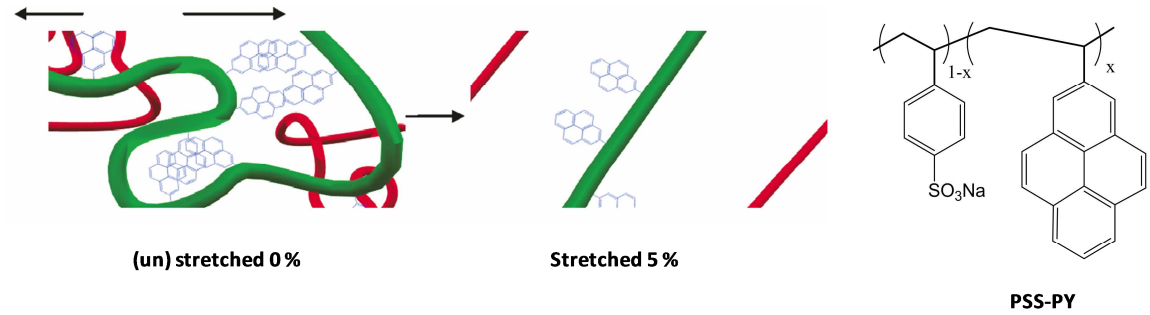

Figure 1. 5. Schematic representation of the effect at unstretched and when stretched. (PSS-PY) with x = 1 and 3%.(Green) PSS-PY polyelectrolyte (Red) PDADMA molecules.

The transformation of mechanical stimulus such as stretching into a chemical or biological reaction is a process that is widely used by nature and that is called transduction.[54] When subjected to mechanical forces, some proteins change their conformation. This change allows the exhibition of hidden active sites, called cryptic sites, that become accessible. For instance fibronectin is able to expose such cryptic sites under stretching.[54-56] Our work has sought to develop films mimicking this property, for instance films containing active compounds which are inaccessible in the non constrained state and become accessible in a reversible way when the surface is stretched.

More recently Mertz[56] et al. describes films with biocatalytic activity induced by stretching. The multilayer architectures were built up on a silicon sheet, Figure 1.6. The films consist in a first exponentially growing multilayer $(PLL/HA)_{15}/PLL/ALP/(PLL/HA)_{15}$ and covered by $(PDADMA/PSS)_6$ that acts as a barrier. ALP (alkaline phosphatase) was embedded in the films. This enzyme hydrolyzes FDP (fluorescein diphosphate). This interaction (ALP-FDP) was displayed when the films is stretched leading to green fluorescence emission. This fluorescence suggests that the cryptic sites have become accessible upon stretching. At rest, only a weak fluorescence was observed.

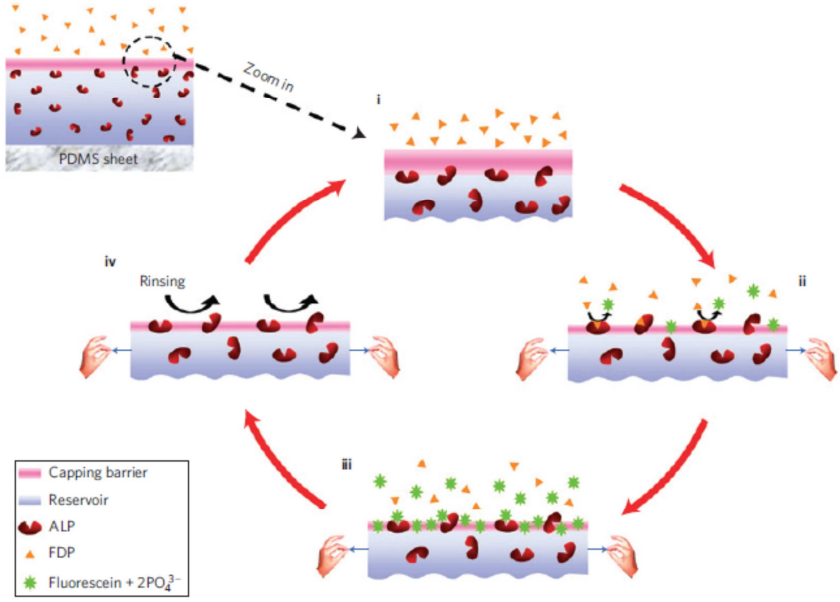

Figure 1. 6. Scheme of the mechanically sensitive biocatalytic coating. (i) At rest the catalysis is off. (ii) under stretching the enzymes are exposed, the biocatalysis is active leading to formation of fluorescein. (iii) Inhibition of enzymes due to strong increase of the concentration of fluorescein and phosphate ions. (iv) Rinsing step to reactivate the enzymes. When the system is brought back to its initial state (i) the enzymes are again masked and the catalysis is desactivated.[56]

These types of architectures demonstrate the utility of PEM to mimic biological systems. Until now, very few studies have been carried out with the functionalization of polyelectrolytes with different molecules for specific biological applications.

1.3 Control of protein adsorption and cell-adhesion on surfaces

1.3.1 Strategy

PEM can coat “virtually” any surface. An interesting perspective is to use them to coat medical implants. One of prime importance for all applications of implants is to control their interactions with the biological environment. For those applications one seeks two main properties.

- It must be protein repellant: this property is necessary to render the implant blood compatible for instance in catheters or heart valves to avoid thrombosis or bacterial infections.
- It must be adherent for the cells: this property is necessary in tissue repair or in bypass systems.

Some applications require both properties (anti-fouling properties and cell adhesion) simultaneously. The PEMs are very prone to adsorb proteins. The proteins can be adsorbed on any polyelectrolytes by electrostatic interactions, depending on the charge of the protein. However even in the case of unfavourable charges, the protein can absorb. Ladam et al.[57] describe the adsorption of negative serum albumin (HSA) that is negative onto positively or negatively charged polyelectrolyte film. On the positive film HAS adsorbs and the thickness of the adsorbed protein layer exceeding several times the typical protein size. On the negative films, HSA still adsorbs and in this case only one monolayer is adsorbed. This behavior is due to hydrogen-bonding and hydrophobic interactions.[58]

Besides physicochemical adsorption, some proteins can be bound to PEM´s by ligand-protein interaction. This can be done by incorporating ligands in the film, which they are accessible to one protein exclusively, as biotin-streptavidin.[59,60] Our strategy is the design of surfaces that can be specific for protein adsorption and adherent to cells.

The next section presents some of antifouling films.

1.3.2 Anti-fouling surfaces

In this chapter we present two antifouling polymeric coatings: the first is based on PEO, the second one on phosphorylcholine (PC) groups.

Surfaces coated or grafted with PEO were introduced in the 80s. For high molecular weights and high grafting densities, PEO forms a brush conformation that sterically impedes protein adsorption.[61] The reduction of protein adsorption is related to the grafting density of PEO, to their surface density and to their length.

In order to coat surfaces with PEO, block copolymers with a hydrophobic block are used to absorb the substrate on hydrophobic surfaces. Adhesion to hydrophobic substrates can also be obtained using methacrylate backbones with alkyl side chains.[62] Polyelectrolytes can be easily modified to form antifouling PEMs: brush copolymers of PLL modified with 5 mol % of PEO (PLL-*g*-PEO) on metal oxide surfaces effectively reduce the adsorption of blood serum and human fibrinogen.[63, 64] Boulmedais et al.[65] have studied multilayers based on (PLL/PGA) and

observed a strong reduction of protein adsorption with a hydrophilic multilayer of (PLL/PGA-*g*-PEO).

The other group of antifouling species, less studied than PEO, are compounds containing phosphorylcholine (PC). Many phospholipids compose the cell membranes and can have either uncharged, positive or negative head groups. But it has been noticed that in blood cells, PC is the major membrane constituent of the external membranes. PC groups lead to blood compatibility because they reduce the adsorption of proteins. [66, 6, 67] Later it has been found that many other zwitterionic groups induce protein resistance, e.g. sulfobetains having equal amounts of $N(CH_3)_3^+$ and SO_3^- groups.

In our group, Reisch et al.[68, 69] have modified many polyelectrolytes with side chains ended by PC (Scheme 1.1). Their inclusion in PEMs strongly reduces protein adsorption even under stretching.

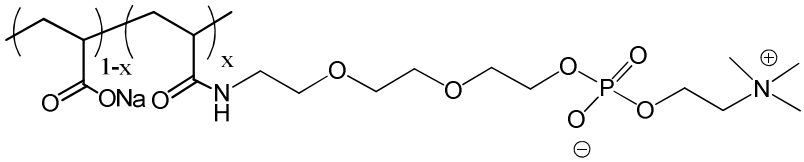

Scheme 1. 1. Chemical structure of $PAA(EO)_3PC$.

Films of $PEI(PSS/PAH)_5/PAA(EO)_3$-PC where $PAA(EO)_3$-PC is the modified PAA depicted Scheme 1.1 proved to be fully protein repellent for rates of modification of 25 %.[69] The same film was built on PDMS and its antifouling capacity was measured under rest and after stretching. The systems was stretched to 100 and 150% after exposure to fluorescein labeled albumin (Alb^{FITC}) and the amount of adsorbed protein was measured by fluorescence microscopy. The results are illustrated Figure 1. 7. The fluorescence slightly increases when it is stretched. One has to deposit two $PAA(EO)_3PC$ top-layers to eliminate all adsorption under stretching. The antifouling properties were also tested with $PAA\text{-}(EO)_3$ with a modification degree of 24%, and proven to be as efficient as with PC.[68]

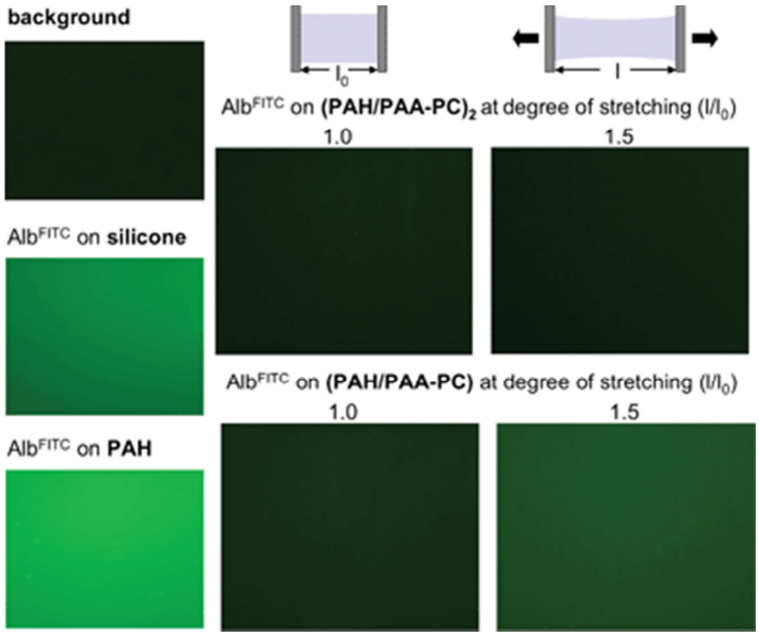

Figure 1. 7. Fluorescence micrograms of protein adsorption of PEI/PAH/PSS/PAH, PEI(PSS/PAH)$_5$ (PAA-(EO)$_3$PC)$_n$ n = 1 or 2 Treated onto silicon surface after adsorption of Alb^{FITC} and rinsing.

These types of systems are one of the main trends in biomedical applications involving modification of polyelectrolytes with bioactive molecules. They are e.g. used as thin films for immunoassays, chemical and biological sensors[70, 71], drug screening, tissue engineering, films to immobilize DNA, proteins and enzymes for biosensors applications. [72]

1.4 Cell-adhesive surfaces

When cell adheres to a substrate, it involves complex biochemical mechanisms. Especially, in the living tissues the cell adhere to the extracellular matrix via membrane proteins called integrins.[73] These proteins mediate cell adhesion by binding to different proteins of the extracellular matrix (ECM).

The tripeptide RGD (arginine-glycine-aspartic acid) is a ligand of integrins and can stimulate cell adhesions when it is adsorbed on surfaces. This sequence was identified in many other ECM proteins e.g. in fitronectin, fibrinogen, collagen, laminin, etc, that trigger cell adhesion.

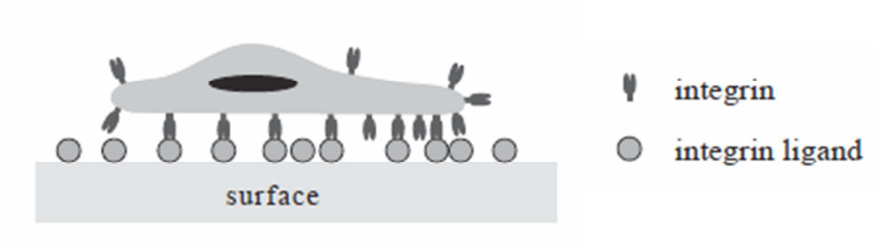

Figure 1. 8. Adhesion and proliferation of the cell.

Therefore, functionalization of polyelectrolyte multilayers with RGD endows them with cell adhesion capacity . This peptide can be easily linked to polymers via covalent amide bonds. The PAH proved to be excellent for binding RGD.[74] When RGD was covalently immobilized in films of alkyne or azide groups (PEG-Alk/PEG-Az)$_5$ it promoted the adhesion and proliferation of cells.[75]

In similar systems RGD is grafted to (PLL-g-PEG/PEG-RGD*x*%) with (x% = 1, 4, 11, 58) The structure is represented in Scheme 1.2 and PEMs with this modified polymer on top were built on a Ni_2O_5 surface. The construction of the film and cell adhesion was monitored by the OWLS apparatus. [76] This film promotes the adhesion of human dermal fibroblasts. In these examples, the films are functionalized at the same time with PEG in order to repel proteins. This double functionalization affords a film that is antifouling for most of the species, but adherent for the targeted cells.

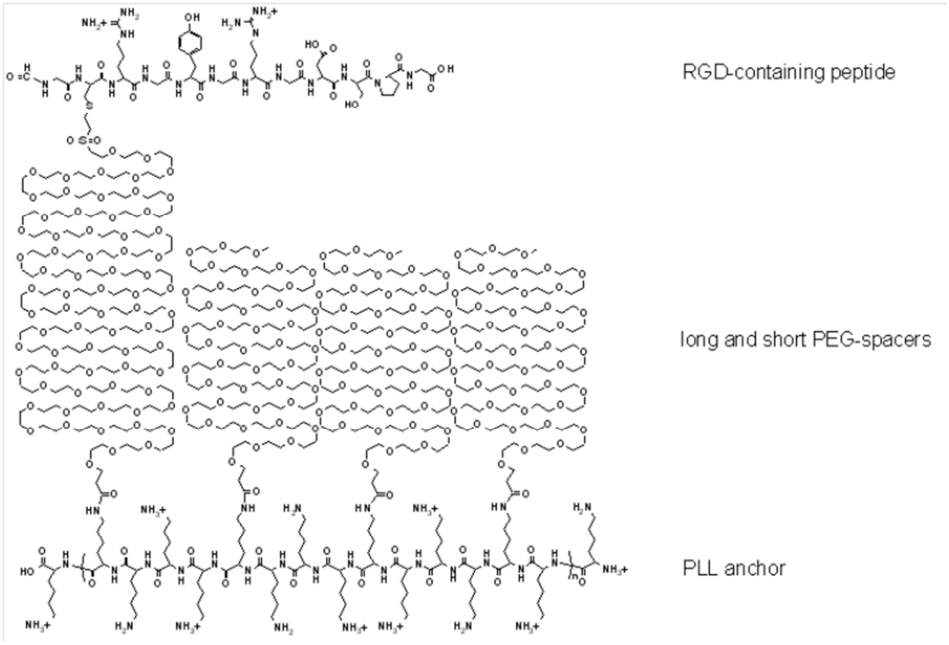

Scheme 1. 2. Scheme of PLL-g-PEG/PEG-RGD

1.5 Biosensor systems using Polyelectrolyte multilayer films

A biosensor has three major components: the *bioreceptor* that is a biomolecule that recognizes a given target, the target molecule or *sensor molecule*, and the *transducer* which converts the recognition into a measurable signal as (optical, piezoelectric, electrochemical, etc). The sensor molecule can consist of a large variety of molecules, e.g. enzymes, antibody, etc.

The principle of biosensors was introduced in 1962 by Leland et al.[77] . His system was able to measureme blood glycemiae and described the first enzyme electrode with immobilized glucose oxidase.

LbL is readily used to prepare biosensors. Multilayer thin films including oxidoreductases (glucose oxidase[78], lactate oxidase[79],) or other proteins[80] by the alternating deposition of proteins and oppositely charged polymers have been prepared. These protein-containing LbL films can be immobilized on electrode surfaces. When the reaction takes place between the enzyme and its substrate,. the oxidation is converted in electric signal via the electrode. This technique has proven to be relatively simple and versatile.

1.5.1 Protein sensors

Many PEM biosensors have been tested with biotin as the sensor and avidin as the bioreceptor. Indeed, biotin-strepatvidin presents the strongest non-covalent biological interaction known, with binding constant of 10^{15} M^{-1}. With this strong interaction, it has been easy for many teams to develop films able to bind biotin or avidin.[57, 81-83]. Biotin is an acid and can be readily coupled to polyelectrolytes, as illustrated in Scheme 1.3.

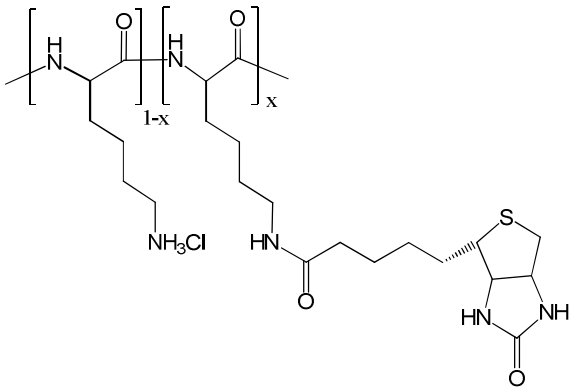

Scheme 1. 3. Example of PE modified by Biotin: poly(L-lysine-*co*-ε-biotinyl-L-lysine).

Roucoules and coworkers.[84], designed surface responsive materials based on PDMS substrates. PDMS was functionalized with carboxylic acid groups by a pulse plasma treatment in the presence of maleic anhydride. COOH groups were used to covalently attach PEG (MW = 2000) and PEG-biotin groups. The studied the non-specific adsorption of proteins, under stretch and at rest in the presence of avidin. Figure 1. 9 illustrates the behavior of the PDMS surface.

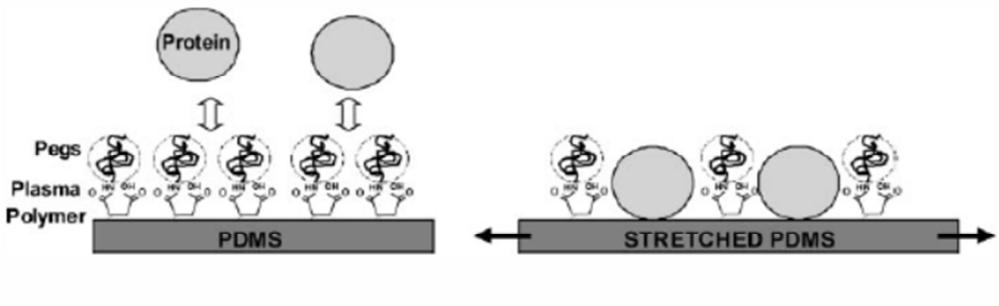

Figure 1. 9. Schematic representation of the PEG-Biotin covalently attached on the PDMS surface in contact with avidin. On the right representation of the surface at rest and on the left the surface under stretch.

The studies of the surface demonstrate that the surfaces are anti-fouling when they are not stretched. This property varies with the elongation of the substrate. When the substrate is stretched at 100% non-specific adsorption of proteins takes place, since the surface is now accessible. Nevertheless, these types of surfaces are precursors for the design of mechanically responsive materials able to resist non-specific adsorption at rest and under stretch.

In one hand PEM can be modified to inhibit the non-specific adsorption of proteins proteins interactions with the surface. On the other hand they can be modified to bind specifically given proteins such streptavidin or avidin. This double capacity offers an interesting perspective to form biosensors.

1.5.2 Immunosensors

Immunosensors exploit the molecular recognition of antigens by antibodies to form a stable complex. The antibodies constitute a class of proteins called immunoglobulins, which are produced by B-cells and they can bind to a foreign substance/molecule (antigen). Immunoglobulins are composed of four polypeptide chains that are connected by disulfide bonds and noncovalent interactions, yielding a Y-shaped protein. There are five types of antibodies called immunoglobulin (Ig), IgM, IgA, IgD, IgE and IgG. They are used in a wide range of

applications e.g., medical implants, drug delivery, clinical diagnostics. Their major application is the detection of drugs in blood or urine. For this purpose, the antibodies are labeled with an enzyme, a fluorescent compound or biotin providing a detectable complex able to be quantified. The construction of these systems with a biological recognition layer is fundamental for their use as biosensors.

The first PEM immunosensors used monoclonal antibodies anti-immunoglobulin G(anti-IgG) embedded in LbL films of $(PSS/PAH)_2$ for the immobilization of the antibodies.[85] The assembly process and the binding capacity of anti-IgG-IgG were monitored using quartz crystal microbalance (QCM) and surface Plasmon resonance (SPR). Other approaches have been reported using LbL assembled on colloidal gold particles.[86]

The performance of immunosensors must be improved by lowering the nonspecific adsorption. As described above, it can be achievd with PEO. Recently,[87] a biosensor with biotinylated PEO grafted to poly($_L$-lysine), (PLL-*g*-PEG/PEG-biotin+PLL-*g*-PEO) provides a surface that is highly resistant to nonspecific adsorption from serum. The film construction was studied by optical waveguide light mode spectroscopy (OWLS). The copolymers of (PLL-*g*-PEO/PEO-biotin+PLL-*g*-PEO) are assembled on the negative surface of niobium oxide (Nb_2O_5). Figure 1. 10(b)

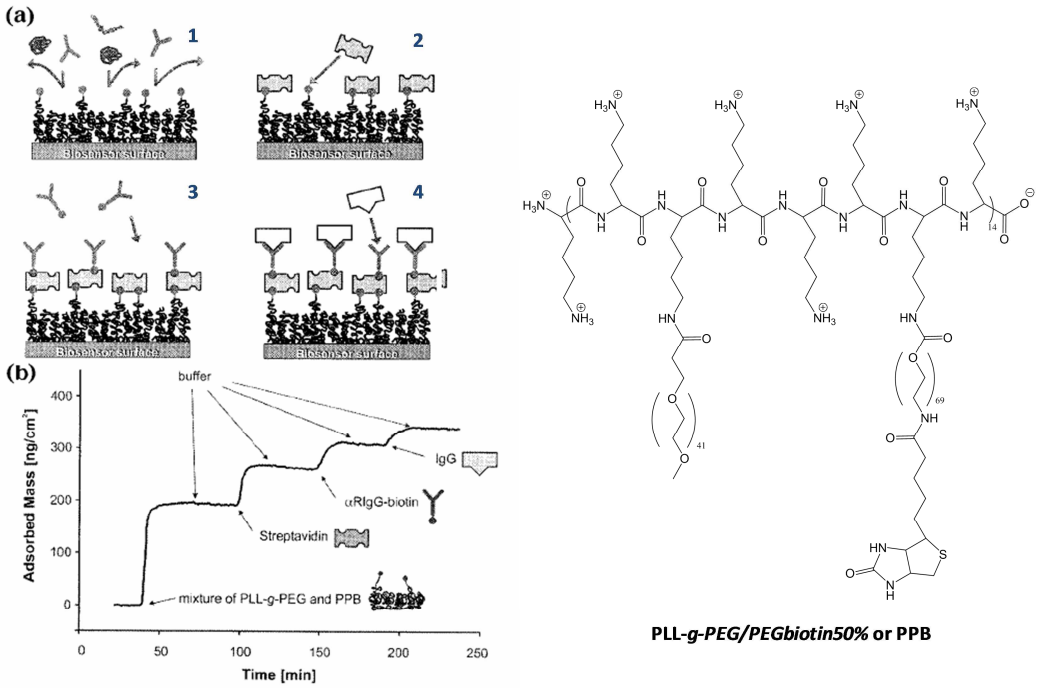

Figure 1. 10. (a) Schematic representation of the different steps in the model of immunoassay on PLL-*g*-PEO/PEO-biotin surface. 1) Surface resist to nonspecific protein adsorption. 2) specific adsorption of streptavidin. 3) αRIgG-biotin binds to streptavidin (antibody). 4) RIgG(antigen) binds αRIgG-biotin. (b) Sequence of streptavidin, antibody and antigen adsorption on PLL-*g*-PEG/PEG-biotin surface by OWLS measurement.[87]

The biotinylated (PLL-*g*-PEG/PEG-biotin) is taken as a model for immunoassays. The presence of streptavidin on the surface of the multilayer film leads the interaction biotin-streptavidin. Once the streptavidin is immobilized on the film, it binds to the antibody (biotinylated goat rabbit immunoglobulin (αRIgG-biotin)), which in turn interacts with the antigen (RIgG). Figure 1. 10

Figure 1. 11(b) shows that the adsorption of αRIgG-biotin is lower than that of streptavidin. This behavior can probably be explained by steric effects of the more closely packed layers of PEG-biotin, blocking biotin or streptavidin free sites. Another reason may be the flexibility of the PEG-biotin chains, allowing the ligands to bind the four sites of the streptavidin, blocking the sites to the adsorption of the antibody. This behavior is represented in Figure 1.11.

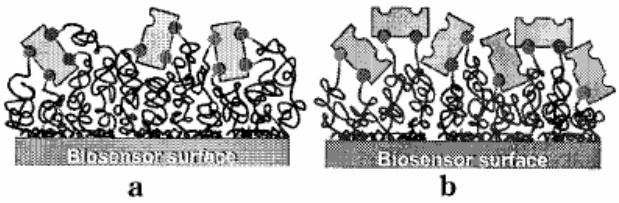

Figure 1. 11. Shematic representation of possible streptavidin configurations. a) PEG-biotin binding to a single streptavidin in there four free sites. b) Steric effects making less accessible the streptavidin or biotin.

To conclude the LbL technique can readily form films with very elaborate surface properties.

1.6 Conclusion

To summarize polyelectrolyte multilayer films can be designed to become anti-fouling, biosensing or cell adhesive. The best known groups that inhibit the non specific adsorption of proteins or cell adhesion are poly(ethylene glycol) and phosphorylcholine.

In addition, PEM can be designed to change their properties under a mechanical stimulus. In the present work, we have elaborated new multilayer films with new biological properties. The first films are model biosensors, that can bind strongly streptavidin, but to repel all other proteins. This study will be described in chapter 2.

The second are mechanoresponsive films for cell adhesion. They embed hidden RGD moieties that become exposed to the surface under stretching. This part of the project will be presented in the chapter 3.

CHAPTER 2:

Polyelectrolyte multilayer films developed for biosensor applications

This chapter describes the design and the buildup of polyelectrolyte multilayer films (PEM) able to bind selectively one protein and in the same time able to repel all others.

We have chosen streptavidin as a model of the protein specifically bounded. As discussed in the previous chapter, biotin can be tethered on PEMs and can bind the protein through a strong interaction. We have developed PEM films with a top layer composed of poly(acrylic acid) (PAA) grafted with biotin. This ligand has been covalently attached to PAA through an oligo(ethylene oxide) $(EO)_n$ spacer having different lengths (3, 9 and 18 EO units) or no spacer for comparison sake. $(EO)_n$Biotin was attached with different grafting ratios (GR), roughly 1%, 5%, 10% and 25%.

Furthermore, we modified PAA both with biotin and phosphorylcholine (PC) groups, to compare their response with streptavidin and their resistance to the non specific adsorption of other proteins, e.g fetal bovine serum (serum). Recently[68, 69], our group proved that modified surfaces with PEM having PC groups on the surface can strongly reduce the adsorption of serum. These results were obtained with PAA functionalized with 25 % of phosphorylcholine groups (PAA-PC).

The first part of this chapter is dedicated to the preparation and characterization of modified PAA. The second part concerns the use of modified PAA as a last layer of PEM films to create a potential biosensor.

2.1 Modifications of PAA by biotin and phosphorylcholine moieties

In order to study anti-fouling property of films and the specific adsorption of streptavidin, we prepared two kinds of modified PAA:

i) PAA modified with EO groups bearing biotin moiety (PAA$(EO)_n$Biotin), with different GR roughly 1 to 25 %.

ii) PAA modified with PC and $(EO)_n$ groups bearing biotin (PAA-PC-$(EO)_n$Biotin) with a GR in PC at ≈ 25 % and in biotin at ≈ 1 %.

In both strategies the length of $(EO)_n$ was varied from n = 0 to n = 18. The selection of $(EO)_n$ as spacer, is due to their hydrophilicity and biocompatibility.[88]

The chemical structure of the modified polyelectrolytes to PAA(EO)$_n$Biotin and PAA-PC-(EO)$_n$Biotin is given in Scheme 2.1.

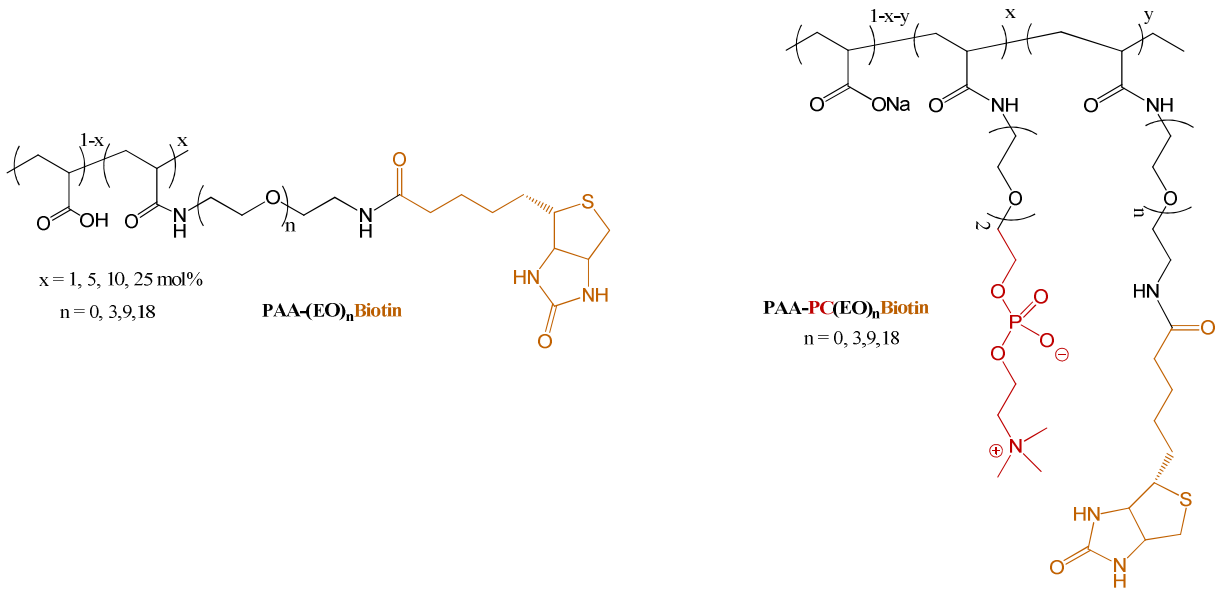

Scheme 2. 1. Structure of PAA-PC-(EO)$_n$Biotin and PAA(EO)$_n$Biotin.

General synthetic pathway is

a) Synthesis of PC and Biotin linkers

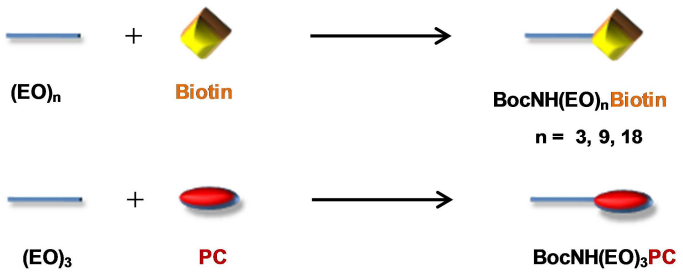

b) Coupling of PC and biotin linkers to PAA

Strategy 1.

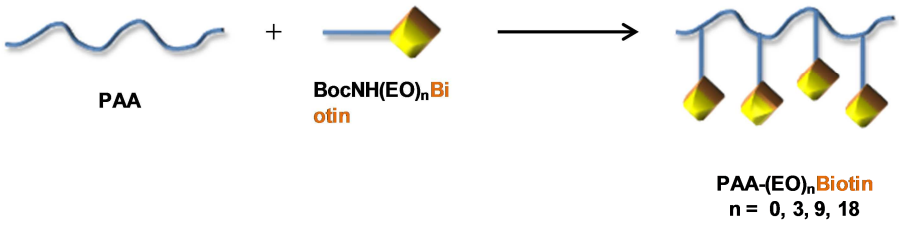

Strategy 2.

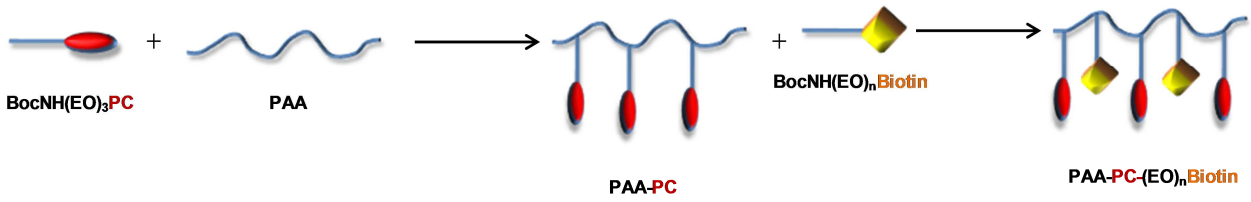

2.1.1 Synthesis of the EO linker

To functionalize PAA, EO_n linkers were prepared with a PC or biotin group on one side and a protected amine on the other side. Biotin linkers synthesis is described for each length of EO_n in Scheme 2.2 and 2.3.

The synthesis of BocNH(EO)$_3$Biotin was done in 6 steps (Scheme 2.2). The linker is acylated by biotin on one side and the other side is reserved to react with carboxylic acid of PAA in the last step. It starts from commercially available tetraethylene glycol. Alcohol functions were replaced by tosyl groups to afford the bis(tosyl) **1**.[89] Tosyl groups as leaving groups have been succesfully used in the modification of oligo and poly(ethylene glycol).[90] This reaction yields to bi-substituted product with up to 40%.

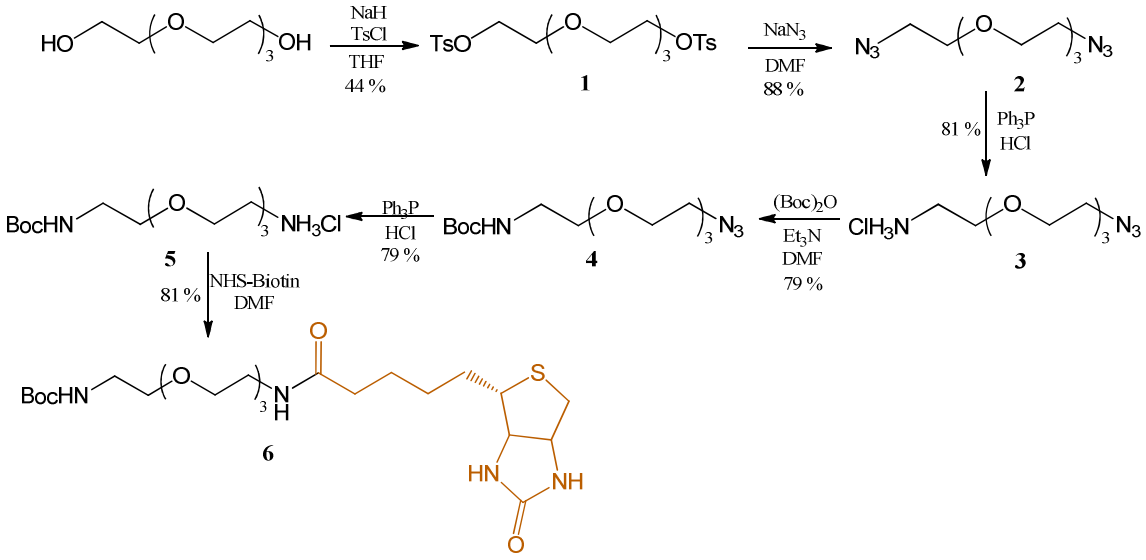

Scheme 2. 2. Synthesis of BocNH(EO)$_3$Biotin.

Bis(azide) **2** was obtained by the reaction with sodium azide in DMF with a yield of 88% from **1**, according to established methods.[89, 91] The mono-reduction to amines was achieved with one equivalent of triphenylphosphine (PPh_3) (Staudinger reduction).[89, 92] This reaction is conducted with EtOAc/acidic water. This set-up allows the solubilisation of the monamine in water and prevents its to bireduction. It affords **3** in 81% yields. The obtained amine group was then protected with $(Boc)_2O$ to obtain **4**. The azide group, on the other side was reduced by using PPh_3 to afford **5**.[93] The last step was acylation of the free amine by NHS-biotin in DMF to obtain **6**.[94, 95]

The synthesis of BocNH(EO)$_9$Biotin **8** and BocNH(EO)$_{18}$Biotin **9** were done in one step. Indeed, the starting compounds BocNH(EO)$_9$NH$_2$and NH$_2$(EO)$_{18}$NH$_2$ are commercially available from Aldrich. The synthesis of **9** was done from the bis(amine) with one stoichiometric equivalent of $(Boc)_2O$ and one equivalent of NHS-biotin. The yield is 40 %.The reactions are represented in Scheme 2.3

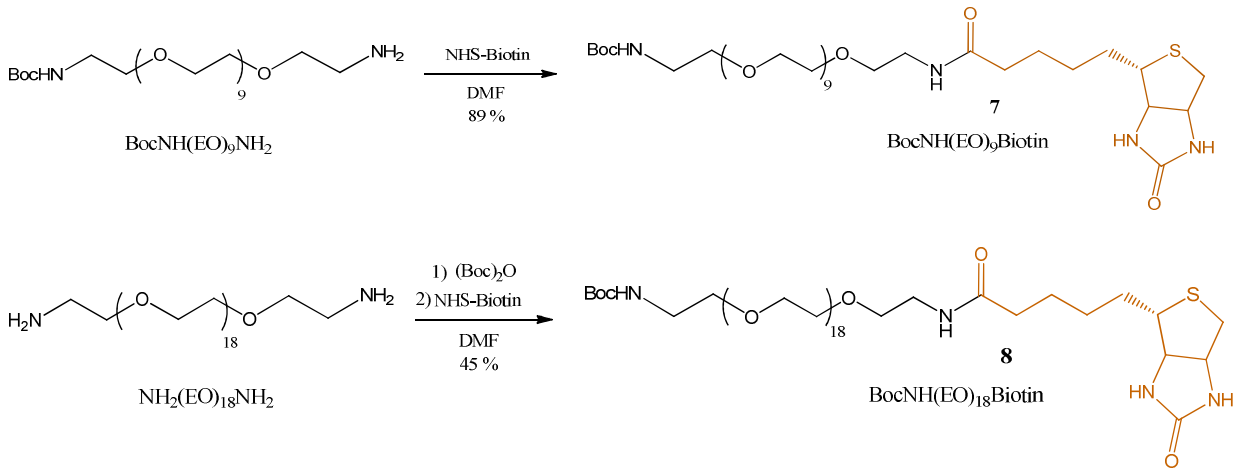

Scheme 2. 3. Synthesis of BocNH(EO)$_9$Biotin 7 and BocNH(EO)$_{18}$Biotin 8.

The PC linkers were synthesized according to the procedure of Brockerhoff et *al.*[96, 97] (Scheme 2.4). The synthesis consists in two successive one-pot reactions: reaction of $POCl_3$ with $BocNH(EO)_3H$ (in the presence of NEt_3), followed by the reaction of the formed compound with with choline tosylate (in the presence of pyridine). After hydrolysis, **9** was obtained with 50 % of yield.

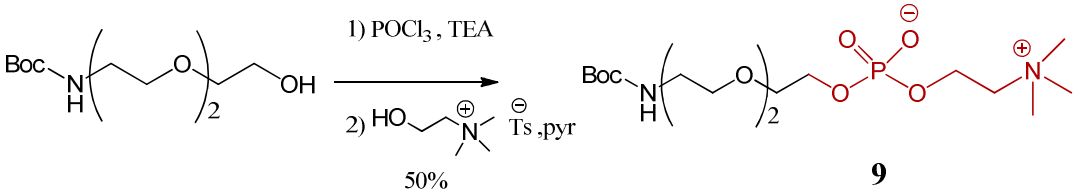

Scheme 2. 4. Synthesis of BocNH(EO)$_3$PC 9.

2.1.2 Coupling reactions of EO linker to Poly(acrylic acid)

EO linkers were covalently coupled to PAA (Mw = 100 000 from Sigma Aldrich) with the coupling procedure described by Reisch et *al.*[97] The GR is defined as a percentage of modified carboxylate functions of PAA. The linkers, described below, were quantitatively deprotected by acidic treatment (HCl, 2.5 M) and coupled *in situ* with PAA in water at pH 5, with an excess of EDCI and HOBt. The polymer was purified by dialysis against water during 5 days.

a) PAA(EO)$_n$Biotin

We synthesized PAA(EO)$_n$Biotin with different lengths of ethylene oxide (n = 0, 3, 9 and 18) and different percentages of modification GR (1, 5, 10 and 25 %). The reactions are illustrated in Scheme 2.5 for EO$_n$ with n = 3, 9 and 18. For n = 0, the modification of PAA was achieved with biotin-hydrazide. Scheme 2.6

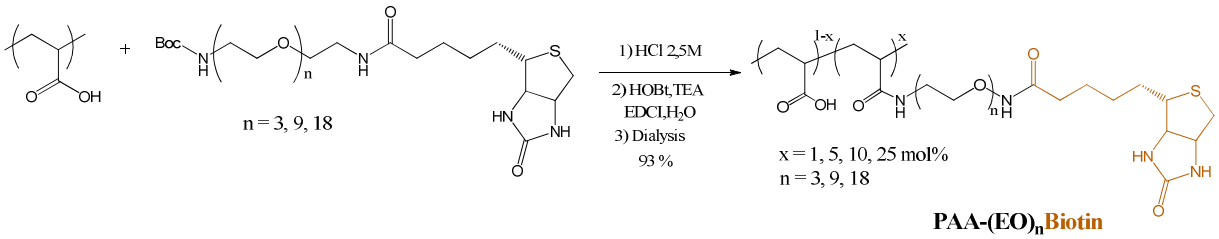

Scheme 2. 5. Coupling reaction between PAA and BocNH(EO)$_n$Biotin, (n = 3, 9, 18) and GR (1 , 5, 10 and 25 %).

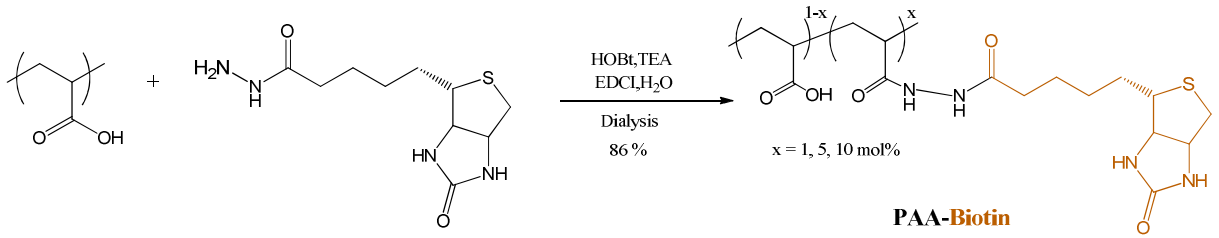

Scheme 2. 6. Coupling reaction between PAA and Biotin hydrazide, GR (1, 5 and 10 %).

The polymers were obtained with an average yield 80-90 % (Table 2.1). Since all the polymers are water soluble, the purification can be obtained by dialysis and gave satisfactory purities.

b) PAA-PC

We first followed the procedure illustrated in Scheme 2.7 described by Reisch et *al.*[97] to modify PAA with BocNH(EO)$_3$PC **9** with a GR of 25 %. As it was described above the linker was first deprotected under acidic conditions and coupled to PAA. The PAA-PC was obtained with a yield of 80 % after dialysis.

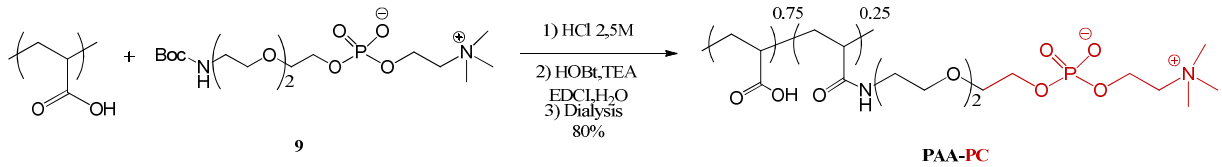

Scheme 2. 7. Coupling reaction between PAA and BocNH(EO)$_3$PC to obtain PAA-PC 25 %.

BocNH(EO)$_n$Biotin (n = 3, 9, 18) was grafted at 1 % on PAA-PC, by the same method as above to afford PAA-PC-(EO)$_n$Biotin , 25 %: 1 % (Scheme 2.8). PAA-PC-Biotin was synthesized by coupling reaction between biotin-hydrazide and PAA-PC.

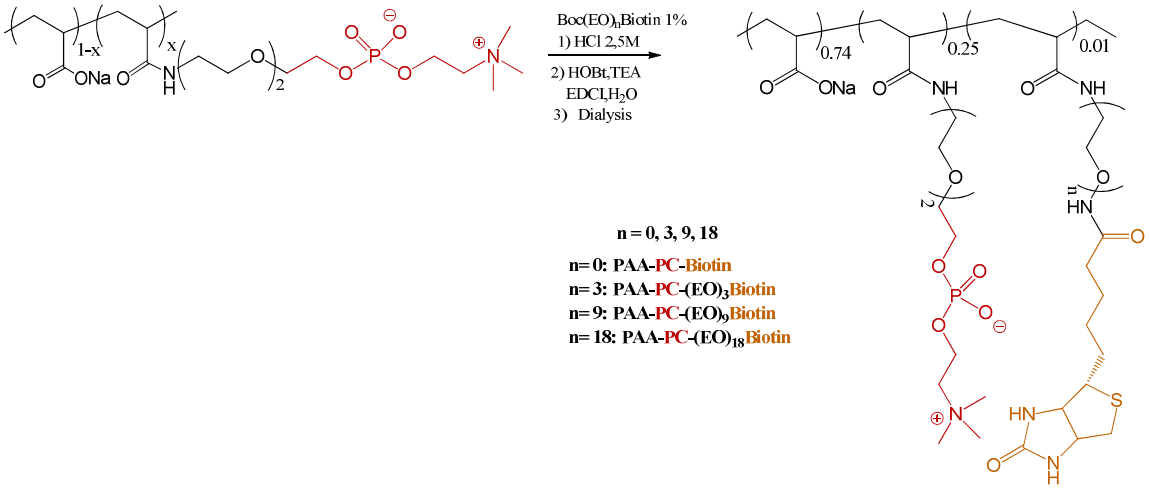

Scheme 2. 8. Coupling reaction between PAA-PC 25 % and BocNH(EO)$_n$Biotin 1 %.

2.2.3 Characterization of modified PAA

GR of PAA-PC polymers was determined by ^{1}H NMR from the integral ratio of the signals at δ = 4.23 ppm of PC (-CH_2OP-) and at δ = 230 ppm of PAA(–CH-). The biotin content was determined by the integral of signals at δ = 2.30 ppm of PAA (–CH-) and the signals at δ = 4.62 - 4.43 ppm of biotin (S-CH_2). The spectra obtained for PAA modified by biotin are consistent with the ones found in the literature for products bearing EO and biotin moieties.[94] The elemental analysis could also provide a measurement of the biotin GR by the sulfur mass, since biotin

contains one atom of sulfur (see materials and methods). These measurements were consistent with those from NMR.

2.2 Buildup of polyelectrolyte multilayer films by QCM

We first followed the adsorption of functionalized PAA by quartz crystal microbalance (QCM). To avoid the influence of the substrate, we first built a PEI(PSS/PAH)$_3$/PAH/PAA as a precursor film. On top of which the modified PAA to be studied was adsorbed. The adsorptions of PEI, PSS and PAH are quite fast, about 5 min. There were, followed by rinsing steps of 5 min. The adsorption and the rinsing step of modified PAA were performed until the stabilization of the QCM signal.

As an example, the buildup of PEI/(PSS/PAH)$_3$/PAA/PAH/PAA-PC-(EO)$_n$Biotin film is given in Figure 2.1. The evolution of the frequency shift Δf at 15 MHz ($\Delta f_3/3$) is representative of the film buildup and is associated to a mass increase at each deposition steps. The measurement of all the frequencies allows to apply the Sauerbrey relation to calculate the mass and the thickness of the film.

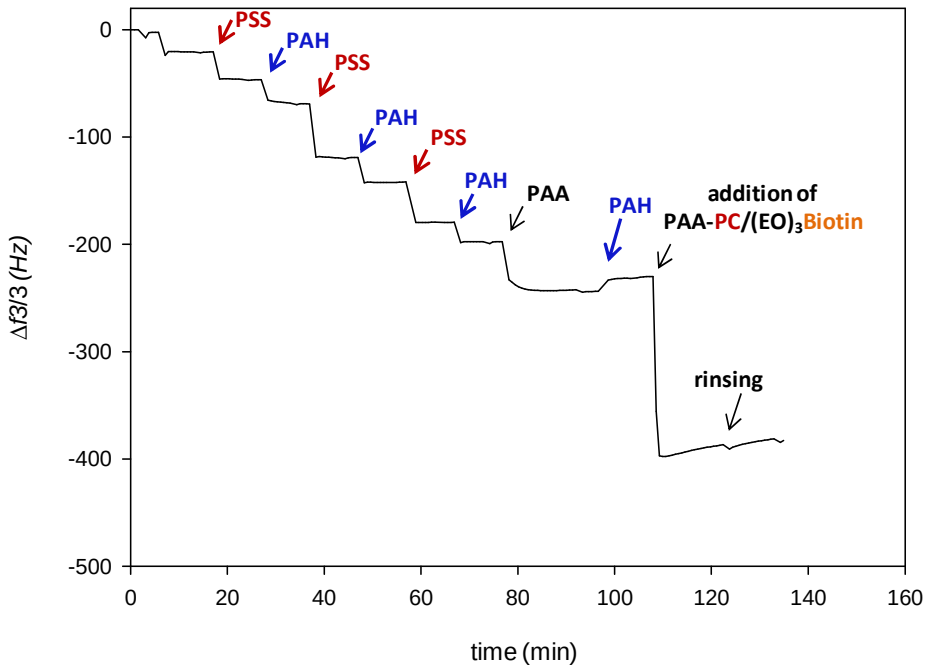

Figure 2. 1. Evolution of the normalized frequency shift at 15 MHz (third harmonic) during the buildup of PEI(PSS/PAH)$_3$/PAA/PAH/PAA-PC-(EO)$_n$Biotin film as a function of time.

The increment of thickness obtained for the different modified PAA and PAA is reported in Table 2.1.The thickness of modified PAA increases with the increase of GR and the length of EO_n linker. This can be explained by the deposition of bound water on the film, due to the strong hydration of ethylene glycol groups.[69]

Table 2. 1. Thicknesses of modified PAA adsorbed on PEI(PSS/PAH)$_3$PAA/PAHcalculated from QCM data by applying the Sauerbrey relation.

	GR in %	GR in %(^{1}H NMR)	Yield %	Thickness nm
PAA	0	-	-	7.7±0.7
PAA-PC	25	24±2	80	24±0.2
PAA-B	1	1±2	83	11.5±0.9
	5	6±4	86	12.8±0.2
	10	12±4	89	16±1.1
PAA(EO)$_3$Biotin	1	1±2	86	8.6±0.9
	5	4±2	93	8.5±0.7
	10	11±4	87	14.4±0.4
	25	25±5	89	18.4±0.6
PAA(EO)$_9$Biotin	1	1±2	85	8.6±0
	5	5±2	93	13.3±1.2
	10	12±4	91	17.4±0.4
	25	24±5	87	31.7±1.3
PAA(EO)$_{18}$Biotin	1	1±2	93	9.7±0.2
	5	6±2	89	16.5±2.4
	10	9±2	81	21.2±1.1
	25	24±2	83	61.7±1.1
PAA-PC/Biotin	25/1	24/1±2	94	25.7±0.8
PAA-PC/(EO)$_3$Biotin	25/1	24/1±2	96	27.3±6.6
PAA-PC/(EO)$_9$Biotin	25/1	24/1±2	95	28.3±0.3
PAA-PC/(EO)$_{18}$Biotin	25/1	24/1±2	96	28.8±1.1

2.3 Serum and Streptavidin adsorption on functionalized films

Once the modified PAA adsorbed on the top of the films, we measured the amount of streptavidin and serum adsorption.

2.3.1 PAA ending films

As a blank, we determined the adsorption of serum and streptavidin on PEI(PSS/PAH)$_3$PAA/PAH/PAA. On these films, the adsorption is necessarily non-specific since it contains no biotin.

The QCM traces during adsorption of serum and streptavidin are shown in Figure 2.2, respectively. A large amount of serum (1252 ng/cm^2) is adsorbed on PAA ending films (Figure2.2(b)) On the contrary, no adsorption of streptavidin is observed, Figure 2.2(a). Thus, PAA adsorb non-specifically serum proteins. It is expected that streptavidin does not bind specifically to the film but it does not bind either by non-specific interactions.

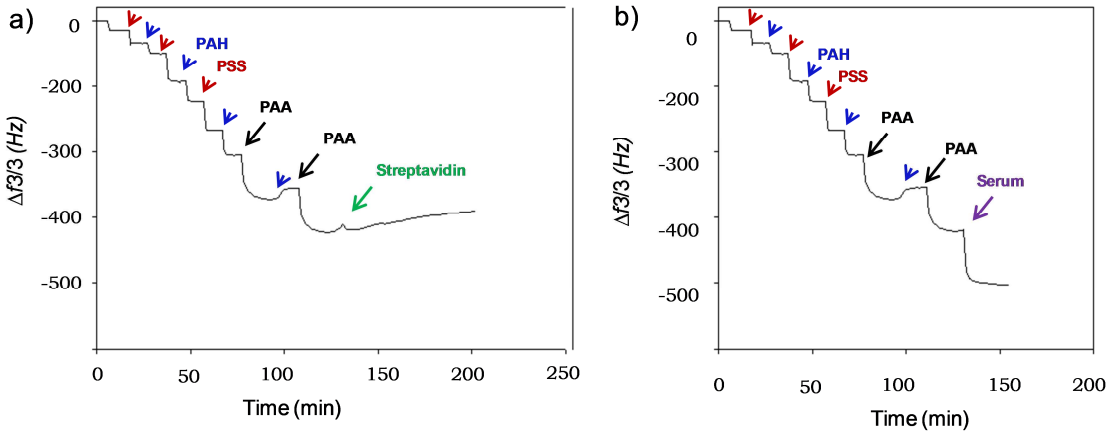

Figure 2. 2. Evolution of the normalized frequency shift measured by QCM at 15 MHz (third harmonic) during the buildup of PEI(PSS/PAH)$_3$/PAA/PAH/PAA as a function of time. a) Film put in contact with streptavidin. b) Film put in contact with serum.

In order to obtain films that prevent non specific adsorption of proteins and induce specific adsorption of streptavidin, we have adsorbed the modified PAA's on top of the PEM films. Depending on the nature of the top layer, two strategies were developed:

1) In the first strategy, the top layer is PAA(EO)$_n$Biotin modified with different spacer lengths (EO)$_n$(n = 0, 3, 9 and 18) at different GR (1, 5, 10 and 25 %).

2) In the second strategy, the top layer is PAA modified both with PC and EO_nBiotin with respective GR of 25 % and 1 %, and with different $(EO)_n$ spacer lengths.

2.3.2 PAA$(EO)_n$Biotin ending films

Strategy 1.

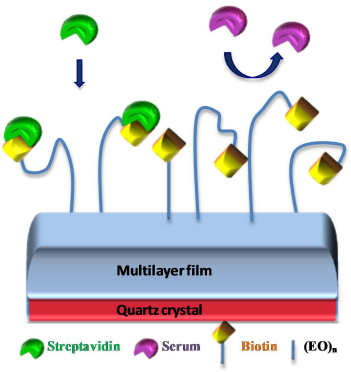

Figure 2. 3. Scheme of functionalized PEM films with PAA$(EO)_n$Biotin, n = 0, 3, 9 and 18.

We built the following films : PEI$(PSS/PAH)_3$PAA/PAH/PAA$(EO)_n$Biotin with n = 0, 3, 9 and 18 and with GR = 1, 5, 10 and 25 %. The adsorption of streptavidin (0.1 mg/mL) was monitored *in situ* by QCM. The mass adsorbed of streptavidin was calculated for QCM data using the Sauerbrey relation. The values are reported in Table 2.2 and plotted in Figure 2.4.

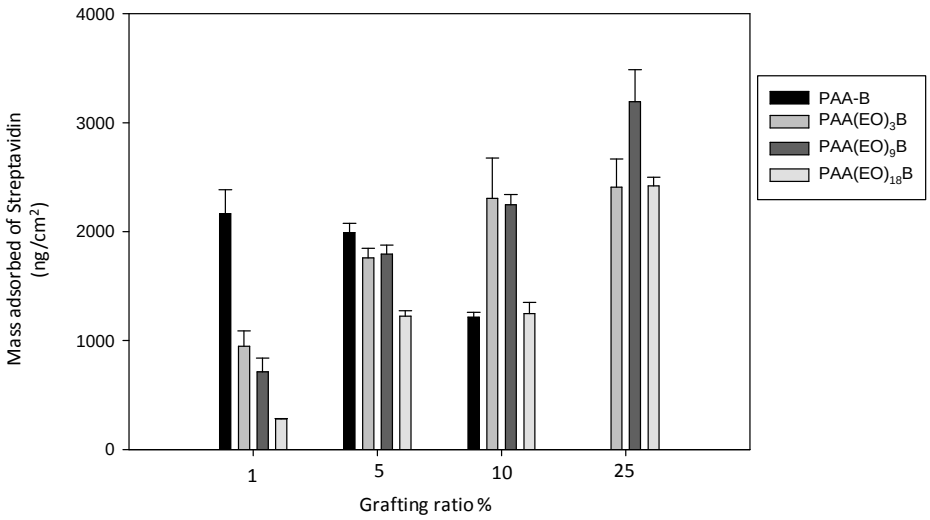

Figure 2. 4. Mass adsorbed of Streptavidin on PEI$(PSS/PAH)_3$/PAA/PAH/PAA$(EO)_n$Biotin with GR = 1, 5, 10 and 25 % and n= 0, 3, 9 and 18, calculated from QCM data using the Sauerbrey relation.

With PAA-Biotin (w/o spacer), streptavidin adsorption is similar for a GR of 1 and 5 % and decreases for a GR of 10 %. The thickness of adsorbed PAA-Biotin increases with GR. The decrease of the adsorbed streptavidin mass is probably due to a non accessibility to biotin due the lack of spacer between PAA and biotin.

With $PAA(EO)_3$Biotin, the mass of adsorbed streptavidin increases when GR increases from 1 to 10 % and has the same value at 25 than 10 %. With $PAA(EO)_9$Biotin and $PAA(EO)_{18}$Biotin, the mass of adsorbed streptavidin increases with GR. The highest adsorbed amount of streptavidin is found for $PAA(EO)_9$Biotin with a GR of 25 %.

To test the anti-fouling property of the films, they were brought in contact with serum at 4.4 mg/mL. The results are illustrated in Figure 2.5 and summarized in Table 2.2.

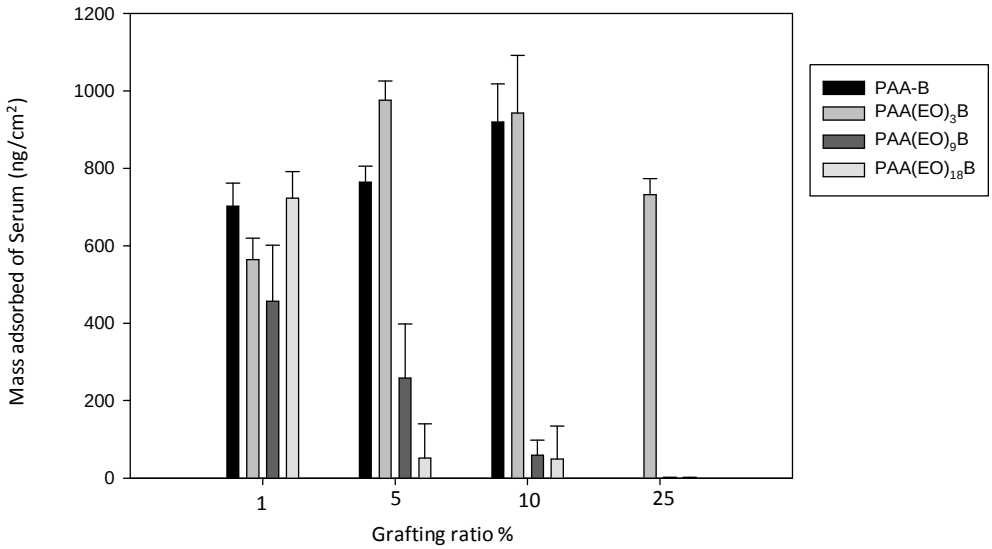

Figure 2. 5. Mass adsorbed of Serum on $PEI(PSS/PAH)_3/PAA/PAH/PAA(EO)_n$Biotin with GR = 1, 5, 10 and 25 % and n= 0, 3, 9 and 18, calculated from QCM data using the Sauerbrey relation.

The adsorption of serum on PAA-Biotin increases when GR increases. On $PAA(EO)_3$Biotin it is independent for the GR. On $PAA(EO)_9$Biotin and $PAA(EO)_{18}$Biotin it decreases drastically when GR increases. At GR = 25 %, the serum adsorption was equal to the detection limit of the QCM.

Table 2. 2. Mass adsorbed of Streptavidn and Serum on PEI(PSS/PAH)$_3$/PAA/PAH/PAA(EO)$_n$Biotin films, calculated from QCM data by applying the Sauerbrey relation.

Nature of the top layer deposited on PEI/(PSS/PAH)$_3$PAA/PAH	GR in %	Streptavidin adsorption (ng/cm^2)	Serum adsorption (ng/cm^2)
PAA	-	<1±1	1252±53
PAA-B	1	2165±218.5	702±59.9
	5	1990±87.3	765±41.8
	10	1241±43.2	920±98.5
PAA(EO)$_3$Biotin	1	947±143.2	564±55.6
	5	1760±87.5	976±49.7
	10	2305±371.3	943±148.9
	25	2407±259.6	732±41.7
PAA(EO)$_9$Biotin	1	714±125.2	457±145.2
	5	1794±59	258±140.5
	10	1483±605.6	40±39
	25	3192±295.7	<1±1
PAA(EO)$_{18}$Biotin	1	281±3.5	723±69.2
	5	1223±51.3	51±88.9
	10	1249±101.4	49±85.4
	25	2419±80.1	<1±1

At 25 % in GR, the amount of adsorbed streptavidin is higher on PAA(EO)$_9$Biotin (3192 ng/cm^2) than on PAA(EO)$_{18}$Biotin (2419 ng/cm^2).(Table 2.2).

Biotin groups of PAA(EO)$_{18}$Biotin are probably not all accessible on surface of the film. This could be explained by the flexibility of the ethylene oxide groups that can fold down.[87]

In the case of PAA(EO)$_9$Biotin, the protein resistance is attributed to the formation of brush layers on the surface that act as a steric barrier. While for PAA(EO)$_{18}$Biotin, the conformation is more like mushroom like form inhibiting the non specific adsorption of proteins. In the same time the biotin moieties are less exposed towards the supernatant and less accessible to streptavidin.

2.3.3 PAA-PC-$(EO)_n$Biotin ending films

As described by Reisch et *al.*[68, 69], PAA-PC with GR = 25 % has anti-fouling properties. Therfore, we have used the same polymers, with the same GR in PC. But in addition we have further functionalized them with $(EO)_n$Biotin with GR = 1 % and we have varied the length of $(EO)_n$.

Strategy 2.

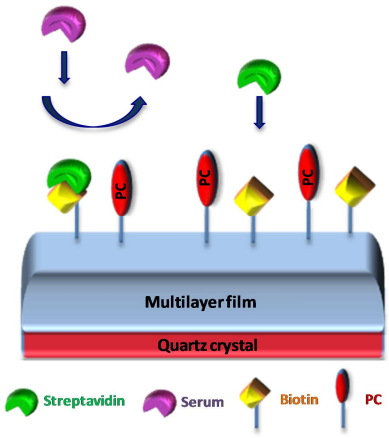

Figure 2. 6. Scheme of functionalized PEM films with PAA-PC-$(EO)_n$Biotin, n = 0, 3, 9 and 18.

After the adsorption of PAA-PC-$(EO)_n$Biotin on the top of the films, the completed films were incubated with serum at 4.4 mg/mL or streptavidin solution at 0.1 mg/mL. The results are displayed in Figure 2.7 and Table 2.3.

Table 2. 3.Mass adsorbed of Streptavidin and Serum on PEI$(PSS/PAH)_3$/PAA/PAH/PAA-PC-$(EO)_n$Biotin films, calculated from QCM data by applying the Sauerbrey relation

Nature of the top layer deposited on PEI/$(PSS/PAH)_3$PAA/PAH	GR %	Streptavidin adsorption (ng/cm^2)	Serum adsorption (ng/cm^2)
PAA-PC/Biotin	25/1	342±8.1	<1
PAA-PC/$(EO)_3$Biotin	25/1	449±64.6	<1
PAA-PC/$(EO)_9$Biotin	25/1	588±166.1	<1
PAA-PC/$(EO)_{18}$Biotin	25/1	445±69.2	<1

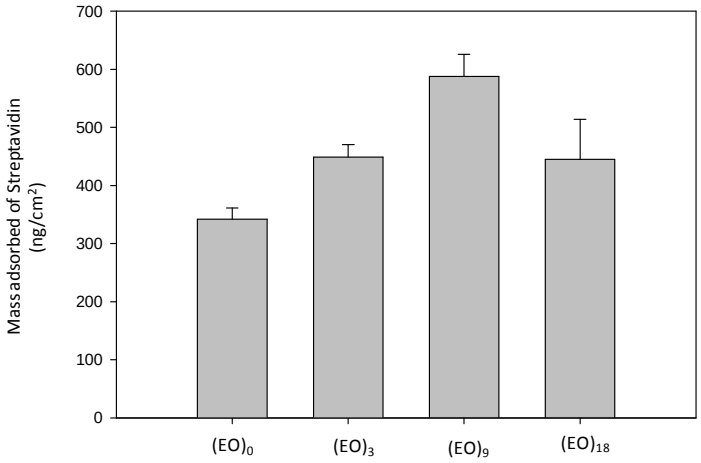

Figure 2. 7. Mass adsorbed of Streptavidin on PEI(PSS/PAH)$_3$/PAA/PAH/PAA-PC-(EO)$_n$Biotin calculated from QCM data using the Sauerbrey relation.

The amount of serum adsorbed for the different films was of the order of the detection limit of the QCM (Table 2.3), which is in agreement with the results of PAA-PC with GR of 25 % reported by Reisch et *a*l.[69]

Figure 2.7 displays the mass adsorbed of streptavidin obtained for PAA-PC-(EO)$_n$Biotin ending film, with different lengths of oligo(ethylene oxide) (EO)$_n$ (n = 0, 3, 9 and 18). The amount of bound streptavidin increases with the spacer length. Streptavidin adsorbs less on PAA-PC-(EO)$_{18}$Biotin than on PAA-PC-(EO)$_9$Biotin. This feature can be explained by the decrease of accessibility to the biotins at the surface due to the fold down of the EO chains. The optimal adsorption is thus found for PAA-PC-(EO)$_9$Biotin.

These surfaces specifically adsorbs streptavidin with higher efficiency for PAA-PC-(EO)$_9$Biotin and at the same time prevent non-specific adsorption. This property can be explained by the presence of PC and EO groups that are well known to have anti-fouling properties. EO displayed anti-fouling properties as well as PC groups.[69] Non specific adsorption of protein decreases with the increase in length of EO and GR.

2.4 Conclusion

In this study, two strategies were applied to obtain a specific adsorption of streptavidin and to prevent the non specific adsorption of serum proteins. Films with PAA-PC-$(EO)_n$Biotin and PAA $(EO)_n$Biotin as last layers specifically adsorb streptavidin. The amount of protein adsorbed depends on the EO length and the modification degree (GR) in linker. The highest ratio of streptavidin adsorption over non specific adsorption is reached for $(EO)_9$.

The non-specific adsorption of serum proteins on PAA-PC-$(EO)_n$Biotin is totally precluded for any $(EO)_n$ linker length. The polyelectrolytes PAA$(EO)_n$Biotin resist to non specific adsorption when the length is 9 or 18 and the GR is 25 %. In both strategies, modified PAA with $(EO)_9$ as linker shows the best results, i.e the highest specific adsorption of streptavidin and the smallest non-specific adsorption.

When comparing both strategies, the films with PAA$(EO)_9$Biotin are able to bound higher amounts of streptavidin than PAA-PC-$(EO)_9$Biotin. In addition, PAA$(EO)_9$Biotin with GR of 25 % is resistant to non specific protein adsorption. This behavior can be explained by the structure of the modified polyelectrolyte on the film surface. The EO groups are strongly hydrated and form a steric barrier as loop-rich layer being most efficient against protein adsorption.

The designed surfaces are a powerful technique to obtain specific adsorption of proteins and to be good candidates for the development of biosensors.

Indeed by using both strategies it is possible to immobilize a biotinylated antibody that can recognize its antigen. (Figure 2.8)

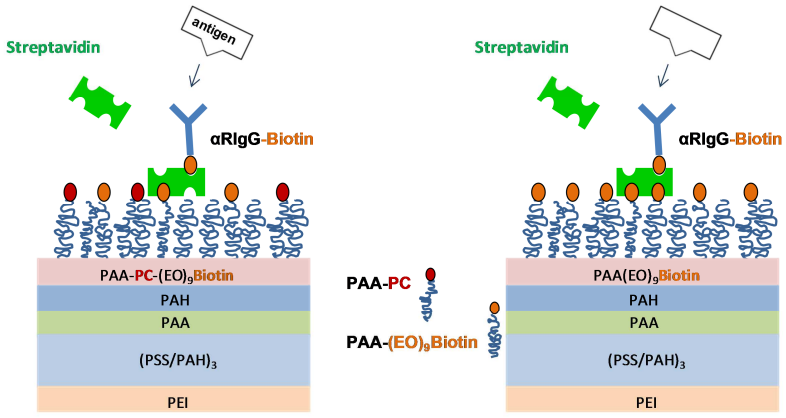

Figure 2. 8. Schematic representation of PEMs as platform for biosensing.

CHAPTER 3:

Cyto-mechanoresponsive Polyelectrolyte Multilayer Films

3.1 Article 1: Cyto-mechanoresponsive Polyelectrolyte Multilayer Films

In this chapter, we have studied films that are able to become cell adherent or to induce specific adsorption of protein by the application of a mechanical stimulus. The design of surfaces that respond under mechanical stimulus has become very attractive field. Only few mechanosensitive surfaces have been described in the literature. One of the first studies was the development of surfaces that present mechanochromic behavior,[98,99] which are able to change their color upon stretching.

In nature, the proteins change their conformation under mechanical forces, exhibiting cryptic sites, e.g. fibronectin are involved in this process where the cryptic sites are exposed under stretching.[54-56] This concept have inspired the development of surfaces containing active compounds which are inaccessible in non stretched state and become accessible when the surface is stretched.[56]

Summary

In this section, we have designed surfaces that exhibit different features, cell adhesion and specific adsorption of proteins when they are stretched. To reach this goal, silicon substrates were used as substrate of PEM films.

In the case of cell adhesion property, PAA was modified by arginine-glycine-aspartic acid (RGD) sequence to obtain PAA-RGD. In order to induce the cell adhesion under stretching, the silicon surfaces were functionalized by PEM films composed by PAA-RGD and PAA-PC. The buildup consist on PEI(PSS/PAH)$_3$ as a precursor film, followed by PAA-RGD embedded by 2 to 6 bilayers of (PAH/PAA-PC) to obtain PEI(PSS/PAH)$_3$/PAA-RGD/(PAH/PAA-PC)$_n$ with n = 2 to 6. It was found that in non stretched state (PAH/PAA-PC)$_2$ film adsorbed onto PEI(PSS/PAH)$_3$/PAA-RGD is needed to render the surface totally resistant to cell adhesion. Furthermore by stretching the functionalized silicon up to 150 % of its original length, cell adhesion is observed.

In the second part of this section, the specific adsorption of proteins was also studied as for cell adhesion, but in this case using modified PAA with biotin moieties. The strong interaction between streptavidin-biotin was used as model system. First of all the film buildup was studied

by QCM, with PEI(PSS/PAH)$_3$/PAA-(EO)$_n$Biotin/PAH/PAA-PC (n = 0, 3 and 9). The results demonstrated that one layer of PAA-PC was enough to prevent the adsorption of streptavidin in (EO)$_n$ (n = 0 and 3). Then the studies with these moieties were carried on silicon substrates to determine their behavior under stretching. Using fluorescein labeled streptavidin (Strep$_{FITC}$) and fluorescence microscopy in non stretched state, the findings were in good agreement with the results obtained by QCM. When the film is stretched, a strong streptavidin adsorption was observed, increasing with the degree of stretching. The reversibility of the films was also studied. When the film is stretched and put back at its non-stretched state, the presence of streptavidin reveals fluorescence intensity. The same behavior is obtained for adhesion of cells on RGD functionalized films. This system seems not reversible.

JACS
JOURNAL OF THE AMERICAN CHEMICAL SOCIETY
Communication
pubs.acs.org/JACS

Cyto-mechanoresponsive Polyelectrolyte Multilayer Films

Johanna Davila,[†,#] Armelle Chassepot,[‡,§,#] Johan Longo,[†] Fouzia Boulmedais,[†,∥] Andreas Reisch,[⊥] Benoît Frisch,[∥,⊥] Florent Meyer,[‡,§] Jean-Claude Voegel,[‡,§] Philippe J. Mésini,[†] Bernard Senger,[‡,§] Marie-Hélène Metz-Boutigue,[‡,§] Joseph Hemmerlé,[‡,§] Philippe Lavalle,[‡,§] Pierre Schaaf,*[,∥] and Loïc Jierry[†,∥]

[†]Centre National de la Recherche Scientifique, Institut Charles Sadron, UPR 22, 67034 Strasbourg Cedex, France
[‡]Institut National de la Santé et de la Recherche Médicale, INSERM Unité 977, 67085 Strasbourg Cedex, France
[§]Université de Strasbourg, Faculté de Chirurgie Dentaire, 67000 Strasbourg, France
[∥]International Center for Frontier Research in Chemistry, 67083 Strasbourg, France
[⊥]Laboratoire de Conception et Application de Molécules Bioactives, CNRS/Université de Strasbourg, UMR 7199, 67401 Illkirch Cedex, France

Supporting Information

ABSTRACT: Cell adhesion processes take place through mechanotransduction mechanisms where stretching of proteins results in biological responses. In this work, we present the first cyto-mechanoresponsive surface that mimics such behavior by becoming cell-adhesive through exhibition of arginine−glycine−aspartic acid (RGD) adhesion peptides under stretching. This mechanoresponsive surface is based on polyelectrolyte multilayer films built on a silicone sheet and where RGD-grafted polyelectrolytes are embedded under antifouling phosphorylcholine-grafted polyelectrolytes. The stretching of this film induces an increase in fibroblast cell viability and adhesion.

The last years have seen the emergence of new domains in materials and surface science. The area of external-stimuli-responsive systems is surely among the most active. Almost any conceivable stimulus has been explored, including pH, ionic strength, electrical potential, light, and magnetic field to cite only a few.[1] Among all of the applied stimuli, mechanical stretching has certainly been less investigated even though it is one of the most widely used in nature. Cell adhesion, tissue growth, and response of organisms to their environment all rely on their response toward externally applied mechanical forces.[2] These forces are then transduced into chemical responses through mechanotransductive processes.[3] Materials or surfaces responding to a mechanical stress are called mechanoresponsive systems. Most of the mechanoresponsive materials developed to date have been designed to change color upon stretching.[4,5] Our group recently introduced the first example of films that respond enzymatically to stretching by using polyelectrolyte multilayers.[6] Two types of polyelectrolyte multilayers, obtained by the alternate deposition of polyanions and polycations, were built on silicone sheets to design such a mechanoresponsive film. A first exponentially growing film was loaded with enzymes that keep their enzymatic activity and then capped by a linearly growing film acting as a barrier for enzyme substrates. Stretching this architecture exposed the enzymes to the solution containing its substrate, allowing the reaction to take place.

Here we present the first cyto-mechanoresponsive surface that responds to stretching by inducing cell adhesion through specific interactions. We used the versatility of polyelectrolyte multilayers to design the most appropriate film architectures.[7,8] Polyelectrolyte multilayers can be deposited on almost any kind of substrate and in particular on bare silicone.[9,10] Our idea was to embed poly(acrylic acid) (PAA)-bearing arginine−glycine−aspartic acid (RGD) adhesion peptides (PAA-RGD, grafting ratio 5%) under a multilayer resistant to cell adhesion and then to expose the RGD peptides by stretching the film (Scheme 1).

Scheme 1. Schematic Representation of the Strategy Used to Design a Cyto-mechanoresponsive Multilayer Film: (a) At Rest, RGD Peptides Are Buried inside the Film; (b) Under Stretching RGD Peptides Are Accessible to Cells

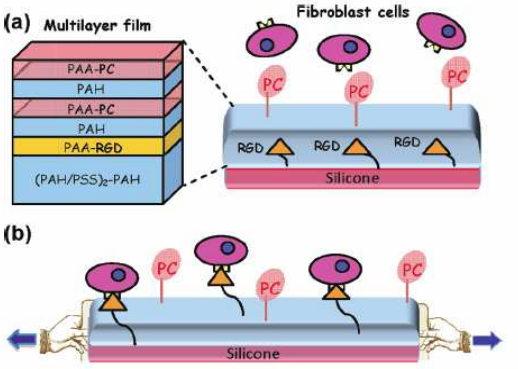

In a previous study, we showed that silicone sheets can be rendered non-cell-adherent at rest as under stretching by

Received: September 23, 2011
Published: December 14, 2011

dx.doi.org/10.1021/ja208970b | J. Am. Chem.Soc. 2012, 134, 83−86

depositing a PAA-PC/PAH/PAA-PC multilayer on a precursor $(PAH/PSS)_2/PAH$ film[10,11] [PAH, poly(allylamine hydrochloride); PSS, poly(styrene sulfonate); PAA-PC, PAA modified with phosphorylcholine (PC) moieties, grafting ratio 25%]. PC groups cover the outer membrane of cells and are known to render surfaces antifouling when grafted at high enough densities on surfaces.[12] Chemical structures of modified PAAs are drawn in Scheme 2. In this study, a $(PAH/PSS)_2/PAH$ precursor film was built on silicone sheets before adsorption of PAA-RGD and capping of the architecture with several PAH/PAA-PC bilayers. Polymer synthesis and all experimental details are given in sections 1, 2, and 3 in the Supporting Information (SI). The stretching ratio (α) is defined as the ratio of the lengths of substrate after and before stretching.

Scheme 2. Molecular Structures of the Functionalized Polymers PAA-Biotin, PAA-PC, and PAA−RGD

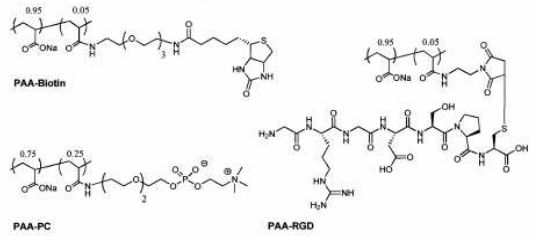

We first followed the buildup of a poly(ethylene imine)/$(PSS/PAH)_3$/PAA-RGD/$(PAH/PAA-PC)_6$ multilayer using a quartz crystal microbalance (QCM) (Figure S1 in the SI). A regular mass increase was observed up to the third (PAH/PAA-PC) bilayer.

The viability and cellular adhesion of primary gingival fibroblasts were then quantified by AlamarBlue assay and immunolabeling for different multilayer architectures deposited on silicone substrates. We first compared, with respect to cell adhesion, the following multilayer films in the nonstretched and stretched states at α =1.5: $(PAH/PSS)_2/PAH$, $(PAH/PSS)_2/PAH/PAA-RGD$, and $(PAH/PSS)_2/(PAH/PAA-PC)_2$ (Figures S2 and S3). Cells were always deposited after stretching of the film. RGD-functionalized films[13] and PAH/PSS multilayers ending with PAH[14] are known for their strong cell adhesion and proliferation tendencies. As expected, strong adhesion and proliferation were observed on multilayers ending with PAA-RGD or PAH and very weak ones on films ending with two PAH/PAA-PC bilayers. Stretching PAA-PC- and PAA-RGD-ended films at α = 1.5 did not modify the cell adhesion and proliferation properties (Figure 1). Next, we determined the minimum number of (PAH/PAA-PC) bilayers required to cover the PAA-RGD layer to obtain a non-cell-adherent film in the nonstretched state. While with one bilayer the cell adhesion and proliferation were only marginally modified, they were strongly reduced with two or more (PAH/PAA-PC) bilayers covering the PAA-RGD (Figure S4).

We then investigated the stretching effect on $(PAH/PSS)_2/PAH/PAA-RGD/(PAH/PAA-PC)_n$ films (denoted as RGD-PCn) with n up to 6 (Figure S5). It appears that under stretching (α = 1.5), cell adhesion takes place for n = 2. On the contrary, RGD-PCn films remain antifouling under stretching for larger values of n. The RGD-PC2 film appears to be the optimal configuration to hinder cell adhesion at rest and allow

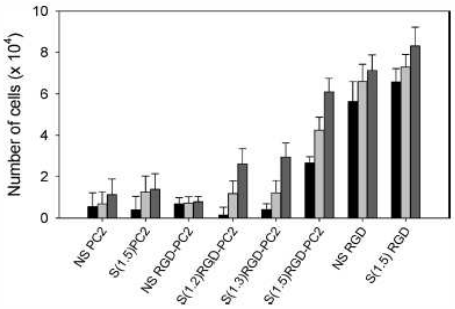

Figure 1. Viability of fibroblast cells as determined by the Alamar Blue test after 1 day (black bars), 2 days (gray bars), and 7 days (dark-gray bars) of culture on different multilayer films built on a silicone basin: a $(PAH/PSS)_2/(PAH/PAA-PC)_2$ film named PC2, a $(PAH/PSS)_2/PAH/PAA-RGD/(PAH/PAA-PC)_2$ film named RGD-PC2, and a $(PAH/PSS)_2/PAH/PAA-RGD$ film named RGD in either the nonstretched state (NS) or the stretched state at a particular α ratio [S(α)]. The reported numbers of cells correspond to means ± standard deviations from three experiments.

cell adhesion under stretching. Thereafter, the experiments were performed with n = 2.

It is known that an increase in RGD density on a surface induces better cell adhesion and spreading.[15] We thus determined the number of adherent cells on RGD-PC2 films stretched at α = 1.2, 1.3, and 1.5 after 1, 2, and 7 days of cell culture (Figure 1). At α = 1.2 and 1.3, the increase in the number of adherent cells was minor and took place only after 7 days of culture. For a film stretched at α = 1.5, the cell viability increased significantly whatever the number of days of culture. In the absence of the PAA-RGD layer [i.e., for the $(PAH/PSS)_2/(PAH/PAA-PC)_2$ film], no increase of the cell number was observed for a film stretched at α = 1.5 relative to the nonstretched one (Figure 1). This clearly indicates that the increase in the number of adherent cells at α = 1.5 was not due to nonspecific interactions but must be attributed to the RGD groups that become accessible to the cells under stretching. Cell adhesion remained smaller for the stretched $(PAH/PSS)_2/PAH/PAA-RGD/(PAH/PAA-PC)_2$ film relative to the $(PAH/PSS)_2/PAH/PAA-RGD$ film (Figure S1), indicating that even for α = 1.5 all of the RGD peptides are not exposed.

Immunostaining allowed checking of the fibroblast morphology. When cells were cultured for 1 week on a nonstretched RGD-PC2 film, only a few cells remained adherent (Figure 2a).

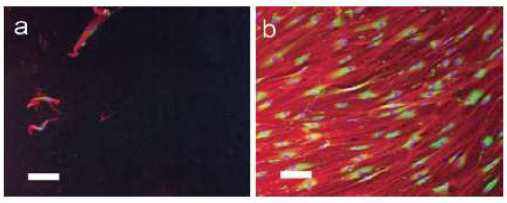

Figure 2. Typical fluorescence microscopy images of fibroblast cells after 1 week of culture on RGD-PC2 built on a silicone basin in (a) the nonstretched (NS) state and (b) a stretched state with α = 1.5 ratio [denoted S(1.5)]. Immunochemical detection of actin fibers of the cytoskeleton by phalloidin (red labeling), collagen type I compounds of the extracellular matrix by anticollagen I (green labeling), and nuclei by DAPI (blue labeling). Scale bars correspond to 100 μm.

dx.doi.org/10.1021/ja208970b | J. Am. Chem.Soc. 2012, 134, 83−86

However, when cells were cultured on the same type of film, RGD-PC2, in a stretched state at α = 1.5, a dramatic proliferation of adherent cells was observed. Cytoskeleton staining showed the presence of actin fibers lying parallel to each other (Figure 2b), a signature of cell spreading and organization. Collagen type I synthesis by cultivated fibroblast cells were investigated as well. Adherent cells revealed the production of collagen type I, the early component of the extracellular matrix produced by fibroblasts, a signature of their good secretory activity.

Next, we verified by atomic force microscopy that the films remained homogeneous over the whole surface under stretching up to α = 1.5. No cracks appeared on the surface, indicating that the silicone substrates remained totally covered by the multilayers under stretching (Figure S6).

To confirm that film stretching renders the embedded RGD sites accessible to cells, RGD peptides were replaced by biotin groups to study their accessibility to fluorescein isothiocyanate (FITC)-labeled streptavidin present in solution. We used biotin because it binds to streptavidin, a 53 kDa protein, through a noncovalent bond known to be the strongest measured in biological systems,[16] making it easier to quantify. In the nonstretched state, the $(PAH/PSS)_2/PAH/PAA\text{-}Biotin/(PAH/PAA\text{-}PC)_2$ film was nonadsorbent to streptavidin, as no fluorescence was observed on the surface after contact with the streptavidin solution followed by rinsing (Figure 3, inset labeled α = 1.0).

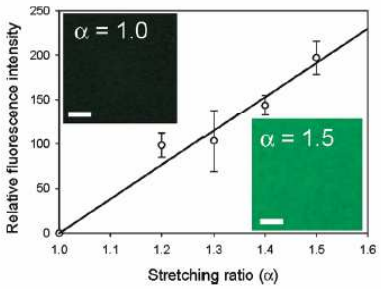

Figure 3. Fluorescence intensity measured from FITC-streptavidin adsorbed on a $(PAH/PSS)_2/PAH/PAA\text{-}Biotin/(PAH/PAA\text{-}PC)_2$ multilayer film built on a silicone sheet at different stretching ratios α. The relative fluorescence intensity was measured using Image J software. The data correspond to means ± standard deviations from three experiments. A strong correlation between the amount of FITC-streptavidin adsorbed and α (R = 0.980) was obtained. The insets represent typical images of the film brought in contact with FITC-streptavidin in the nonstretched (α = 1.0) and stretched (α = 1.5) states. The scale bars represent 20 μm.

Increasing α from 1.0 to 1.5 led to a roughly linear increase in the fluorescence with α when the film was in contact with FITC-streptavidin (Figure 3 and its inset labeled α = 1.5). This indicates that an increasing number of biotin groups became available on the top of the film. In a control experiment with no PAA-Biotin embedded [i.e., a $(PAH/PSS)_2/PAH/PAA/(PAH/PAA\text{-}PC)_2$ film], no fluorescence was observed after contact with FITC-streptavidin in either the stretched or nonstretched state (data not shown). The fluorescence was thus due to specific interactions between biotin and streptavidin.

These results can be interpreted as follows: in the nonstretched state, the ligands (RGD or biotin) embedded under two or more PAH/PAA-PC bilayers are not accessible to their receptors. When the film is stretched, resulting in a thinning of the capping layer, an increasing number of ligands become accessible as α increases. However, a critical RGD density must be reached for fibroblasts to adhere correctly. This critical density seems to be obtained at α = 1.5 (Figure 1). When the ligands are embedded under four or more PAH/PAA-PC bilayers, exposure becomes impossible even at α = 1.5 and cells thus hardly adhere (Figure S5).

Finally, we also addressed the reversibility of the system with respect to stretching. We stretched a $(PAH/PSS)_2/PAH/PAA\text{-}RGD/(PAH/PAA\text{-}PC)_2$ film at α = 1.5 for 30 min before returning it to the nonstretched state during 1 h. We then seeded the surface with cells in this nonstretched state (Figure S7). Only partial recovery of the nonadherent effect was observed. This can be explained by film restructuring consecutive to the stretching/relaxation steps. Thus, only a partial remasking of the RGD peptides takes place, leading to a slight decrease in cell adhesion.

To summarize, we have presented here a new type of mechanotransductive film that becomes cell-adherent under stretching by rendering RGD ligands accessible to cells. This mechanotransductive film was obtained using multilayer technology with polyelectrolytes bearing RGD ligands embedded under nonadhesive polyelectrolytes bearing phosphorylcholine. The effect is partially reversible upon stretching/relaxation. Up to now, only a few synthetic mechanotransductive materials and films have been reported, most leading to a change in color when stretched. This change of color can be due to a chemical reaction that takes place with the stretched molecules.[5] None of these processes induced by stretching are reversible, even partially. For films becoming enzymatically active under stretching, the process is reversible to some extent. Our next goal is to design fully reversible cyto-mechanoresponsive materials that induce changes in behavior of already adherent cells. Through gradual changes in the density of adhesion ligands, the fate of adherent cells could be modified simply by stretching, allowing one to envision applications in tissue engineering.

■ ASSOCIATED CONTENT

Supporting Information

Polymer modification; multilayer buildup and characterization; cellular viability and adhesion method; buildup of $(PAH/PSS)_2/PAH/PAA\text{-}RGD/(PAH/PAA\text{-}PC)_6$ films monitored by QCM; polydimethylsiloxane characterization; and fibroblast viability and adhesion on different stretched and nonstretched multilayers. This material is available free of charge via the Internet at http://pubs.acs.org.

■ AUTHOR INFORMATION

Corresponding Author

pierre.schaaf@ics-cnrs.unistra.fr

Author Contributions

#These authors contributed equally.

■ ACKNOWLEDGMENTS

We gratefully acknowledge Karim Benmlih for stretching device design, Bernard Guérold for the chemical peptide synthesis, and Delphine Toulemon for technical help in QCM measurements. J.D. was supported by a fellowship from FONACIT (Government of Venezuela). This work was supported by ANR-10-BLAN-0818 "Biostretch" and icFRC. J.L. acknowledges IRTG for financial support.

REFERENCES

(1) Cohen Stuart, M. A.; Huck, W. T. S.; Genzer, J.; Muller, M.; Ober, C.; Stamm, M.; Sukhorukov, G. B.; Szleifer, I.; Tsukruk, V. V.; Urban, M.; Winnik, F.; Zauscher, S.; Luzinov, I.; Minko, S. *Nat. Mater.* **2010**, *9*, 101−113.
(2) DuFort, C. C.; Paszek, M. J.; Weaver, V. M. *Nat. Rev. Mol. Cell Biol.* **2011**, *12*, 308−319.
(3) Vogel, V. *Annu. Rev. Biophys. Biomol. Struct.* **2006**, *35*, 459−488.
(4) Caruso, M. M.; Davis, D. A.; Shen, Q.; Odom, S. A.; Sottos, N. R.; White, S. R.; Moore, J. S. *Chem. Rev.* **2009**, *109*, 5755−5798.
(5) Davis, D. A.; Hamilton, A.; Yang, J. L.; Cremar, L. D.; Van Gough, D.; Potisek, S. L.; Ong, M. T.; Braun, P. V.; Martinez, T. J.; White, S. R.; Moore, J. S.; Sottos, N. R. *Nature* **2009**, *459*, 68−72.
(6) Mertz, D.; Vogt, C.; Hemmerlé, J.; Mutterer, J.; Ball, V.; Voegel, J. C.; Schaaf, P.; Lavalle, P. *Nat. Mater.* **2009**, *8*, 731−735.
(7) Decher, G. *Science* **1997**, *277*, 1232−1237.
(8) Hammond, P. T. *Adv. Mater.* **2004**, *16*, 1271−1293.
(9) Fruh, J.; Kohler, R.; Möhwald, H.; Krastev, R. *Langmuir* **2010**, *26*, 15516−15522.
(10) Reisch, A.; Hemmerlé, J.; Chassepot, A.; Lefort, M.; Benkirane-Jessel, N.; Candolfi, E.; Mésini, P.; Letscher-Bru, V.; Voegel, J. C.; Schaaf, P. *Soft Matter* **2010**, *6*, 1503−1512.
(11) Reisch, A.; Voegel, J. C.; Decher, G.; Mésini, P. J.; Schaaf, P. *Macromol. Rapid Commun.* **2007**, *28*, 2217−2223.
(12) Chen, S.; Zheng, J.; Li, L.; Jiang, S. *J. Am. Chem. Soc.* **2005**, *127*, 14473−14478.
(13) Picart, C.; Elkaim, R.; Richert, L.; Audoin, T.; Arntz, Y.; Cardoso, M. D.; Schaaf, P.; Voegel, J. C.; Frisch, B. *Adv. Funct. Mater.* **2005**, *15*, 83−94.
(14) Kerdjoudj, H.; Berthelemy, N.; Boulmedais, F.; Stoltz, J. F.; Menu, P.; Voegel, J. C. *Soft Matter* **2010**, *6*, 3722−3734.
(15) Liu, J. C.; Tirrell, D. A. *Biomacromolecules* **2008**, *9*, 2984−2988.
(16) Merkel, R.; Nassoy, P.; Leung, A.; Ritchie, K.; Evans, E. *Nature* **1999**, *397*, 50−53.

3.1.1 Article 1 (SUPPORTING INFORMATION)

Abbreviations (alphabetic order)**:** AFM= atomic force microscopy, BSA= bovine serum albumin, DAPI= 4',6'-diamidino-2-phenylindol Dihydrochloride, DMEM= Dulbecco's modified eagle medium, **DMF= dimethylformamide,** EDCI= *N*-(3-Dimethylaminopropyl)-*N*′-ethylcarbodiimide hydrochloride, EDTA= ethylene diamine tetraacetic acid, PAA= poly(acrylic acid), **EO= ehtylene oxide,** RGD = GRGDSPC sequence, **ES= electrospray,** FBS= fetal bovine serum, FITC= fluorescein isothiocyanate, FTIR= Fourier Transformed InfraRed Spectroscopy, FMOC= 9-fluorenylmethoxycarbonyl, HEPES= **4-(2-Hydroxyethyl)piperazine-1-ethanesulfonic acid, HOBT= N-hydroxybenzotriazole,** HPLC= high performance liquid chromatography, **MALDI-TOF=** matrix-assisted laser desorption/ionization-time of flight, MWCO= molecular weight cut-off, NMR=nuclear magnetic resonance, **PAA= poly(acrylic acid),** PAA-Biotin= poly(acrylic acid) modified by grafting 5% of biotin groups, PAA-PC= poly(acrylic acid) modified by grafting 25% of phosphorylcholine groups, PAA-RGD= Poly(acrylic acid) modified by grafting 5% of RGD sequence peptide, PAH= poly(allylamine hydrochloride), PBS= phosphate buffered saline, PDMS= polydimethylsiloxane, PEI= poly(ethylene imine), PFA= paraformaldehyde, PS= penicillin-streptomycin, PSS= poly(styrene sulfonate), QCM= quartz crystal microbalance, **SULFO-NHS= N-hydroxysulfosuccinimide sodium salt, TBAI= tetrabutylammonium iodide, THF= tetrahydrofuran, TLC= thin layer chromatography,** UV= ultraviolet.

SECTION-1: Preparation of PAA-Biotin, PAA-PC and PAA-RGD

All starting materials were obtained from commercial suppliers and were used without further purification. ^{1}H NMR and ^{13}C NMR spectra were recorded on Bruker Advance DPX400 (400 MHz) spectrometers. The NMR chemical shifts are reported in ppm relative to tetramethylsilane ($CDCl_3$ or MeO-d_4) or *tert*-butanol (1.24 ppm) in D_2O (s: singlet, t: triplet, q: quadruplet, dd: doublet of doublet, br: broad). Infrared spectra were obtained on a Thermo Electron Corporation Nicolet 380 FT-IR equipped with ATR. Merck RP-18 F254S plates were used for analytical thin layer chromatography. Silica gel 60 (particle: 40 – 60 μm) was used for flash chromatography.

Preparation of PAA-PC

The synthesis of the modified PAA-PC polyelectrolyte was described in detail previously: Reisch et *al.*, *Macromol. Rapid Commun.* **2007**, *28*, 2217-2223.

Preparation of PAA-RGD

Peptide sequence synthesis

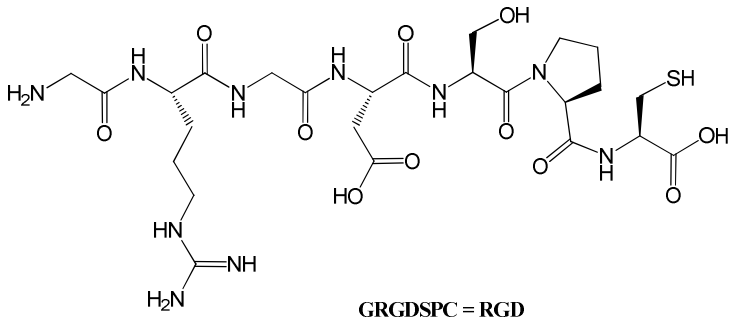

GRGDSPC = RGD

The peptide, GRGDSPC named RGD, was synthesized using standard Fmoc solid-state chemistry on an Applied Biosystems 433A peptide synthesizer (Life Technologies **SAS**, Courtaboeuf, Villebon Sur Yvette, **France)**. Crude peptide preparation was purified by HPLC using a Dionex system (Ultimate 3000, Voisins Le Bretonneux, France) with a Vydac HPLC Protein and Peptide C-18 column (Grace Division Discovery Sciences, Epernon, France). During

HPLC purification, the main peak detected at 214 nm was collected and the identity of the peptide was confirmed by matrix-assisted laser desorption ionization mass spectrometry.

^{1}H NMR (D_2O, 400 MHz, δ ppm): 4.56 (t, ^3J = 5.0 Hz, 1H), 4.52 (m, J = 4.5 Hz, 1H), 4.38 (t, ^3J = 5.0 Hz, 1H), 3.97 (s, 2H), 3.87 (s, 4H), 3.74 (m, 3H), 3.27 (t, ^3J = 6.5 Hz, 2H), 2.92 (m, 2H), 2.82 (m, (t, J = 6.0 Hz, 2H), 2.31 (br m, 1H), 2.04 (br m, 3H), 1.78 (br m, 3H), 1.67 (br m, 2H).

MALDI-TOF: calculated $[M+H]^+$=691.28, found $[M+H]^+$=691.077.

PAA-RGD has been prepared according to general scheme depicted below:

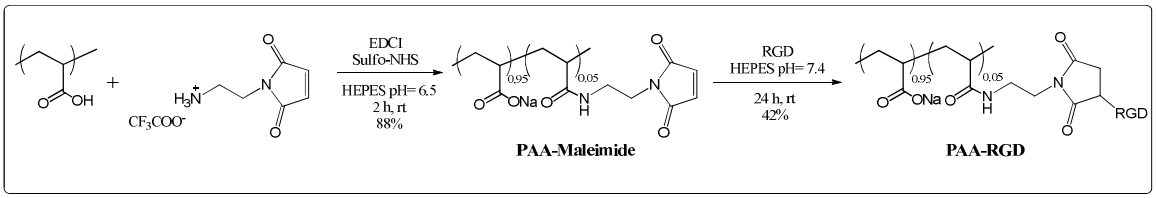

PAA-Maleimide (5%), Poly(acrylic acid) (PAA, Mw 100 000, 35% in water, provided by Sigma-Aldrich company, 60 mg, 0.83 mmol. of acrylic acid units) was dissolved in 30 mL of 10mM HEPES buffer (pH 6.5) followed by the addition of EDCI (117 mg, 0.75 mmol, 0.9 eq.), and sulfo-NHS (33 mg, 0158 mmol, 0.2 eq.). Then N-(2-aminoethyl)maleimide trifluoroacetate (24 mg, 0.0094 mmol, 0.11 eq.) was added. The reaction was stirred at room temperature for 2 h. The solution was dialyzed with a cellulose ester membrane (MWCO 12000-14000) against 0.5 M NaCl for one day and against pure Milli-Q water for 5 days. The final solution was freeze dried to give PAA-Maleimide (88.3 mg, 88% yield).

^{1}H NMR (D_2O, 400 MHz, δ ppm): 7.09 (brs, 0.1H), 3.67 (brs, 0.1H), 3.18 (brs, 0.1H), 2.26 (m, 1H), 1.60 (m, 2H). The signal in 7.09 ppm (s, Mal CH=CH) comparing with the signal at 2.26 ppm (CHα of PAA) give 5% of degree of modification.

FTIR (neat): 1698 cm^{-1} (ν_s CONH), 1650 cm^{-1} (ν_s COO^-).

PAA-RGD (5%), PAA-Maleimide (10 mg, 0.035 mmol) was dissolved in 1.5 mL of 10mM HEPES buffer (pH 7.4), the 7-amino-acid containing the RGD sequence was dissolved in 1 mL of DMF and added to the mixture. After the solution was stirred for 24 h at room temperature, the solvent was evaporated under reduced pressure. The residue was dissolved into

Milli-Q water, and the pH was adjusted at pH 7 with 0.1 M NaOH solution. Then, the solution was dialyzed with a cellulose ester membrane (MWCO 12000-14000) against 0.5 M NaCl (5L) and against pure Milli-Q water (5L). The solution was lyophilized to give (17.1 mg, 42% yield).

^{1}H NMR (D_2O, 400 MHz, δ ppm): 4.56 (br m, 0.1H), 4.36 (br s, 0.05H), 3.96 (br s, 0.1H), 3.88 (br s, 0.2H), 3.75 (br s, 0.15H), 3.21 (br s, 0.1H), 2.88 (br s, 0.2H), 2.41 (br s, 1H+0.2H), 1.77 (br m, 2H+0.25H).

Preparation of PAA-Biotin

*Synthesis of biotin precursor **6***

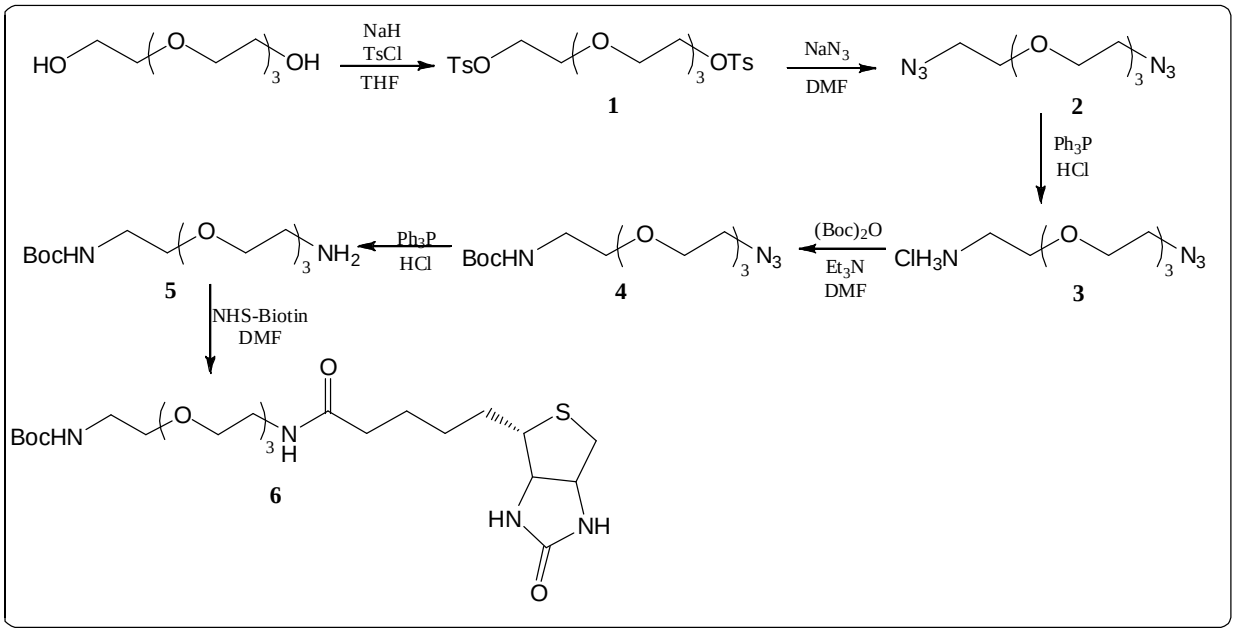

1,14-Ditosyl-3,6,9,12-trioxatetradecane (1). To a solution of tetra(ethylene glycol) (112.5 mg, 0.58 mmol, 1 eq.) in 2 mL of CH_2Cl_2, *p*-Toluenesulfonyl chloride (221 mg, 1.16 mmol, 2 eq.) was added and the mixture was cooled at 0 °C. KOH (260 mg, 4,64 mmol, 8 eq.) was added slowly in small portions, keeping the mixture below 3 °C for 2h. After stirring for 3h at 0 °C, CH_2Cl_2 (5 mL) and ice-water (3 mL) were added. The organic layer was separated and the water layer was extracted with CH_2Cl_2 (2 × 5 mL). The combined organic layers were washed with water (1 × 3 mL) and dried over anhydrous $MgSO_4$. Evaporation of the organic solvent provides **1** as colorless oil (255.7 mg, 44% yield).

^{1}H NMR ($CDCl_3$, 400 MHz, δ ppm): 7.78 (d, ^{3}J = 8.1 Hz, 4H), 7.35 (d, ^{3}J = 8.2 Hz, 4H), 4.15 (t, ^{3}J = 4.5 Hz, 4H), 3.66 (t, ^{3}J = 4.5 Hz, 4H), 3.61 (s, 8H), 2.45 (s, 6H).

^{13}C NMR ($CDCl_3$, 100 MHz, δ ppm): 144.9, 132.9, 129.8, 127.9, 70.6, 69.2, 68.7, 21.6**.**

1,11-Diazido-3,6,9-trioxaundecane (2). Ditosylated triethyleneglycol **1** (376 mg, 0.75 mmol) was dissolved in DMF (2.5 mL). NaN_3 (195 mg, 3 mmol, 4 eq.) and TBAI (13.85 mg, 0.038 mmol, 5 mol %) were added and the mixture was heated at 80 °C for 18h. The DMF was evaporated and the solid residue was suspended in Et_2O. The insoluble salts were filtered and the filtrated concentrated. This procedure was repeated twice to afford **2** as a colorless liquid (875 mg, 88% yield).

^{1}H NMR ($CDCl_3$, 400 MHz, δ ppm): 3.74 (m, 12H), 3.52 (t, ^{3}J = 4.8 Hz, 4H).

^{13}C NMR ($CDCl_3$, 100 MHz, δ ppm): 70.32, 51.06.

FTIR (neat): 2101 cm^{-1} (ν_{as} N_3), 1108 cm^{-1} (ν_{as} C-O-C).

1-amine-11-azido-3,6,9-trioxaundecane hydrochloride (3). A solution of diazide **2** (315 mg, 1.61 mmol) in 10 mL of EtOAc and 2 mL of HCl (1M). To this, Ph_3P (422 mg, 1.61 mmol, 1 eq.) was added and the reaction was vigorously stirred for 12 h at room temperature. The mixture was diluted with water (2 mL) and washed twice with EtOAc. The aqueous phases were concentrated under reduce pressure to yield **3** as a colorless oil (389 mg, 81% yield).

^{1}H NMR ($CDCl_3$, 400 MHz, δ ppm): 3.67 (m, 10H), 3.59 (t, ^{3}J = 5.2 Hz, 2H), 3.46 (t, ^{3}J = 5.2 Hz, 2H), 2.87 (t, ^{3}J = 5.4 Hz, 2H).

^{13}C NMR (MeO-d_4, 100 MHz, δ ppm): 71.6, 71.6, 71.5, 71.3, 71.2, 62.1, 51.9, 40.9.

FTIR (neat): 3350 cm^{-1} (NH_2), 2103 cm^{-1} (ν_{as} N_3), 1104 cm^{-1} (ν_{as} C-O-C).

m/z (ESI): calcd for C8H18N4O4 $[M+H]^+$ 219.15, observed 219.14.

Boc-amine-11-Azido-3,6,9-trioxaundecane (4). 450 mg (2.06 mmol) of **3** was dissolved in DMF (8 mL), and $(Boc)_2O$ (495 mg, 2.26 mmol, 1.1 eq.) was added to the mixture. The reaction was stirred at room temperature for 12h. The solvent was removed under reduced pressure. The crude product was purified by silica gel chromatography (EtOAc: Cyclohexane 1:1) to yield **4** as a colorless oil (355 mg, 79% yield).

^{1}H NMR ($CDCl_3$, 400 MHz, δ ppm) 5.25 (brs, 1H), 3.63 (m, 10H), 3.54 (t, ^{3}J = 4.8 Hz, 2H), 3.39 (t, ^{3}J = 5.2 Hz, 2H), 3.32 (q, ^{3}J = 5.4 Hz, 2H), 1.45 (s, 9H).

^{13}C NMR ($CDCl_3$, 100 MHz, δ ppm): 155.9, 79.1, 70.6, 70.5, 70.4, 70.2, 70.1 70.0, 50.6, 28.4.

FTIR (neat): 2105 cm^{-1} (ν_{as} N_3), 1704 cm^{-1} (ν_s O-C=O), 1389-1365 cm^{-1} (ν_s $(CH_3)_3C$) 1109 cm^{-1} (ν_{as} C-O-C).

Boc-amine-11-Amino-3,6,9-trioxaundecane (5). Triphenylphosphine (250 mg, 0.95 mmol, 1.2 eq.) was added to a solution of **4** (253 mg, 0.81 mmol) in dry THF (3.5 mL), under argon atmosphere at room temperature. The reaction was monitored by TLC in SiO_2 (EtOAc: Cyclohexane 5:1), then 1 mL of water was added and the mixture stirred for 2 additional hours. The solvent was removed under reduced pressure and to the residue 10 mL of toluene and 15 mL of water were added and stirred for 10 min. The aqueous layer was extracted with toluene (10 mL) twice, water was evaporated off and the residue dissolved in CH_2Cl_2, dried over $MgSO_4$. After remove of the solvent under reduce pressure, **5** were obtained as yellow oil (186 mg, 79% yield).

^{1}H NMR ($CDCl_3$, 400 MHz, δ ppm) 5.27 (s, 1H), 3.65 (m, 12H), 3.52 (q, ^{3}J= 5.9 Hz, 2H), 3.31 (q, ^{3}J= 6.8 Hz, 2H), 2.87 (t, ^{3}J = 5.2 Hz, 2H), 1.45 (s, 9H).

^{13}C NMR ($CDCl_3$, 100 MHz, δ ppm): 156.4, 79.4, 70.8, 70.7, 70.5, 70.4, 42.2, 40.5, 28.8.

FTIR (neat): 3351 cm^{-1} (NH_2), 1704 cm^{-1} (ν_s O-C=O), 1389-1365 cm^{-1} (ν_s $(CH_3)_3C$) 1104 cm^{-1} (ν_{as} C-O-C).

***N*-Boc-*N'*-biotinyl-3,6,9-trioxaundecane-1,11-diamine (6).** Triethylamine (0.11 mL, 0.81 mmol) and **5** (200 mg, 0.68 mmol, 1.2 eq.) were dissolved in DMF (5 mL). After, the solution was stirred for 30 min, and *N*-hydroxsuccinimidobiotin (280.6 mg, 0.88 mmol, 1.2 eq.) was added. The reaction mixture was stirred for 12h at room temperature and then concentrated in vacuum. The residue was purified by silica gel column chromatography (acetone: methanol 9:1) as eluent to afford **6** (285 mg, 81% yield) as a white solid.

^{1}H NMR (MeO-d_4, 400 MHz, δ ppm) 4.49 (ddd, $^{3}J_{trans}$ = 8.0 Hz, $^{3}J_{trans}$ = 5.5 Hz, $^{3}J_{cis}$ = 1.0 Hz 1H), 4.30 (dd, $^{3}J_{trans}$ = 8.0 Hz, $^{3}J_{trans}$ = 5.5 Hz, 1H), 3.63 (m, 8H), 3.52 (t, ^{3}J = 5.5 Hz, 2H),

3.49 (t, ^{3}J =5.5 Hz, 2H), 3.36 (br t, ^{3}J =5.5 Hz, 2H), 3.22 (m, 2H), 2.93 (dd, ^{2}J = 13.0 Hz, $^{3}J_{trans}$ =5.0 Hz, 1H), 2.70 (d, ^{2}J = 13.0 Hz, 1H), 2.22 (t, ^{3}J=7.5 Hz, 2H), 1.66 (m, 6H), 1.43 (s, 9H).

^{13}C NMR (MeOD, 100 MHz, δ ppm): 176.3, 174.8, 166, 71.5-70.5, 63.3, 61.5, 56.8, 41.2, 40.9, 40.2, 36.7, 29.6, 29.3, 28.6, 26.7, 26.1.

FTIR (neat): 2927 cm^{-1} (ν_{as} CH_2-C), 2867 cm^{-1} (ν_s CH_2-C), 1693 cm^{-1} (ν_s O-C=O), 1693 cm^{-1} (ν_s CO-NH), 1390-1365 cm^{-1} (ν_s $(CH_3)_3C$) 1104 cm^{-1} (ν_{as} C-O-C).

m/z (ESI): calcd for $C_{23}H_{42}N_4O_7S$ $[M+H]^{+\cdot}$ 519.68, observed 519.28.

Anal. Calcd. for $C_{23}H_{42}N_4O_7S$: C, 53.26; H, 8.16; N, 10.80; S, 6.18; found C, 53.26; H, 8.14; N, 10.88; S, 6.17.

PAA-Biotin

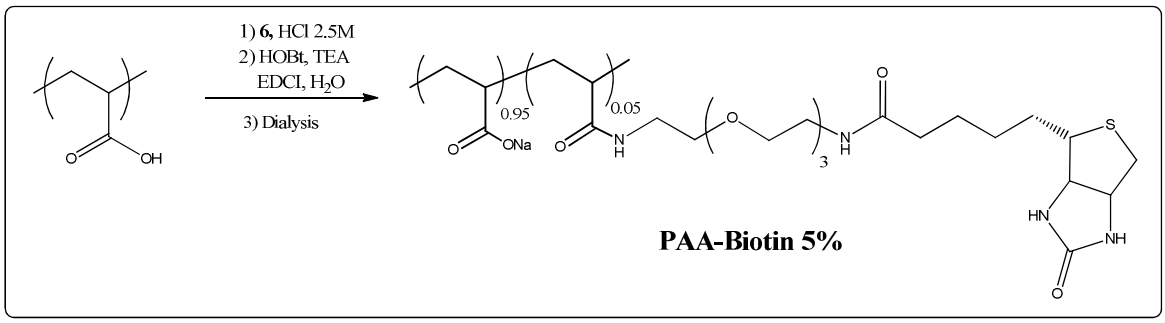

PAA-Biotin (5%). BocNH(EO)$_3$Biotin **6** (28.7 mg, 0.055 mmol, 0.05 eq.) was mixed with aq. HCl (1 mL, 2.5M) and stirred at room temperature for 2 hours. The mixture was dried under vacuum. The residue and poly(acrylic acid) (PAA, Mw 100 000, 35% in water, provided from Sigma-Aldrich company, 123.1 mg, 1.11 mmol. of acrylic acid units, 1 eq.) were dissolved in 4 mL of water, followed by the addition of HOBt (74.9 mg, 0.55 mmol, 0.5 eq.) to the mixture and the minimal amount of NEt_3 to allow the dissolution of HOBt. The pH of 5 was adjusted with HCl (0.1 M), and EDCI (153.5 mg, 0.99 mmol, 0.9 eq.) was added at 0°C. The reaction mixture was stirred at room temperature for 18 hours. The solution was dialyzed with a cellulose ester membrane (MWCO 12000-14000) against 1 M NaCl solution for one day and against pure water for 5 days. Lyophilization of the solution afforded PAA-Biotin as a white solid (83% yield).

^{1}H NMR (D_2O, 400 MHz, δ ppm): 4.62 (dd, ^{3}J =7.5 Hz, ^{3}J =5.0 Hz, 0.05H), 4.43 (dd, ^{3}J =7.5 Hz, ^{3}J = 5.0 Hz, 0.05H), 3.78 (br s, 0.40H), 3.64 (br s, 0.20H), 3.4 (br t, ^{3}J =5.0 Hz, 0.10H), 3.33 (br m, 0.10H), 2.90 (dd, ^{2}J = 13 Hz, ^{3}J = 5.0 Hz), 2.78 (d, ^{2}J = 13 Hz), 2.30 (very

br s, 1H), 2.27 (t partially overlapped with previous broad s, ^{3}J =7.0 Hz, 0.10H), 1.87 (very br s, 0.10H), 1.65 (br m, 2H+0.10H), 1.43 (m, 0.10H).

^{13}C NMR (D_2O, 100 MHz, δ ppm): 176.6, 165.2, 69.7, 69.5, 68.9, 62.1, 60.2, 55.4, 39.8, 38.9, 35.5, 28.0, 27.8, 25.3.

FTIR (neat): 3370 cm^{-1} (ν_s CONa), 2925 cm^{-1} (ν_{as} CH_2-C), 2875 cm^{-1} (ν_s CH_2-C), 1699 cm^{-1} (ν_s CO-NH), 1552 cm^{-1} (COO^-), 1449-1403 cm^{-1} (ν_{as} CO-NH), 1069 cm^{-1} (ν_{as} CH_2-O- CH_2). **Anal. Calcd.** 5% of biotin groups along the PAA backbone determined by 1H NMR (see above) is in good agreement with the S proportion measured by elemental analysis; found S, 1.82; calculated S, 1.85.

SECTION-2: Multilayer buildup and characterizations

Materials

Poly(acrylic acid) (PAA, Mw 100 000, 35% in water, Sigma-Aldrich), Poly (allylamine hydrochloride) (PAH, Sigma-Aldrich M_w 70000), poly (sodium 4-styrene sulfonate) (PSS, Sigma-Aldrich M_w 70000), Trizma^R (Prolabo), sodium chloride (Prolabo) were used as received. Synthetic procedures to prepare the modified poly(acid acrylic) PAA-PC, PAA-Biotin and PAA-RGD are described below. Silicone (poly (dimethyl siloxane, PDMS) basins 15×17×4 mm were purchased from Statice (Besançon, France). Prior to use, these silicone basins are successively pre-treated with absolute ethanol, HCl 0.1 M, NaOH 0.1 M and water in ultrasonic baths. The silicone sheets (254 μm thick, Speciality Manufacturing Inc. SMI, Saginaw, Michigan, USA), measuring 18 × 18 mm^2, were cleaned as silicone basins prior to use.

Dulbecco's Modified Eagle Medium (DMEM) containing 1 g/L glucose and L-glutamine used for primary fibroblasts culture, fetal bovine serum (FBS), penicillin-streptomycin (PS), PBS, trypan-blue stain (0.4%) and trypsin-EDTA (0.5%) were purchased from Gibco, France.

AlamarBlue was purchased from Biosource. Paraformaldehyde (Sigma), PBS (Gibco), Triton (Sigma), BSA (Euromedex), Phalloidin-Tetramethylrhodamine B isothiocyanate (Sigma), Anti-collagen I (ab-cam ab34710), DAPI (Euromedex), FITC Anti-rabbit IgG (Rockland), mounting medium (Dako). Streptavidin-FITC salt-free, lyophilized powder, 5 units/mg protein, was purchased from Sigma-Aldrich (catalog number: S3762).

Silicone pre-treatment and characterizations

Prior to use, silicone substrates were treated with absolute ethanol, HCl 0.1M, NaOH 0.1M and water in ultrasonic baths. This surface treatment is done to render the surface clean and sterile before cell adhesion. No differences between native silicone (Statice France and SMI) were observed before and after surface treatment by contact angle measurements, infrared spectroscopy and atomic force microscopy.

Contact angle measurements. Contact angles were measured on untreated silicone from Statice France and SMI and are respectively of 98° and 97°. After treatment, these values changed to 90° and 100° indicating that the hydrophobicity of the surface does not vary.

Infrared spectroscopy. Perfect overlapping of ATR-IR spectra of treated and non-treated silicone surface (Statice France and SMI) indicates that the surface is not modified chemically. In particular, there is no appearance of OH groups at 3450 cm^{-1} (see FTIR spectra figure below). These observations are in agreement with contact angle measurements indicating that the surface treatment does not affect the chemical nature of the surface.

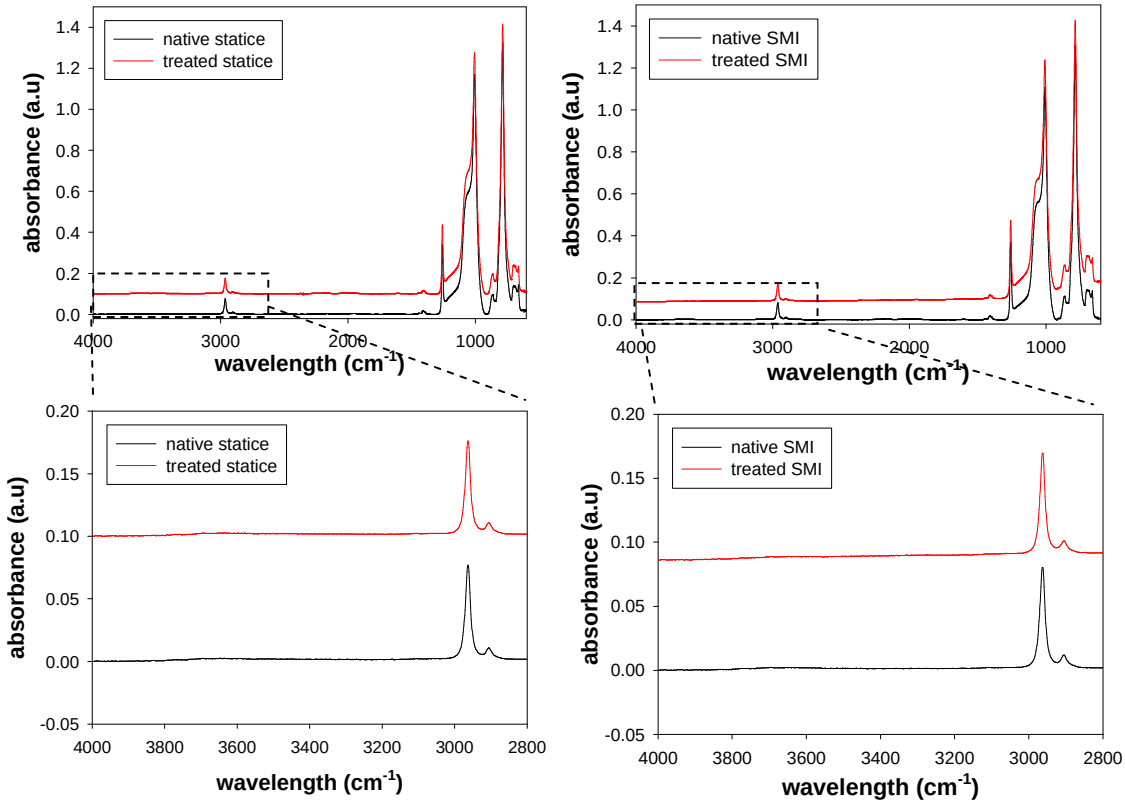

FTIR-ATR spectra of silicone surfaces from Statice France and SMI before and after washing treatment: (a) and (b) spectra represent the whole IR spectra from 600 to 4000 cm^{-1} of Statice and SMI silicone sheets respectively. (c) and (d) are respective zooms between 2800 and 4000 cm^{-1}. For the sake of clarity, spectra corresponding to treated (red line) and untreated (black line) silicone surfaces have been represented one over the other.

Surface morphologies. The silicone sheet topography was observed by AFM. AFM images are similar before and after treatment for both silicones (see AFM images figure below). RMS values change from 20.8 nm (untreated) to 22.7 nm (treated) for silicone sheets purchased from SMI. RMS values change from 25.2 nm (untreated) to 24.2 nm (treated) for silicone purchased from Statice France.

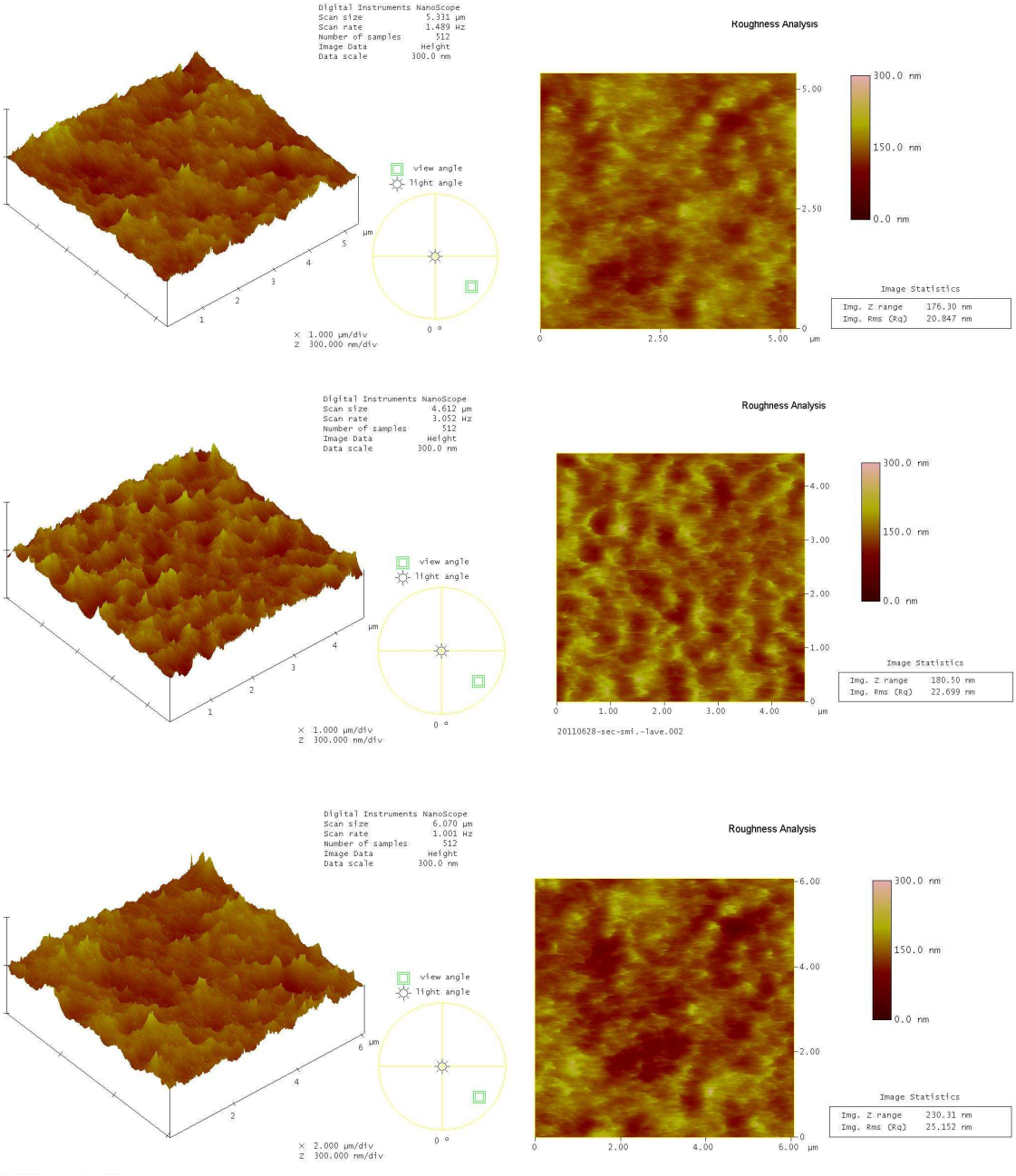
Digital Instruments NanoScope
Scan size 5.331 µm
Scan rate 1.489 Hz
Number of samples 512
Image Data Height
Data scale 300.0 nm
view angle
light angle
X 1.000 µm/div
Z 300.000 nm/div
Roughness Analysis
300.0 nm
150.0 nm
0.0 nm
Image Statistics
Img. Z range 176.30 nm
Img. Rms (Rq) 20.847 nm
Digital Instruments NanoScope
Scan size 4.612 µm
Scan rate 3.052 Hz
Number of samples 512
Image Data Height
Data scale 300.0 nm
view angle
light angle
X 1.000 µm/div
Z 300.000 nm/div
Roughness Analysis
300.0 nm
150.0 nm
0.0 nm
Image Statistics
Img. Z range 180.50 nm
Img. Rms (Rq) 22.699 nm
20110628-sec-smi.-lave.002
Digital Instruments NanoScope
Scan size 6.070 µm
Scan rate 1.001 Hz
Number of samples 512
Image Data Height
Data scale 300.0 nm
view angle
light angle
X 2.000 µm/div
Z 300.000 nm/div
Roughness Analysis
300.0 nm
150.0 nm
0.0 nm
Image Statistics
Img. Z range 230.31 nm
Img. Rms (Rq) 25.152 nm

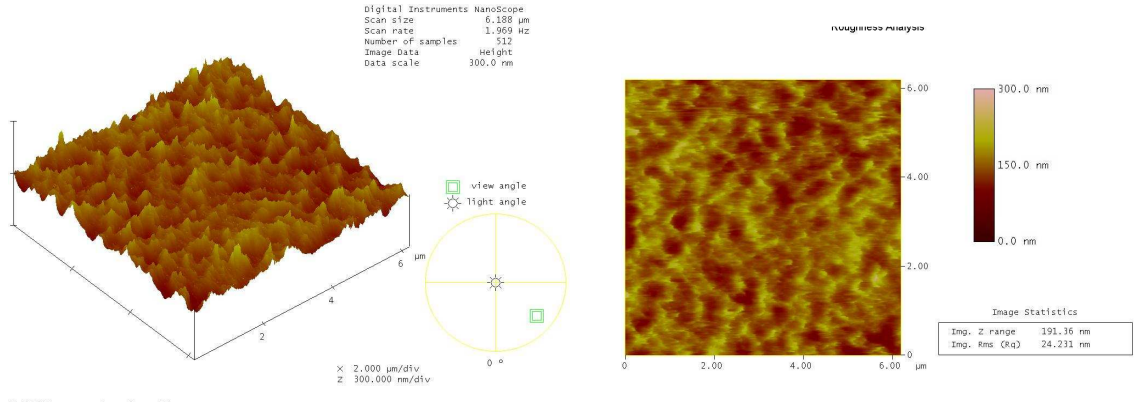

AFM images, obtained in contact mode, of silicone sheets: (**a**) untreated and (**b**) treated SMI sheets and (**c**) untreated and (**d**) treated Statice France sheets.

Preparation of polyelectrolyte multilayer films in silicone basins or on silicone sheets.

All polyelectrolytes are dissolved in 10 mM Tris, 150 mM NaCl buffer at pH 7.4. Concentrations of polyelectrolyte solutions are 1 $mg.mL^{-1}$ for PAH and PSS, 0.5 $mg.mL^{-1}$ for PAA-PC and 0.1 $mg.mL^{-1}$ for PAA-RGD and PAA-Biotin. The pH is adjusted to 7.4. All solutions are filtered (Millex GV membranes, pore diameter of 0.22 µm).

Polyelectrolyte multilayer films are prepared in pre-treated silicone basins (see previous paragraph). Multilayers were assembled by bringing silicone substrate in contact with polyelectrolyte solutions for 5 min in the case of PAH and PSS, for 15 min for PAA-PC or PAA-Biotin and 1h for PAA-RGD. Each deposition was followed by three rinsing steps of 2 min with buffer solution.

Stretching device

Silicone basins or sheets **(a)** are placed in the stretching device (**b**) to stretch it and fix it at the required stretched ratio. The stretched ratio (α) is defined as the ratio between length of substrate after and before stretching. Silicone basins and sheets were stretch at an average speed of 0.5 cm per min. The ratio used in our experiments was between 1.2 and 1.5.

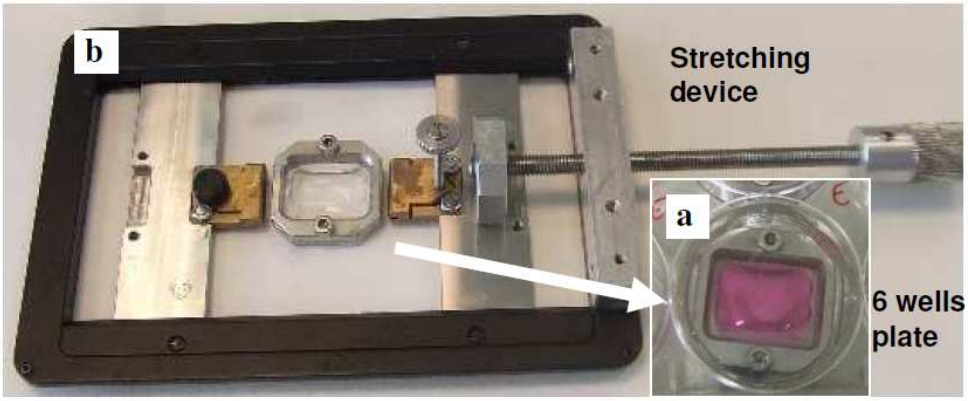

Quartz Crystal Microbalance measurements

Quartz crystal microbalance (QCM) measurements were performed on a QCM-D D300 apparatus from Q-Sense AB (Gothenburg, Sweden) by monitoring the changes in the resonance frequency f and the dissipation factor D of an oscillating gold coated quartz crystal upon adsorption of a layer. The quartz crystal was excited at its fundamental frequency (5 MHz), and the measurements were performed at the first, third, fifth and seventh overtones, corresponding to 5, 15, 25 and 35 MHz. Only the third, fifth and seventh overtones were taken into account in the processing of the experimental data.

Atomic Force Microscopy

Atomic force microscopy (AFM) images were obtained in contact mode in liquid conditions with the Nanoscope IV from Veeco (Santa Barbara, CA). The images were carried out with silicone nitride cantilevers, spring constant 0.03 N/m (Model MSCT, Bruker). Several scans were performed over a given surface area. These scans had to give reproducible images to ascertain that there was no sample damage induced by the tip. Deflection and height mode images were scanned simultaneously at a fixed scan rate (2 Hz) with a resolution of 512×512 pixels. Data evaluation was performed with the NanoScope software version 5.31r1 (Digital Instruments, Veeco).

Fluorescence Microscopy

Images were obtained on an inverted light microscope (Nikon Microphot-FXA, Japan) equipped with a mercury lamp and operating between 470 and 490 nm for excitation and above 520 nm for detection. A 40× dry objective and a digital camera were used. Image analysis was

performed using ImageJ (U.S. National Institutes of Health, Bethesda, Maryland, USA, http://rsb.info.nih.gov/ij/).

Fluorescein labeled Streptavidin ($Strep_{FITC}$) was used at 0.1 $mg.mL^{-1}$ in buffer (10 mM Tris, 150 mM NaCl at pH 7.4) and let adsorbed 2 min on multilayer the film before rinsing 5 × 2 min with buffer. Then, fluorescence microscopy images were taken.

With respect to streptavidin adsorption under physiological conditions the film behaviour was first investigated by quartz crystal microbalance (QCM), a technique that allows the determination of the deposited mass, including the bound water. Film architecture similar to the one study for cell adhesion (but with PAA-Biotin instead of PAA-RGD) shows no detectable streptavidin adsorption. Then, in order to test the influence of stretching on the anti-fouling/streptavidin adsorption properties of this multilayer, the film was built on a silicone sheet according to the same procedure described above in this SI (part entitled "Preparation of polyelectrolyte multilayer films", page 9). Fluorescein labeled streptavidin (StrepFITC) was used and its adsorption on PEI/$(PAH/PSS)_3$/PAH/PAA-Biotin/$(PAH/PAA\text{-}PC)_2$ multilayer built on silicone sheets. The StrepFITC adsorption was monitored at rest and under stretching by detecting the fluorescence intensity using the same exposure conditions. After exposure to StrepFITC solution followed by a rinsing step, a $(PAH/PSS)_3$/PAH/PAA-Biotin/$(PAH/PAA\text{-}PC)_2$ film, built on a silicone sheet, was imaged by fluorescence microscopy. In the main text, Figure 3a and 3b correspond to the fluorescent images obtained respectively in a non-stretched state and in stretched state at α = 1.5. No fluorescence signal of StrepFITC is visible on non-stretched film (comparable to the background, i.e. before exposure to StrepFITC) meaning that the amount of streptavidin adsorbed is of the order of the detection limit. Under stretching up to 1.5 times its original length, characteristic green fluorescence is observed. Even after several rinsing steps, this fluorescence stays on the multilayer film. This observation can be explained by the availability of biotin groups when the material is stretch up to 1.5: specific interaction occurs between StrepFITC and its natural ligand. When the material returns to rest, the fluorescence does not disappear.

SECTION-3: Methods for cellular adhesion tests

Cell culture

Gingival fibroblasts were isolated from human gingival connective tissue of healthy individuals according to a protocol approved by the ethics committee for patient protection of CPP Strasbourg Hospitals. Gingival tissues were obtained from gingival samples without inflammation removed for tooth extraction purposes, cut into small pieces, placed into culture dishes, and incubated in a humidified atmosphere of 95% air and 5% CO_2 at 37°C for 30 min. Then, DMEM culture medium (with 20% FBS, 100 µg/mL penicillin-streptomycin and 2 µg/mL fungizone, Gibco) was added. After confluence was reached, the cells were harvested using 0.25% trypsin. Cells were used between the 4^{th} and 6^{th} passage. The cells were maintained at 37°C in 5% CO_2 in 75 cm^2 flask in DMEM medium containing 10% FBS and 100 IU/mL PS until confluency. For viability tests, basins with polyelectrolyte films were sterilized by UV irradiation during 15 minutes and 2×10^4 cells per basin were distributed.

Viability test (AlamarBlue™ assay)

Viability was assessed by AlamarBlue™ assay after 1, 2 and 7 days. After rinsing, 10% reagent in complete medium was incubated for 3 hours. After incubation optical density (OD) at 570 nm and 630 nm were determined with a microplate reader. The percentage of reduction of AlamarBlue™ was calculated and standard curve numbers of cells were determined.

Cellular fluorescence labelling

Cells were fixed with 4% PFA at 4°C, permeabilized with 0.25% PBS-Triton and saturated with 1% BSA. To label collagen type I, an incubation of anti collagen I (1/200) during 2 h with a rinsing step is followed by an incubation of a secondary antibody for 2 h with a rinsing step. 50 $ng.mL^{-1}$ Phalloïdin solution was incubated for 30 min for labelling of actin filaments. After 3 rinsing steps, 50 $ng.mL^{-1}$ DAPI was incubated for 1 min and washed to label nuclear markers. Samples were mounted in glass with mounting medium. Microscope images were taken. For each experiment and each film condition three samples were tested.

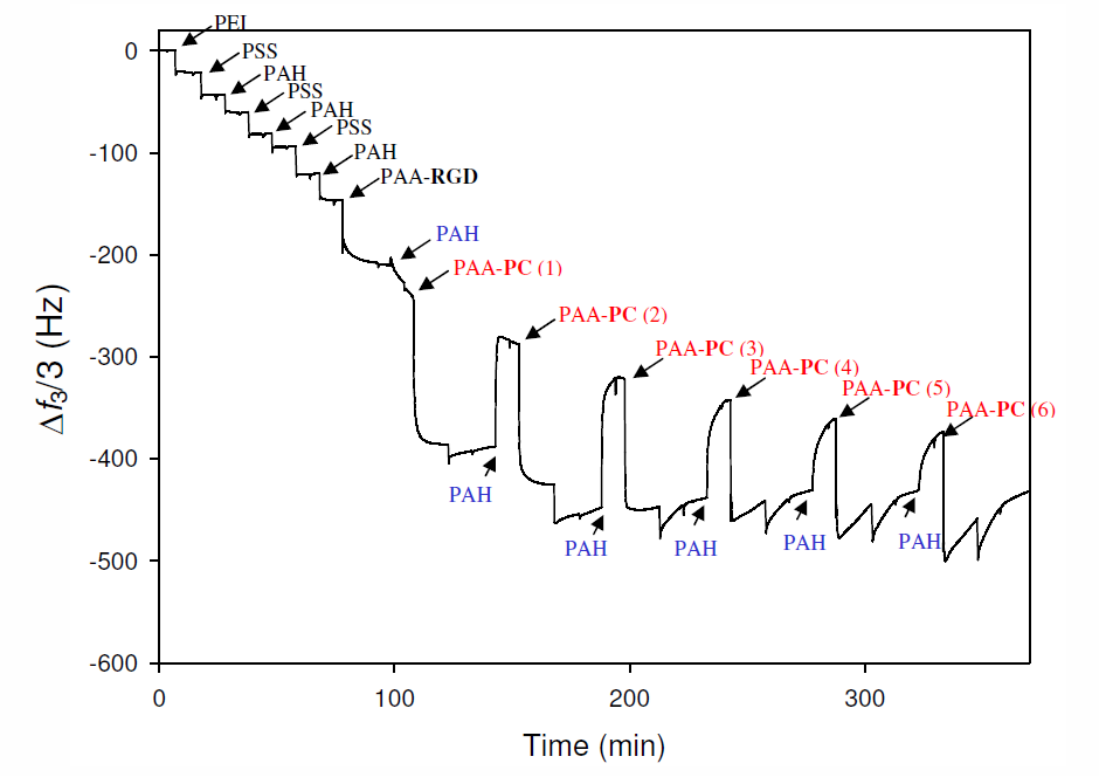

Figure S1. Quartz Crystal Microbalance monitoring of PEI/(PSS/PAH)$_3$/PAA-RGD/ (PAH/PAA-PC)$_6$ film construction. Concentration of the polyelectrolytes solutions are 1 mg.mL^{-1} for PEI, PAH and PSS, 0.5 mg.mL^{-1} for PAA-PC and 0.1 mg.mL^{-1} for PAA-RGD in buffer (10 mM Tris, 150 mM NaCl at pH 7.4). The pH is adjusted to 7.4. All solutions are filtered (Millex GV membranes, pore diameter of 0.22 µm). The quartz crystal is brought in contact with the PEI, PSS and PAH solutions during 5 min and 15 min with the PAA-PC or PAA-RGD solutions. Each deposition step was followed by a rinsing step (5 min) with buffer. The data correspond to the evolution of the frequency shift of the third harmonic (15 MHz). The frequency shifts are proportional, in first approximation, to the mass adsorbed on the crystal surface. A regular mass increase is observed up to the third (PAH/PAA-PC) bilayer. The film buildup seems to stop afterwards. Yet one observes an increase of the deposited mass when the film is brought in contact with PAA-PC and a decrease when it brought in contact with a PAH solution. This could be explained by an adsorption of PAA-PC when the film is brought in contact with the PAA-PC solution, followed by a removal of the deposited PAA-PC when the film is brought in contact with the PAH solution. This process could be accompanied by a film restructuration that is not visible on QCM data because it would not affect the deposited mass.

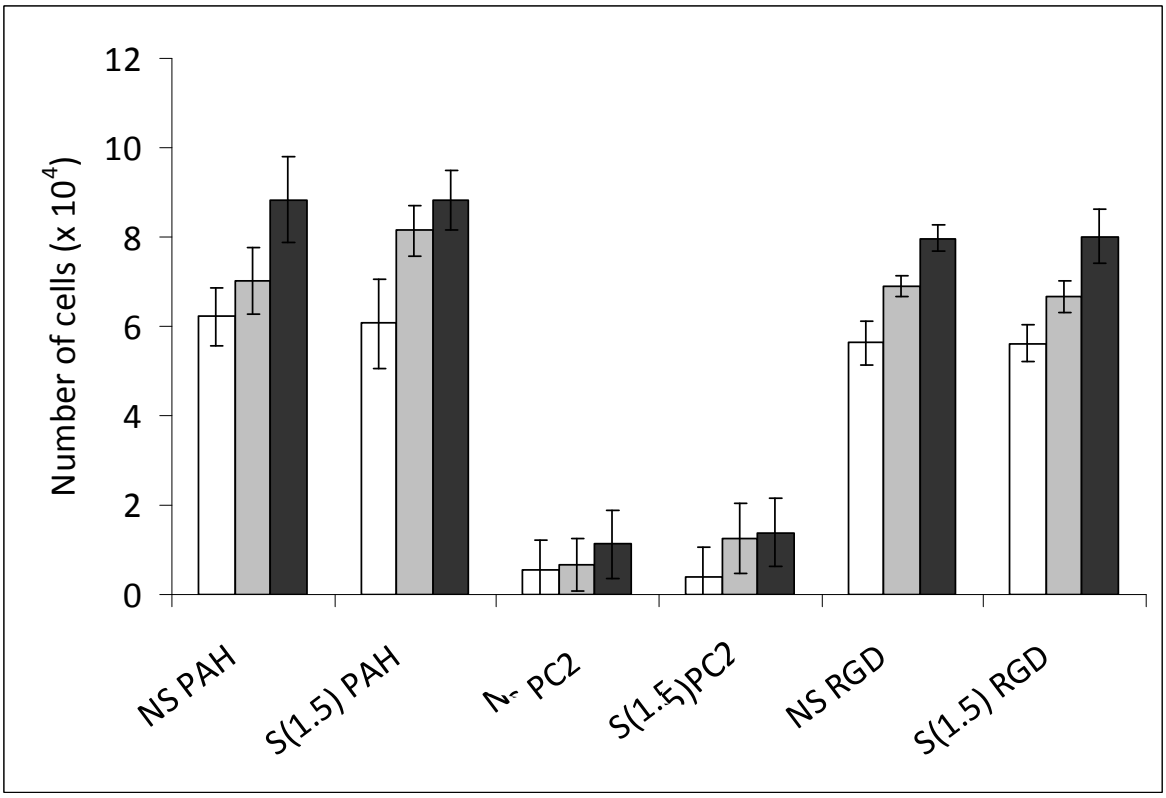

Figure S2. Viability of fibroblasts determined by the AlamarBlue™ test, after 1 day (open bars), 2 days (grey bars) and 7 days (black bars) of culture on different multilayer films built in silicone basins: $(PAH/PSS)_2/PAH$ named PAH; $(PAH/PSS)_2/(PAH/PAA\text{-}PC)_2$ film named PC2 and $(PAH/PSS)_2/PAH/PAA\text{-}RGD$ film named RGD in non-stretched state (NS) and stretched state at 1.5 stretching ratio (S(1.5)).

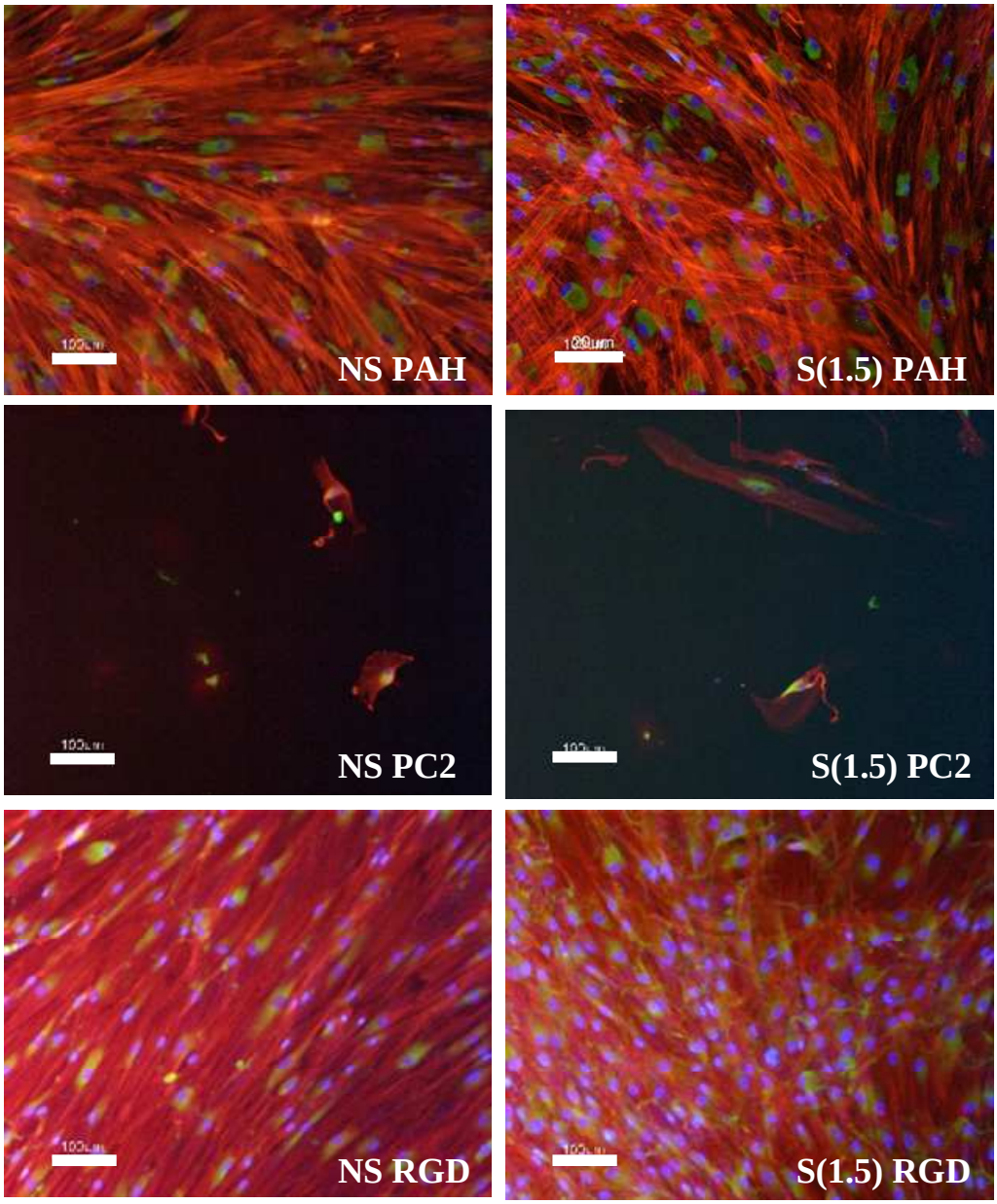

Figure S3. Images of adherent fibroblasts after 7 days of culture on non stretched (left, NS) and stretched (right, S(1.5)) $(PAH/PSS)_2/PAH$ film named PAH, $(PAH/PSS)_2/(PAH/PAA\text{-}PC)_2$ film named PC2 and $(PAH/PSS)_2/PAH/PAA$-RGD films named RGD, built in silicone basins. The stretching ratio was 1.5. Detection of actin markers of the cytoskeleton by phalloidin (red labeling) and collagen type I marker of the extracellular matrix by anti-collagen I (green labeling) by immunochemistry and nuclear marker by DAPI (blue). The scale bars represent 100 µm.

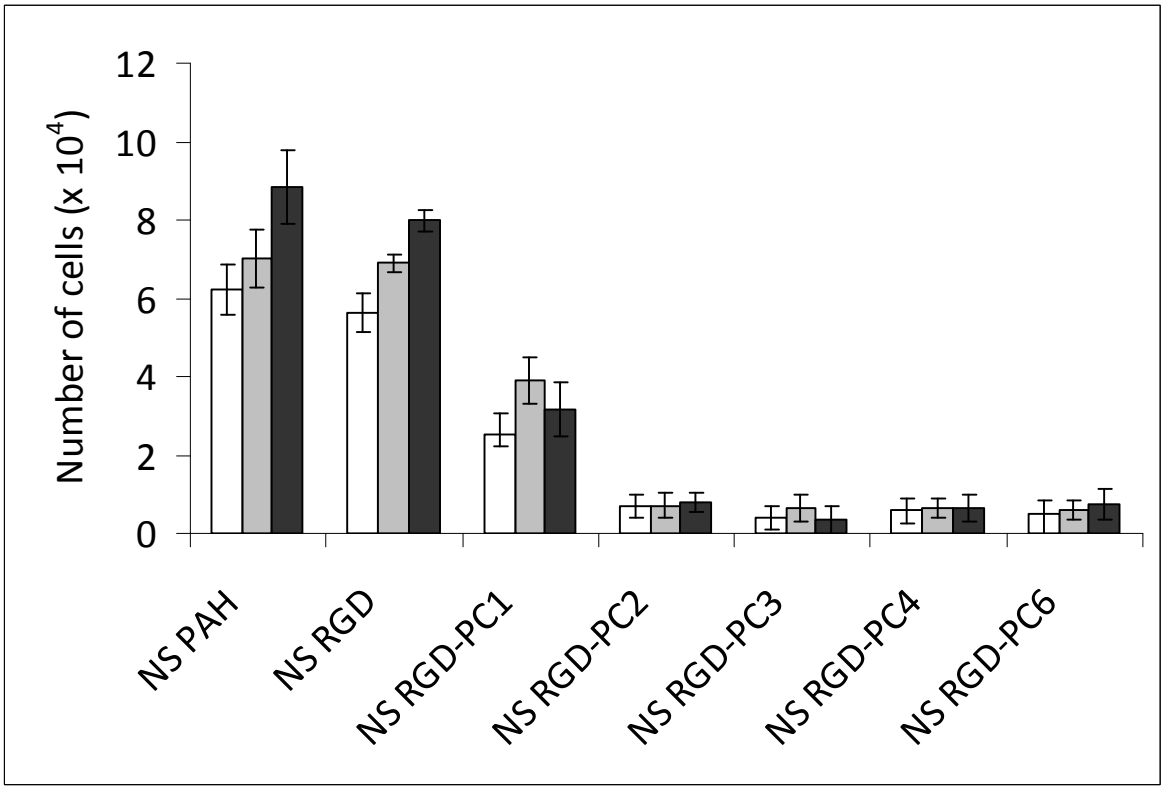

Figure S4. Viability of fibroblasts determined by the AlamarBlue™ test, after 1 day (open bars), 2 days (grey bars) and 7 days (black bars) of culture on different multilayer film built in silicone basins in non-stretched state (NS): $(PAH/PSS)_2/PAH/PAA$-RGD film named RGD, $(PAH/PSS)_2/PAH/PAA$-RGD/$(PAH/PAA\text{-}PC)_1$ film named RGD-PC1; $(PAH/PSS)_2/PAH/$ PAA-RGD/$(PAH/PAA\text{-}PC)_2$ film named RGD-PC2; $(PAH/PSS)_2/PAH/PAA$-RGD/ $(PAH/PAA\text{-}PC)_3$ film named RGD-PC3; $(PAH/PSS)_2/PAH/PAA$-RGD/$(PAH/PAA\text{-}PC)_4$ film named RGD-PC4; $(PAH/PSS)_2/PAH/PAA$-RGD/$(PAH/PAA\text{-}PC)_6$ film named RGD-PC6.

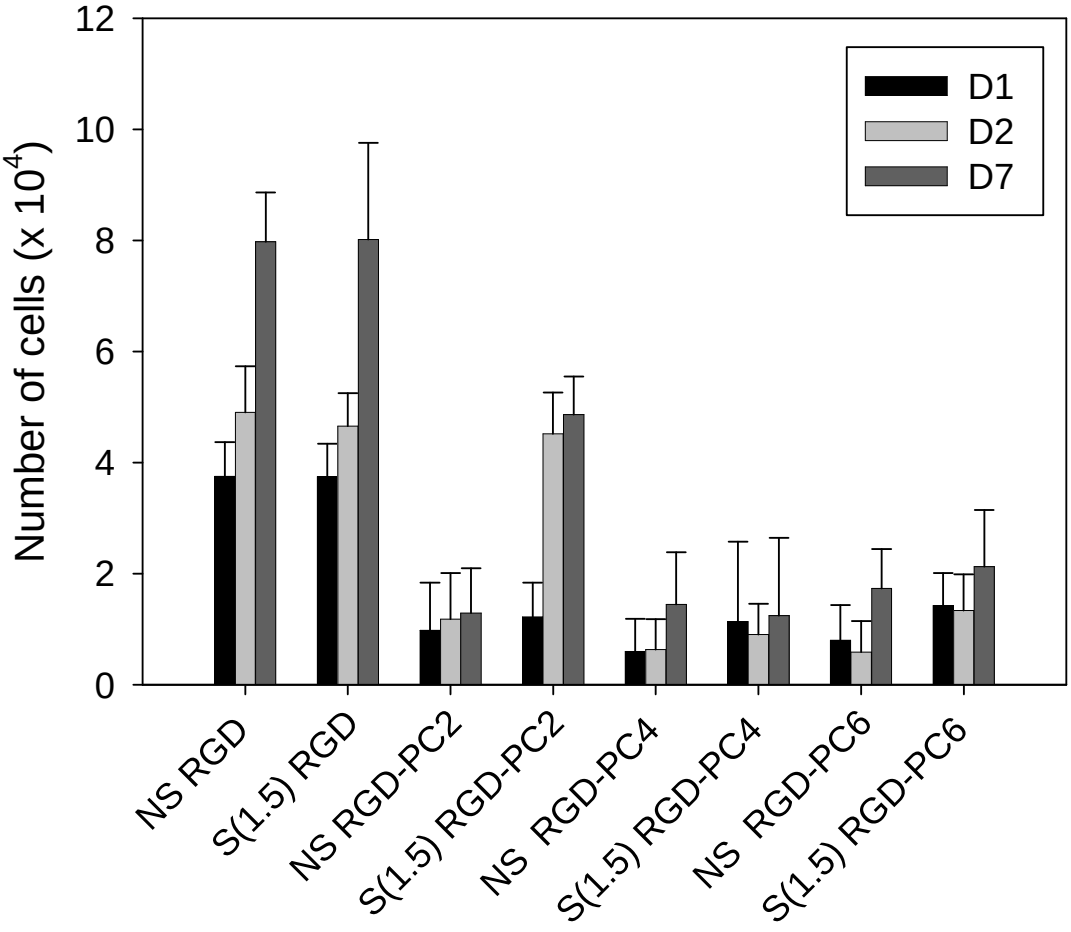

Figure S5. Viability of fibroblast cells determined by the Alamar Blue™ test after 1 day (black bars), 2 days (grey bars) and 7 days (dark grey bars) of culture on different multilayer films built on a silicone basin: $(PAH/PSS)_2/PAH/PAA\text{-}RGD$ film named RGD, $(PAH/PSS)_2/PAH/PAA\text{-}RGD/(PAH/PAA\text{-}PC)_2$ film named RGD-PC2, $(PAH/PSS)_2/PAH/PAA\text{-}RGD/(PAH/PAA\text{-}PC)_4$ film named RGD-PC4 and $(PAH/PSS)_2/PAH/PAA\text{-}RGD/(PAH/PAA\text{-}PC)_6$ film named RGD-PC6 in non-stretched state (NS) and stretched state at an α ratio (S(α)). The data correspond to the mean and the standard deviation of three experiments.

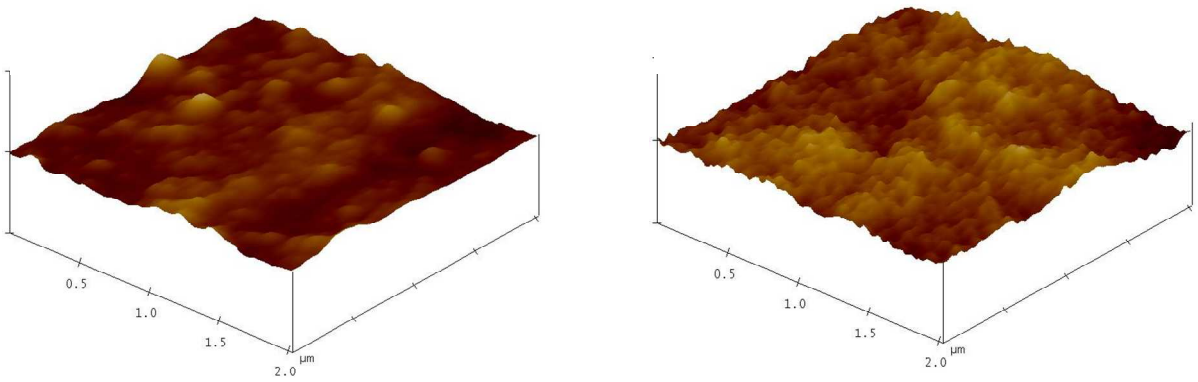

Figure S6. Atomic force microscopy images, obtained in contact mode and in liquid state, of $(PAH/PSS)_2/PAH/PAA\text{-}RGD/(PAH/PAA\text{-}PC)_2$ film (a) in a non-stretched state and (b) in a stretched state at a ratio of 1.5. The z scale is 150 nm.

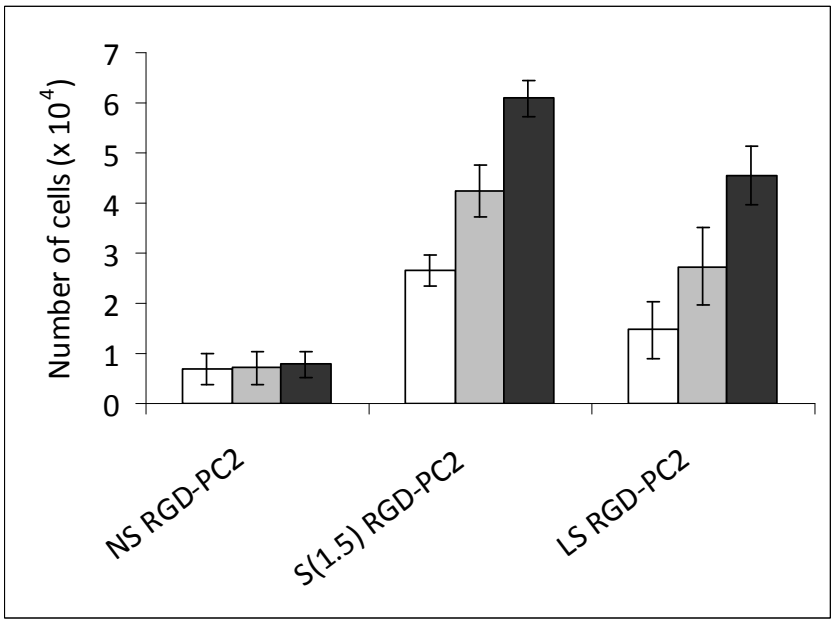

Figure S7: Viability of fibroblasts determined by the AlamarBlue™ test after 1 day (open bars), 2 days (grey bars) and 7 days (black bars) of culture on a $(PAH/PSS)_2/PAH/PAA\text{-}RGD/(PAH/PAA\text{-}PC)_2$ film named RGD-PC2, deposited on a silicone substrate, in the non-stretched state (NS), after stretching at a stretching ratio of 1.5 (S(1.5)) and after stretching at a

ratio of 1.5 for 30 min and brought back in the non-stretched state for 1 hour before the deposition of the cells (LS, i.e. loosened system).

CHAPTER 4:

Associating polymers for therapeutic hydrogels

Goals of the work

This work has been performed in order to design new antibiotic delivery systems to struggle against a pathogenic bacterium: *Pseudomonas Aeruginosa*. This study has been conducted as part of a project supported by the "Association vaincre la mucoviscidose" (beating cystic fibrosis).

Pseudomonas aeruginosa is an opportunistic pathogen, meaning that it exploits some break in the host defenses to initiate an infection. In fact, *Pseudomonas aeruginosa* is the epitome of an opportunistic pathogen of humans. The bacterium almost never infects uncompromised tissues, yet, there is hardly any tissue that it cannot infect if the tissue defenses are compromised in some manner. It causes urinary tract infections, respiratory system infections, dermatitis, soft tissue infections, bacteremia, bone and joint infections, gastrointestinal infections and a variety of systemic infections. Pseudomonas aeruginosa infection is a serious problem in patients hospitalized with cancer, cystic fibrosis,[100] and burns[101]. The case fatality rate in these patients is near 50 percent.

Pseudomonas aeruginosa is primarily a nosocomial pathogen. According to the American Center for Disease Control and Prevention (CDC),[102, 103] the overall incidence of *Pseudomonas-. aeruginosa* infections in U.S. hospitals averages about 0.4 %, and the bacterium is the fourth most commonly isolated nosocomial pathogen accounting for 10.1 % of all hospital-acquired infections. Similar figures are reported in Europe[104] and Africa.[105] *Pseudomonas aeruginosa* has a trend to become drug and multidrug resistant, which worsens the situation.[106]

The goal of this section is the design of drug carrier polymers that can able to form hydrogels under physiological conditions and then this gels can be degraded in the presence of *Pseudomonas aeruginosa*. These bacteria release exoproteins such as lipases. The lipases are able to catalyze the hydrolysis of esters functions in liquid-liquid interface.

For this purpose we have studied associating polymers with a hydrophilic main chain poly(methacrylic acid) (PMA) modified by hydrophobic chains through ester moieties. These polymers are expected to be associating in aqueous solutions. Once the gel is obtained, the hydrophobic parts can be cleaved by the action of the lipases released from the bacteria. The

hydrolysis will be determined by the decrease of the viscosity of the gel and eventually become liquid.

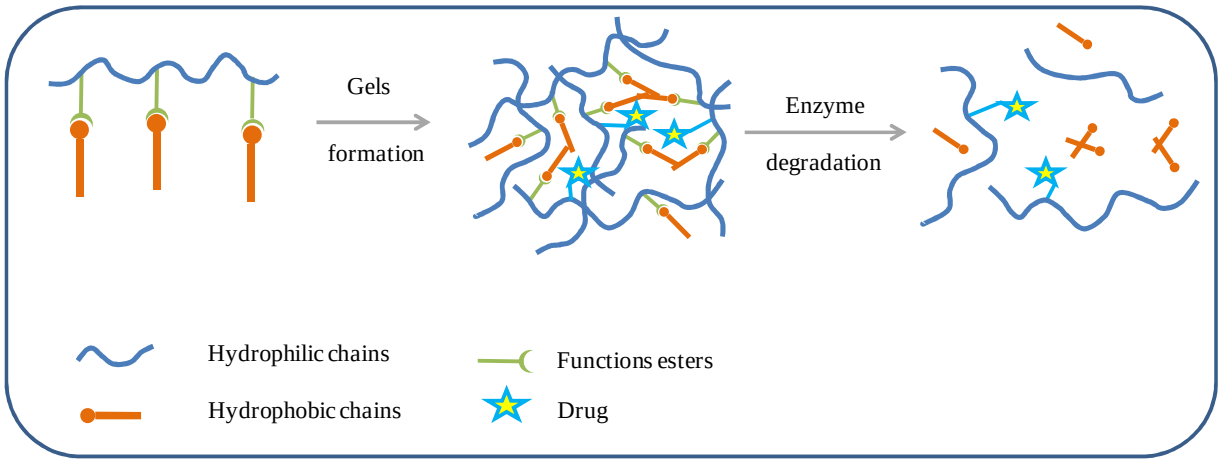

Figure 4. 1. Schemetic illustration of associating polymers.

The targeted material is thus responsive to infections. It is illustrated in Figure 4.1. If a drug is linked to the polymer scaffold, the response will be accompanied by the release of this drug. But this work is limited to the mere associating polymeric system; no drug has been attached to the polymmer.

This bibliographical chapter presents the different key elements to understand the whole design and synthesis of the polymeric material.

In the first part of the chapter will survey the tolerance and toxicity of polyelectrolytes for medical applications, with a focus on poly(methacrylic acid) and poly(acrylic acids). Then we will remind the general structure of associating polymers and the influence of different parameters on their rheological in aqueous solutions. At the end, the acting bacterial enzyme will be briefly presented.

4.1 Relevance and suitability of synthetic polyelectrolytes for biomedical applications

A wide range of polymers has been used for biomedical applications and Table 4.1 gives a summary of the nature of these polymers, classified in biodegradable and non-biodegradable.

Table 4. 1. Representative list of polymers used in drug delivery.

Classification	Polymers
Natural polymers	
Protein-based polymers	Collagen, albumin, gelatin
Polysaccharides	Agarose, alginate, cellulose, chitosan, dextran, hyaluronic acid
Synthetic polymers	
Biodegradable	
Polyesters	Poly(lactic acid), poly(glycol acid), poly(terephthalic acid)
Polyamides	Poly(imino carbonate), poly(amino acid)
Phosphorus-based polymers	Poly(phosphazene), poly(phosphate), poly(phosphonate
Others	Poly(ethylene glycol), poly(dihydropyran), poly (acetal)
Non-biodegradable	
Cellulose derivates	Carboxymethyl cellulose, cellulose acetate, cellulose acetate propionate, ethyl cellulose
Silicones	Poly(dimethylsiloxane), colloidal silica
Acrylic polymers	Poly(methacrylate), poly(methylmethacrylate), poly(hydroxy(ethylmethylacrylate), Sodium polyacrylate and its derivates with n-alkyl chains.
Others	Poly(ethylene-co(vinyl acetate)), poloxamer, poly(vinylpyrrolidone), poly(propylene)

From Table 4.1 it is obvious that most of the polymers used in biomaterials are neutral ones. The charges themselves are absolutely necessary in only a few cases. Transfection vectors for gene therapy need to be polycationic in order to form complexes with DNA strands.[107, 108] Another kind of biomaterials where the charges are needed is the material coating by polyelectrolyte multilayers as studied in the previous chapter.

For other biomedical applications, what is the benefit of charged systems? In the first place, it is expected that highly hydrosoluble polymers like polyelectrolytes were easily excreted via urinary tract. But intraveneous or intraperitoneal administration of high molecular weight sodium polyacrylate causes the death of rat at doses of 25 mg/kg after hypotension, widespread hemorrhages and cardiac arrhythmias.[109] Heavy weight in sodium is the main cause of the cardiac symptoms. Some other effects like depressor effects are explained by the complexation of calcium ions.

Despite this low lethal doses, gels of polyelectrolytes are used as antidhesive materials to prevent post-operation adhesion in abdominal and cardiac surgery.[110, 111] Polyglutamate and polylysine have antiadhesive properties for peritoneal at doses of 1 mg/kg. However this is too

close to their intraperitoneal median lethal dose, ip LD50 (around 40 mg/kg). Polyacrylates have the highest antiadhesive effects, but their LD50 is also low. So the most used polyelectrolytes for this purpose, are NaHA (sodium hyaluronate) and NaCMC (sodium carboxymethyclellulose) that are less toxic since they can be resorbed faster.[112] However these polymers have low antiadhesive activity and must be mixed with low amounts of polyacrylates to increase the performance. [113]

Polyacrylates can be administrated orally with no significant effects.[114] The intraoral median lethal dose i.o. LD50 for polyacrylate is > 40 g/kg, which means that there are not toxic when uptake is oral. Polyacrylates are present in many topical formulations, including cosmetic ones. Numerous toxicological studies have proved that polyanions and polycations do not cause any dermal lesion, irritation or allergy.[115] In conclusion, polyeclectrolytes are seldom used in internal applications, in this case they can be used a low doses (5 mg/kg) mainly because of their chelating properties and high counter-ions content. They are suitable for topical, subcutaneous or oral applications.

Polyelectrolytes are really efficient in mucosal applications because of their mucoadhesive properties.[116, 117] Mucoadhesive polymers are necessary to deliver a drug by mucosal tract (ocular, nasal, buccal or intestinal). They allow to increase the residence times of the drugs in contact with the targeted mucous membrane: they counter the natural clearance. For instance the ocular clearance time is about 90 s and can be increased to 12 h with the suitable polymers in the formulation. Some of those polymers are cationic (PLL, chitosan) or neutral (PVP, HPC). But the majority of these polymers are anionic polymers: alginate, hyaluronic acid, NaCMC. The most used polymers for these formulations are sodium polyacrylate[9] crosslinked with sucrose (Carbomer) or with divinylglycol (Polycarbophil).

Crosslinked weak polyelectrolytes have been used to form stimuli dependant gels. The swelling ratio of the gels strongly depends on the pH. For instance for a polyamine, at pH above the pKa the basic functions are ionized and the gels swells. This has been exploited to make gels that respond to glucose concentration to deliver insulin.[118] Poly(dimethyamino-ethylemethacrylate) gels are synthesized with an enzyme, Glucose Oxidase, and insulin enbedded in the network. The enzyme transforms the glucose into gluconic acid. Therefore when the glucose concentration increases, its degradation in the gels leads to a local acidity, that protonates the polyamine chains, makes the gels swell and release insulin.

This survey has shown that polyelectrolytes are efficient for topical and mucosal delivery. This property can be sought to prevent some nosocomial infections on wound or after surgery. PMA and PAA have always a good activity but their main drawback is their lack of degradability that slows down their excretion. However we have chosen those polymers because they are available and can be easily modified. We also have an experience in their modification for instance our group has been able to modify PAA with PC that are fragile groups with modification rate up to 25 %. In this preliminary work we were interested in proving the validity of our model. The chemistry to target another polymer can always be adjusted in the follow up studies. Another reason for the choice of a non-degradable polymer is to perform the bacterial tests were the degradation of the backbone of the polymer can interfere with the results of the selective degradation of the hydrophobic parts.

For some applications, the polyelectrolytes are often hydrophobically modified to form associating polymers, and to obtain correct gallenic formulation. The next sections recall the structures of associating polymers and the parameters that govern the properties of the resulting hydrogels, before we survey the use of associating polyelectrolytes in biomedical fields.

4.2 Structure of associating polymers

Associating polymers are amphiphilic macromolecules that have a hydrophilic main chain and a few hydrophobic groups. Some of them are called, hydrophobically modified water-soluble polymers (HMWSP) and were introduced in 1951 by Strauss[119] to mimic the conformation of proteins.

In aqueous solution, these polymers present thickening properties: in solution their viscosity is much higher than those of the polymers of the same nature but without hydrophobic part.[120, 121]. This rheological property is caused by intermolecular interactions between the hydrophobic groups. It results in a reversible three-dimensional network that leads to a high viscosity solution and can eventually form hydrogels.

Associating polymers can have the usual topologies of all polymers (linear, brush, star, blockcopolymer, etc). But most of the known associating polymers belong in two large categories, depending on the location of the hydrophobic parts. In the first one, the hydrophobic

parts can be distributed all along the hydrophilic chain and these are often referred as 'multistickers'. In the second one, the hydrophobic groups are located only at the end of the hydrosoluble chains. This is the case of telechelic polymers or triblock copolymers. (Figure 4.2)

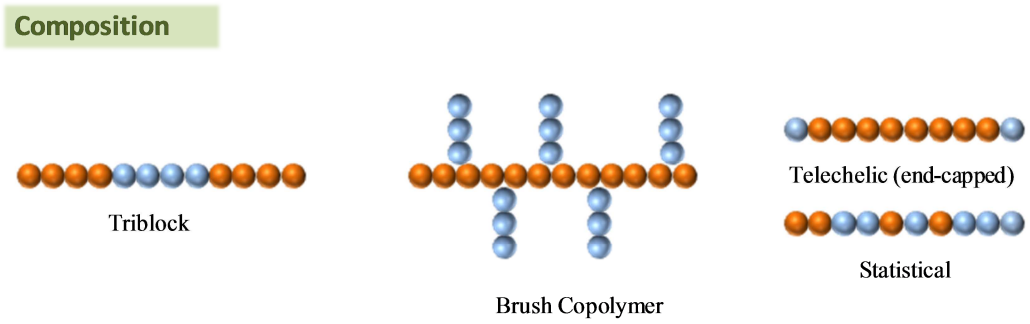

Figure 4. 2. Schematic representation of associating polymers architectures. A: hydrophilic groups (orange), B: hydrophobic groups (bleu).

We will present their chemical structure and when applicable show examples of biomedical use.

4.2.1 Telechelic or end capped polymers and block copolymers

They are linear hydrophilic polymers with hydrophobic group at their ends (end-capped). The hydrophilic backbone generally has low molecular weight (< 100 000 $g.mol^{-1}$). The ends are alkyl chain, comprising 8 to 18 carbons, aromatics groups or fluorinated chains. Usually, these polymers are based upon poly(ethylene oxide) (PEO) with hydrophobic end groups. At the origin, the hydrophobic parts were linked exclusively through urethane spacers[122, 123] and their names HEUR (hydrophobic ethoxylated urethane) originates from this chemistry. Since then polymer with other types of binding between hydrophilic chain and hydrophobic tails have been developed, e.g. ether bounds.[124, 125]

Some block copolymers with hydrophobic and hydrophilic blocks can be considered as an extension of the previous case. An example is PPO-PEO-PPO polymer, where the hydrosoluble poly(ethylene oxide) PEO block is between two poly(propylene oxide blocks (PPO). These polymers have a rather high critical aggregation concentration. They are less used and less known than the Pluronic polymers that have the reverse structure : PEO-PPO-PEO. Pluronics can behave as thickeners but with a different mechanism than the previous associating polymers. They form micelles and depending on the PEO/PPO ratio those micelle can be spherical or

cylindrical. In the last case on obtain gels at concentrations of a few percents. PPO-PEO polymers have high biocompatibility and low immunogenicity and are readily excreted via urinary tract. At higher concentration they form gels when they are heated from room to body temperature, which make them suitable for subcutaneous formation of gels.[126]

4.2.2 Multisticker copolymers

a) Natural polymers derivates

Many multisticker polymers can be obtained from polysaccharides. They are often used in biomedical devices

Some of them are neutral polymers and are obtained by hydrophobic modification of guar, pullulan,[127] dextran [128] or hydrosoluble cellulose derivatives as (hydroxyethyl)cellulose (HEC),[129-141] ethyl(hydroxy-ethyl)cellulose (EHEC), [142-153] and (hydroxypropyl)cellulose (HPC).[154, 155] Charged associating polymers can be obtained from HEC [139] or HPC [156], or from modification of naturally charged polysaccharides such as alginates,[157-162] chitosans,[163, 164] carboxymethylcellulose,[165] carboxymethylpullulan[166] and pectin.[167, 168] The hydrophobic units are usually hydrocarbon alkyl chains or fluorocarbon groups.[169] In order to develop biological applications such as drug release, the hydrophobic parts can be designed to be degradable. This has been done for instance by Durand and coworkers.[170, 171]

b) Polymers based on polyacrylamide

These polymers are copolymers of acrylamide as the hydrophilic monomer and a hydrophobic monomer.[172] *N*,*N*-dimethylacrylamide,[173-175] and *N*-isopropylacrylamide, [176-178] close enough to acrylamide have been also used as hydrophilic monomers. The hydrophobic comonomer may bear a long hydrocarbon chains, an aromatic group (eventually flurescent for photophysical characterization),[178-181] a fluorocarbon group [169, 175, 178] or a siloxan.[182]

Selb and Candau[183] have widely studied hydrophobically modified poly(acrylic acid) and poly(acrylamide). They have shown that micellar copolymerization is an appropriate tool to synthesize long chain hydrophilic polymer and to control the distribution of the hydrophobic chains along the backbone.

c) Thermoresponsive polymers

Poly(*N*-isopropylacrylamide) (PNIPAM) is associating because its low critical solution temperature (LCST) in the range of 25-32 °C in water. Below LCST, the side groups are solvated by water. Above the LCST, the monomers are no longer linked to water, become hydrophobic and tend to link with each other to create crosslinking H-bonds. The same mechanism underpins the formation of gels by Pluronic described above. Because the LCST of pNIPAM is close to the body temperature, they have been widely investigated for drug delivery applications.[184] Poly(*N*-isopropylacrylamide-*co*-methacrylic acid),[185, 186] poly(*N*-isopropylacrylamide-*co*-propylacrylic acid)[187] are able to from hydrogels that are pH and temperature sensitive. Such polymers have been used as carriers for oligonucleotides for gene therapy.[184]

d) Hydrophobically modified polyelectrolyte

One has widely studied polyelectrolytes grafted with hydrocarbon[188] and fluorocarbon.[189-191,192] Usually hydrophobic chains[193] are randomly distributed. These polymers have higher molecular weight than telechelic polymers between (500 000 – 2 000 000 $g.mol^{-1}$).

In 1988, Iliopoulos et al.[189] were the first to report the modification of a polyelectrolyte PAA poly(acrylic acid) with octadecylamine and their viscometric behavior. Then, McCormick and coworkers[194] studied the copolymerization of acrylamide with 0.5 mol % of *N*-[(1-pyrenylsulfonamido)ethyl]acrylamide. These polymers have been extensively used for their thickening properties, in the paper, textile and coatings industries.[195]

In the recent literature Chang et al.[196] studied the free radical copolymerization in aqueous media of methacrylic acid and alkyl methacrylate, with alkyl chain length between 12 and 18 and the mole percentage of the hydrophobic moiety between 0-30 mol %. The hydrophobic domains on the polymer were studied by fluorescence with pyrene as the fluorescence probe. These copolymers show a high potential as drug delivery systems. There are used as polymer-liposomes complexes with phosphatiylcholine/cholesterol to generate liposomes that can respond to 2 stimuli: temperature and pH to deliver drugs.[197, 198]

More complex structures have been developed for biological applications. Copolymers of PAA grafted by (PEO-PPO-PEO, or Pluronic) (PAA-*g*-Pluronic)[199], present better properties than pure pluronic. They have a rapid thermogelation in diluted solutions, and a lower CMC. They have been used as drug carriers in topical, oral[200] and ophthalmologic formulations.[199, 201] They also show bioadhesive properties.[202]

4.3 Structure and physical-chemical parameters that influence the thickening of modified PAA and PMAA

Many studies have lead to a good understanding of the mechanism of associations, and one has clearly established the relationships between the rheological properties, and the different relevant physical parameters or their structural features of associating polymers. The physical parameters are concentration, shear rate and pH. The structural parameters are proportion of the alkyl chains, length of the alkyl chains, microstructure and molecular weight.

4.3.1 Physical parameters

a) Influence of the concentration

The viscosity of solutions of associative polymers strongly depends on the concentration of the polymer. Unmodified and modified polymers have a different behavior when the concentration varies:

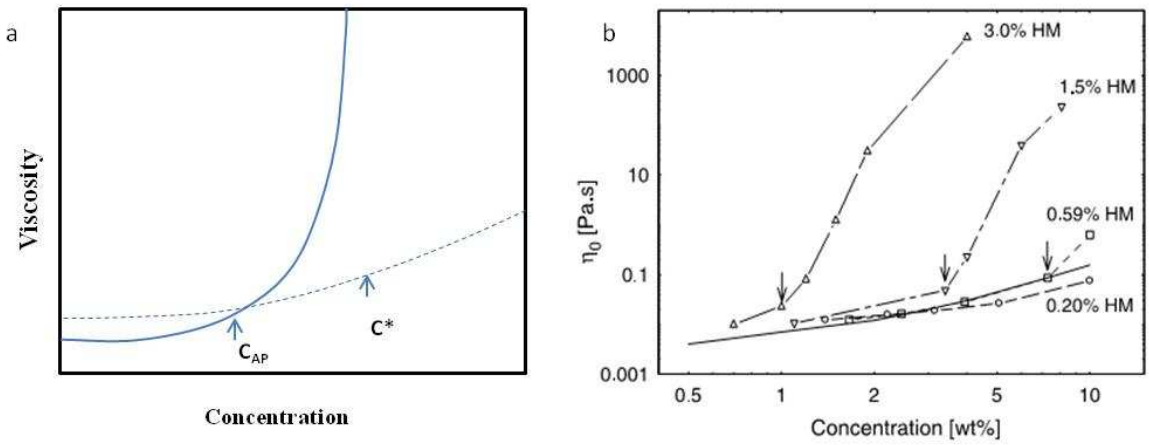

Figure 4.3. Schematic representation of viscosity-concentration relationship. a) Ideal behavior for homopolymer C* (--) and Associating polymer C_{AP} (–). b) Effect of the viscosity-concentration relationship for PAA-C_{18} Mw= 250 000 g/mol, with substitution degree between 0.2-3 mol%. (-) PAA.[203]

In the case Unmodified polymer, the viscosity increase after a critical concentration C*. (Figure 4a). This fact is explained by different concentration regimes : one is called diluted solution when (C < C*) and the second is semi-diluted solution when (C > C*), the transition between two behaviors is defined as critical aggregation concentration C* beyond where the polymer chains are in contact, represented in Figure 4.4.

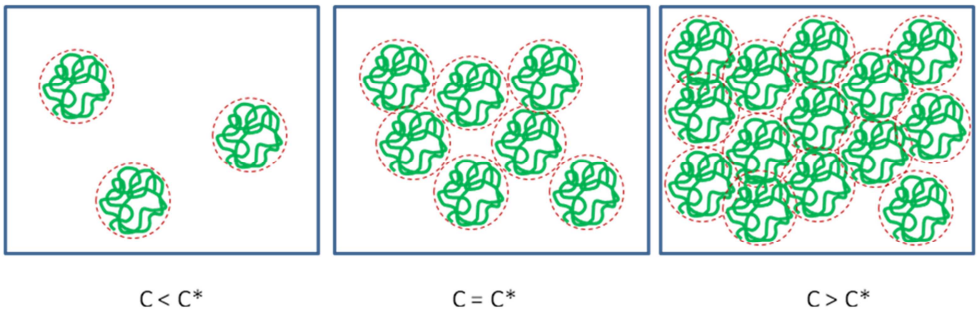

Figure 4.4. Schematic representation of a sketch where the chains are entangled for C > C*.

In the case of modified polymer, Figure 4.3(a) shows that at low concentrations the viscosity is lower than for unmodified polymer. It can be explained by the fact that in diluted solutions, the interactions between hydrophobic units are mostly intramolecular. For a given concentration, called concentration of associating polymer (C_{AP}), the viscosity increases, which is interpreted by the fact that the hydrophobic interactions become intermolecular.[113, 116, 117] C_{AP} is lower than the concentration C^* of the unmodified polymer. (Figure 4.3(a))

In Figure 4.3(b) shows the variations of viscosity vs. concentration for unmodified PAA and PAA modified with C_{18} at different rates.[111] The solid line represents the unmodified polymer (PAA). The polymers with degree of modification between 0.2 and 0.59 % have almost the same viscosity as the homopolymer. For 1.5% modification the viscosity increases at C_{AP} = 3.4 wt % and for higher modification rate (3%) the viscosity increase occurs at a lower concentration C_{AP} (1 wt%). For a given concentration, the more modified the polymer, the more viscous the solution.

b) Influence of shear rate

Figure 4.5 shows the viscosity of hydrophobically modified polymers and the parent homopolymer, when the shear rate increases. The homopolymer behaves as a newtonian fluid, with constant viscosity; for HMWSP the viscosity decreases with shear stress.[183, 204] This effect, called shear thinning effect, increases when one increases either the length alkyl or the molecular weight. In some cases, when the shear rate increases the shear thinning is followed by shear thickening, due to breaking of intramolecular interactions under shear to form more intermolecular interactions.

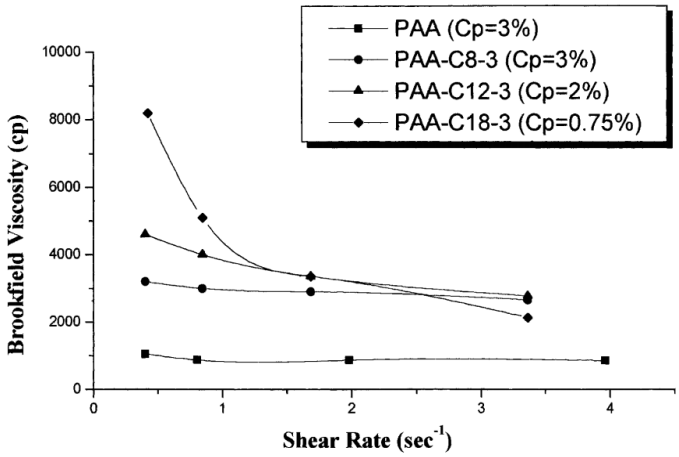

Figure 4. 3. Effect of shear rate on solution viscosity of polymers.[205]

c) pH

pH also influences the viscosity. The Figure 4.6 shows the differences between modified and unmodified PAA. For PAA the viscosity increases when the pH increases and reaches a plateau at pH 7. Above pH 12, the viscosity decreases. At low pH, the polyelectrolyte is only partially charged, and the chain is coiled. As the pH increases more and more acid groups are neutralized and charge repulsion forces the backbone to extend, which increases the viscosity. When the pH is further increased, the excess NaOH increases the salt concentrations and screens the electrostatic interactions, which tends to coil the chains. The curve corresponding to modified PAA with C_{18}-3 mol%, shows that at lower pH, until 6, the viscosity increases, then decreases to be stable stable until pH 12, where more drastic increase occurs. When the pH increases the increasing charge rate on the chain tends to extend the chain but here it is accompanied by the

formation of hydrophobic aggregations that explain the higher viscosity of the modified polymer than that of the unmodified one. When the charge rate increases, the electrostatic repulsions lead both to extend the chains and also induce interactions between chains. When the pH increases above 6 the second effect prevails and the viscosity decreases. It is about constant until pH 12. Above 12 the excess salts screens the electrostatic interactions and makes the hydrophobic interactions prevail again.

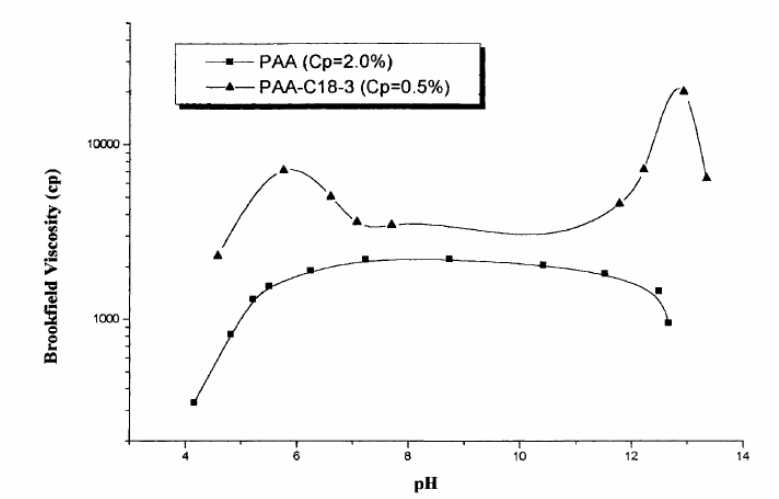

Figure 4. 4. Effect of pH on solution viscosity of PAA and PAA-C18 3mol %.[205]

When the polymer is crosslinked, the degree of swelling can be controlled by pH.[206] Figure 4.7 shows the swelling ratio for different networks of modified and unmodified PAA. When the pH increases the gel swells, because the charges of the backbone create an osmotic pressure. Modified poleleyctrolytes need higher pH to reach a given swelling than the unmodified ones. This pH rises even more when the fraction of hydrophobic units or the length of the alky chain increases. Thus, the hydrophobic modification can tune the swelling pH. At pH values higher than 10 a deswelling is observed, which can be explained by charge screening.

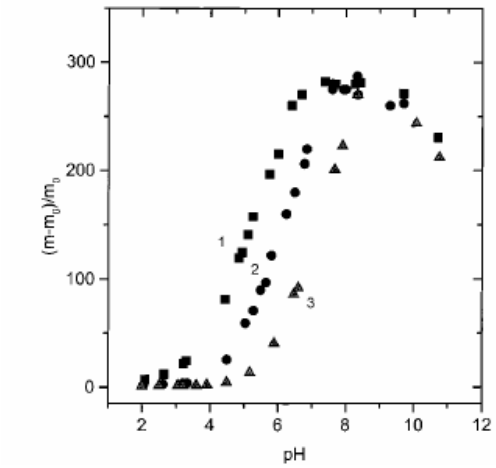

Figure 4. 5. Degree of swelling on the pH of the solution. (1) PAA gel. (2) PAA-C8-5%. (3) PAA-C18-5%.[206]

This sensitivity of these polyelectrolyte networks toward pH has been exploited for oral drug delivery in the gastrointestinal tract. [206, 207] The stomach has an acidic pH (pH of 1-2), while the duodenum has a basic one, so pH sensitive hydrogels can retain the drug in the stomach and release them later in the intestine. Poly(methacrylic acid-g-ethylenglycol) hydrogels are able to incorporate and protect the insulin from release in acidic media. Under acidic environments the hydrogel forms intermolecular associations and the release of the drug occurs when the gel swell at alkaline conditions in the intestine.[208]

4.3.2 Structural parameters

a) Influence of the proportion and length of alkyl chains [203, 207, 209]

These parameters are really important in these systems. The introduction of hydrophobic units onto the hydrophilic backbone, should increase the thickening properties, but maintaining the solubility in aqueous solutions. There is a range of optimal modification between the competitions of inter and intra molecular associations to get a polymer with excellent rheological properties. Figure 4.8 represents the influence of the nature of the alkyl chains on the viscosity. Its shows that viscosity increases when the length of the hydrophobic groups increases.

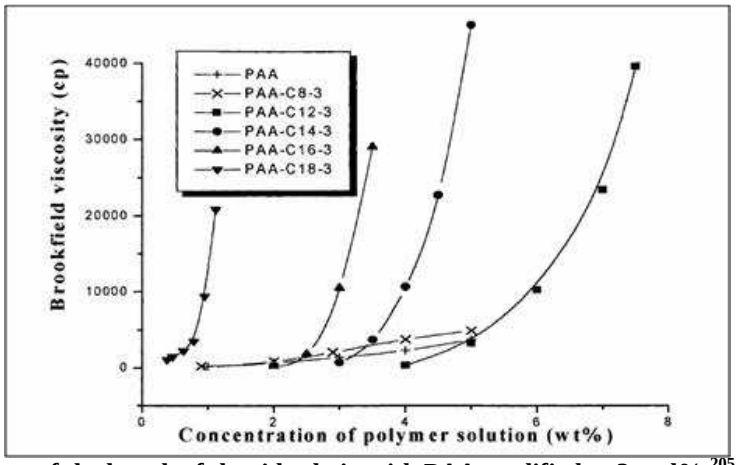

Figure 4. 6. Effect of the length of the side chain with PAA modified at 3 mol%.[205]

The higher the hydrophobic content of the polymer, the lower the concentrations needed to increase the viscosity. The minimal size of hydrophobic groups necessary to increase the viscosity of the modified polymers is 12 or 14 of carbon atoms.[205, 210, 211]

b) Influence of the microstructure

The distribution of the hydrophobic groups affects the properties in aqueous solution. Magny et al.[211]studied the PAA modified with (C_8, C_{12} and C_{18}), resulting in polymers with random and block structure. The higher associating properties were obtained by block copolymers. The same behavior was observed by Volpert et al. by acrylamide polymers modified with alkyl acrylamides (1-5 mol%).[183]

In conclusion, this survey of the literature shows that associating polyelectrolytes can be used for biomedical applications, although the applications are still rare. These polymers are more widely used in other fields : adhesives, adsorbents and paint adjuvants.[212] In the medical field,, they are efficient in formulations that are close to the coating applications, like bioadhesives, wound dressing mucoadhesives. Their behavior vary strongly with different parameters such as temperature or pH, which is an asset to elaborate systems able to respond to temperature or pH. Another advantage is that their behavior has been studied in depth by physicochemists and this knowledge is a sound frame to design new materials from them.

4.4 Biological target: *Pseudomonas aeruginosa* and its lipase

When bacteria infect a tissue, they release exoproteins,[213] which means proteins that are excreted in the extracellular medium. These proteins include hydrolytic enzymes, such as elastases (LasA and LasB), an alkaline protease and a phospholipase. These proteins are virulence factors: they break down the physical barriers by lysing tissues and damaging host cells. Elastase also lyses fibronectin to expose receptors for bacterial attachment on the mucosa of the lung. It disrupts the respiratory epithelium and interferes with ciliary function. Alkaline protease interferes with fibrin formation and will lyse fibrin. Together, elastase and alkaline protease destroy the ground substance of the cornea and other supporting structures composed of fibrin and elastin. Phospholipase is responsible for hemolysis. The virulence factors are therefore responsible for the symptoms associated to the infectious diseases. Lipase is also one of the exoproteins that are present during infection and interferes with the release of inflammatory mediators.[214]

Virulence factors are exoproteins and are therefore suitable targets for our purpose, since the bacteria spontaneously export them in the extracellular medium.

Lipases are enzymes that catalyze the hydrolysis of esters. Esterases are able to catalyze the same reaction, but the distinction is done according the nature of the substrates: esterases hydrolyze soluble substrates whereas lipases act on insoluble substrates. Lipases are also named triacylglycerol hydrolases in reference to the hydrolysis of triglycerides represented in Scheme 4.1.

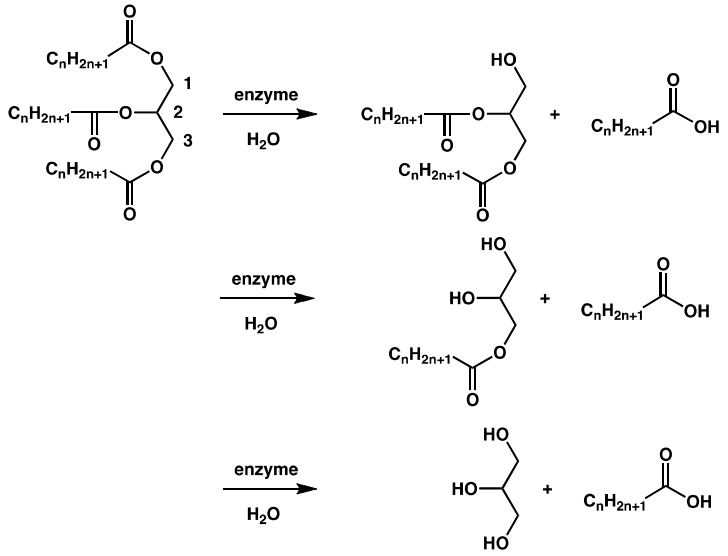

Scheme 4. 1. Hydrolysis of triacylglycerol.

The active site of the lipases comprises three aminoacids that form the catalytic triad encountered in most hydrolases : Aspartic acid, Histidine and Serine. Because of this catalytic triad the lipase belongs in the family of the serine hydrolases. The enzyme proceeds through a transesterification as a first step to yield an acyl-serine intermediate. The alcohol is released in this first step, while the acyl part is covalently bound to the serine. In a second step, the acyl-enzyme complex is hydrolyzed, more slowly, to release the acid.

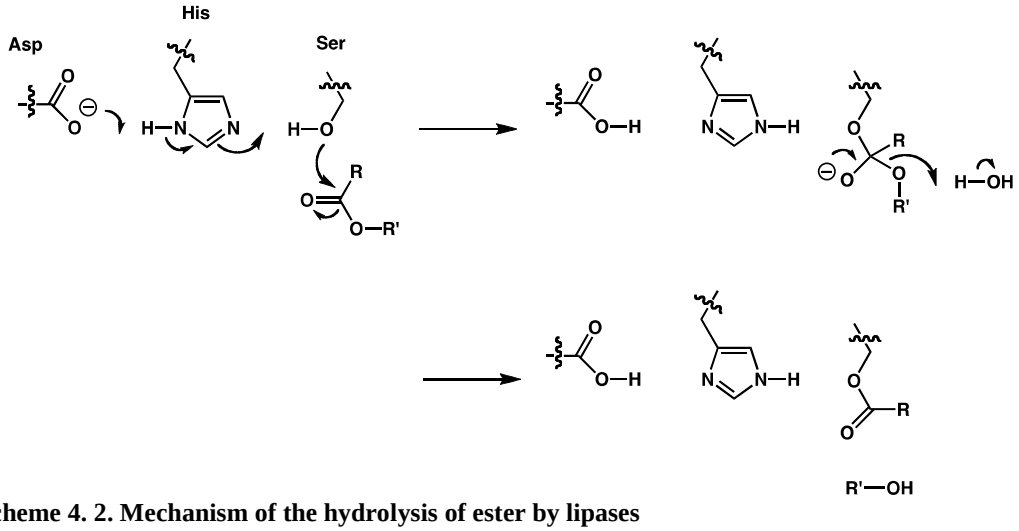

Scheme 4. 2. Mechanism of the hydrolysis of ester by lipases

Unlike other enzymes that are very substrate-specific, the lipases have a rather wide range of substrates. They can easily degrade triglyceride, preferentially with short chains C_{12} and with a slight preference for the 1-3 esters over the 2 ester.[215]

The hydrolysis of fatty acid esters is also catalyzed by this enzyme. This hydrolysis of *p*-nitrophenol (*p*-NP) ester is also the basis of a colorimetric assay. *p*-NP has a UV-spectrum that is different from the starting ester, which allows its titration when its released by hydrolysis. Thanks to this test, the activity of the enzyme toward several *p*-NP is known. The rate of hydrolysis increases when the length of the fatty chains increases, reaches an optimal activity and finally decreases when the ester length further increases. The optimal length has been found of 10-12 carbons for many strains,[216] but can be higher for other strains.[217] But the activity is still appreciable for chains longer than this optimum.

From the survey of this properties, it is worth testing synthesizing simple associating polymers having hydrophobic chains linked through ester to the main hydrophilic chain. In the usual associating polymers, the hydrophobic chains are n-alkyl chain with lengths comprized between 12 and 18 C. The low selectivity of this enzyme makes it possible to accept substrates like modified polymers. Since lipase is an exoprotein it is ideal for our goal: it will get into contact of the gel and it will signal the presence of the bacteria.

4.5 Conclusion

To reach our goal we have chosen polyelectrolytes because these are polymers that are strongly hydrophilic and because we have the know-how in their functionalization. Beyond these practical reasons, some other consideration make them attractive: they show good performance in all topical and oral drug delivery systems; they can be easily functionalized, both with hydrophobic parts, and with drugs (for future studies); their behavior is well documented in the literature.

The design that can be done for the target polymers is guided by the literature: one needs to link short alkyl chains (C12 to C16) to the main chain. The link needs to be an ester. The viscosity can be tuned either by the length of the hydrophobic parts or the modification ratio. The

next chapter develops in details the synthesis of those polymers, the study of their rheological properties in presence and in absence of lipase.

CHAPTER 5:

Synthesis and use of associating polymers for enzymatically responsive gels

The first part of this chapter describes the synthesis and the characterization of the studied polyelectrolytes. The second part, describes the formation of the gels from these polyelectrolytes and a detailed study of their rheological behavior in relation with the different structural parameters of the polymers. In the last part, the degradation of the gels under enzymatic conditions was studied by rheological measurements. Finally, we tested the degradation by cultures of *Pseudomonas aeruginosa*.

The associating polymers that we have chosen for the studies are the copolymers of methacrylic acid and alkyl methacrylate shown Figure 5.1. As discussed in chapter 1, these copolymers were selected because the ester chains can associate under physiological conditions inducing the formation of gels. Magny et al.[211] and Zhuang et al.[205] demonstrated that alkyl chain with a minimum of 12 carbons are necessary to enhance the viscosity solutions. We have selected alkyl chains with C_{12} and C_{18}. We have considered a third monomer, MBL, to insert a spacer between the cleavable ester and the hydrophilic chain. This was designed to offer the enzyme a better access to the cleavable site and to move it apart from the hydrophilic chain. The structures are illustrated in Scheme 5.1.

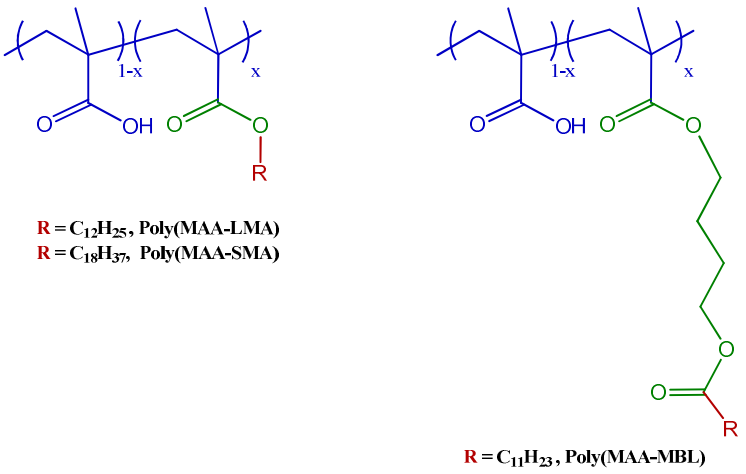

Scheme 5. 1. Structure of amphiphilic copolymers.

We shall remind here that the goal of the work is to investigate whether the gels can be degraded by enzymatic cleavage of their esters moieties, as represented in Figure 5.1.

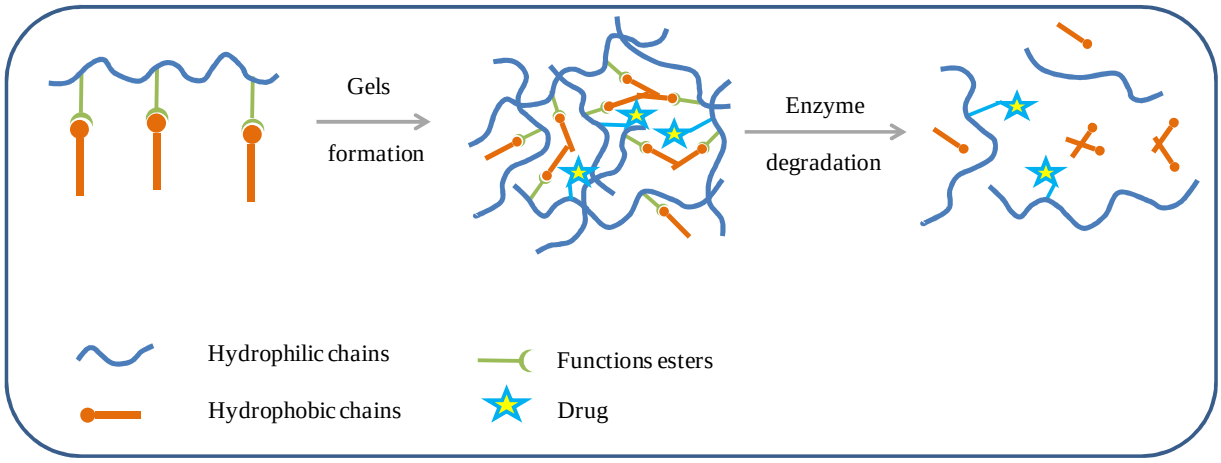

Figure 5. 1. Schematic representation of the formation of gels and degradation.

5.1 Synthesis and characterization of the copolymers

5.1.1 Choice of the synthetic route

Anionic polymerization of methacrylaytes is possible but difficult to set-up and gives high polydispersity.[218] This is because the active centers in anionic polymerization reacts with the ester carbonyl group in competition with the Michael addition to the conjugated double bond. This side reaction forms enolates and diminshes polymerization yields.[219] Well-defined block methacrylate copolymers can be obtained by atom transfer radical polymerization (ATRP) and reversible addition fragmentation chain transfer (RAFT) techniques. These polymerizations maintain a relatively narrow molecular weight distribution ($Mn/Mw < 1.5$).[220] However, the copolymerization of carboxylic acid monomers by ATRP is still complicated, because the acid monomers can poison the catalyst by coordination to the transition metal.[220] In addition the molecular weight obtained by these techniques does not exceed 10^3 $g.mol^{-1}$, which is not sufficient to obtain gels.

Chang and coworkers[196] reported the free radical copolymerization in ethanol of methacrylic acid and *n*-alkyl methacrylate in C_{12} and C_{18} with proportions of the hydrophobic moiety between 0 and 30 mol. % (Scheme 5.2). They have estimated the molecular weight and polydispersity index by size exclusion chromatography (SEC) in THF through a conventional calibration with polystyrene standards. As an example, for the copolymer with 5 mol % of C_{12},

they have obtained the following characteristics: *Mw* = 11 200 and polydispersity index (PDI) of 1.47.

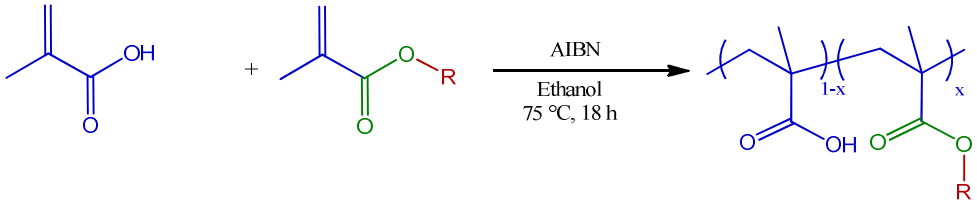

Scheme 5. 2. Copolymerization of methacrylic acid with lauryl methacrylate. R = $C_{12}H_{25}$.[196]

We have followed the same procedure with methacrylic acid and lauryl methacrylate (C_{12}) (5 mol %) but in dioxane at 60 °C. In our hands, the final copolymer showed a molar mass *Mw* = 152 000 and PDI = 2.7. So we obtained copolymers with higher molecular weights but also with much higher polydispersity than reported in the literature.

We have tried another route : the free radical copolymerization of *tert*-butyl methacrylate and *n*-alkyl methacrylate. The literature reports that associating copolymers can be synthesized from monomers with protected acid groups. The protecting groups used for this purpose are *tert*-butyl,[221, 222] benzyl[223] and oxazoline[224] groups. The *tert*-butyl group is widely used as a protecting groups in anionic[225] and both free and controlled radical copolymerization. It can be cleaved easily by acidic treatment to yield the hydrophilic segments of methacrylic acid (MAA).

We have hence developed a synthesis of our associating copolymers in two steps as described in Scheme 5.3. The first one is the copolymerization of alkyl methacrylate with the *tert*-butyl methacrylate. Both monomers are hydrophobic during this step. The second step is the hydrolysis of *tert*-butyl groups to form the hydrophilic parts and afford amphiphilic macromolecules.

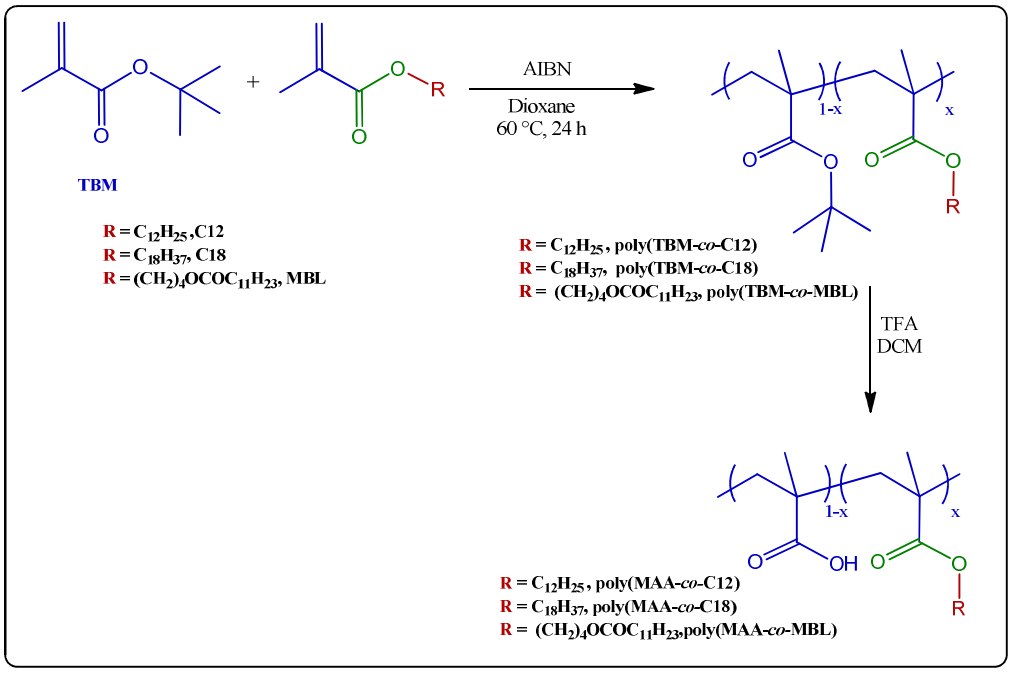

Scheme 5. 3. Scheme of synthesis of the associative copolymers. $_X$= 1, 5, 10.

The copolymerization and homopolymerization of *tert*-butyl methacrylate[226, 227] and *n*-alkyl-methacrylate[220, 228, 229] with different monomers have been described in the literature with success in almost all methods of controlled radical polymerization. But the free radical copolymerization of *tert*-butyl methacrylate (TBM) with lauryl methacrylate (C12), stearyl methacrylate (C18) or methacryloyloxybutyl laurate (MBL) is not reported in the literature. However, we were interested only in obtaining rapdly the targeted amphiphilic polymers to study their degradation. Therefore we have tried only classical radical polymerization with those monomers.

5.1.2 Synthesis of copolymers poly(*tert*-butyl methacrylate-co-*n*-alkyl methacrylate)

We will discuss the three steps of the synthesis of the polymers (Scheme 5.3): (i) synthesis of monomers; (ii) free radical copolymerization between *tert*-butyl methacrylate and *n-alkyl* methacrylate; (iii) hydrolysis of *tert* butyl groups.

Three of the selected monomers are commercial available: TBM, C12 and C18. The fourth monomer MBL was synthesized as described below.

a) Synthesis of MBL

This monomer was synthesized in two steps (Scheme 5.4). The first one was the mono-esterification of 1,4 butanediol with dodecyl chloride to obtain **1**. This step has been completed without protection-deprotection steps and the yield of 40 % nears the maximal statistical yield of 50 % that can be obtained. The second step was the acylation with methacryloyl chloride. The purification of this last product was difficult due to the presence of unidentified vinylic impurities and necessitated chromatography, so the scale of the synthesis is limited to the order of the gram.

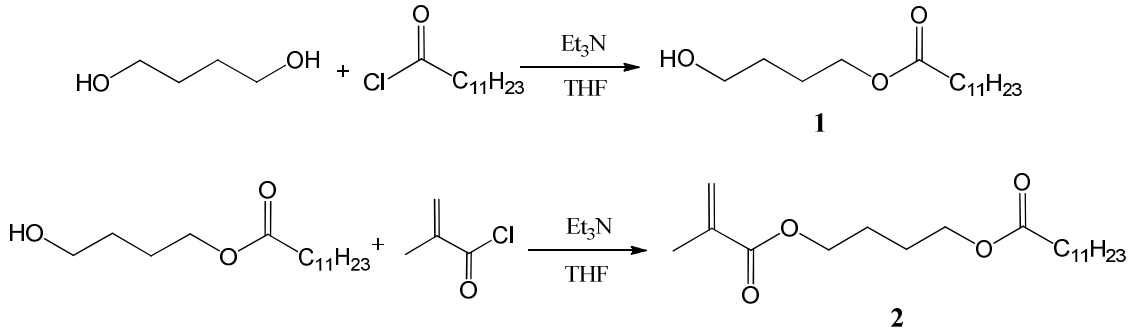

Scheme 5. 4. Synthesis of the monomer MBL (methacryloyloxybutyl laurate).

b) Synthesis and characterization of poly(TBM-co-n-alkyl methacrylate)

(i) Copolymerization

The copolymerization between *tert*-butyl methacrylate and the *n*-alkyl methacrylates is illustrated Scheme 5.5.

In a preliminary study, the quantity of initiator was varied from 0.01 to 0.1% with respect to the monomer. The quantity of 0.05 % of AIBN was found optimal to obtain higher molecular weight and narrower polydispersity. The copolymerization proceeds with yields above 75% after purification.

The copolymers were synthesized with different proportions of *n*-alkyl chains, in order to study the influence of the hydrophobic content on the final copolymers. The feed proportions were with 1, 5 and 10 mol %.

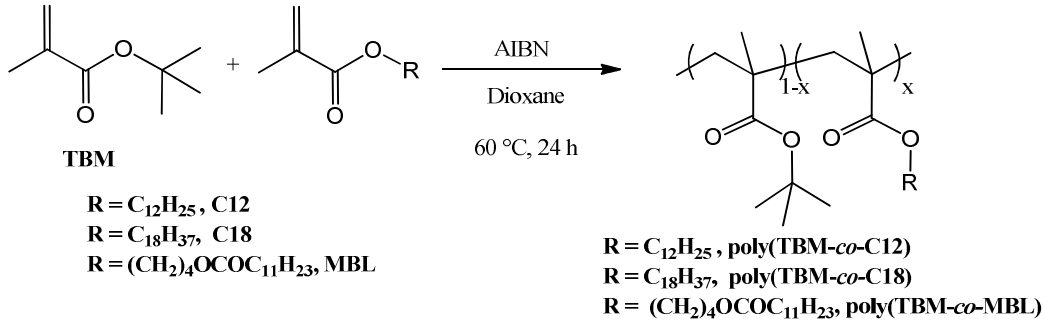

Scheme 5. 5. Free radical copolymerization of poly(TBM-*co*-*n*-alkylmethacrylate)

(ii) Determination of the proportion of n-alkylchains

The chemical structure and the composition of the copolymers were determined with NMR by three methods:

• **by ^{1}H NMR** (Figure 5.2) from the integral ratios of the signals of $–OCH_2$ at (δ = 3.9 ppm, H_d) and -C-CH_2-C- at (δ = 1.8 ppm, H_c). The results are reported in Table 5.1. The signal corresponding to *tert*-butyl groups in ^{1}H NMR is difficult to integrate, because it overlaps the signals of the alkyl chain. For this reason, we have sought other methods to measure the ratio of alkyl chains.

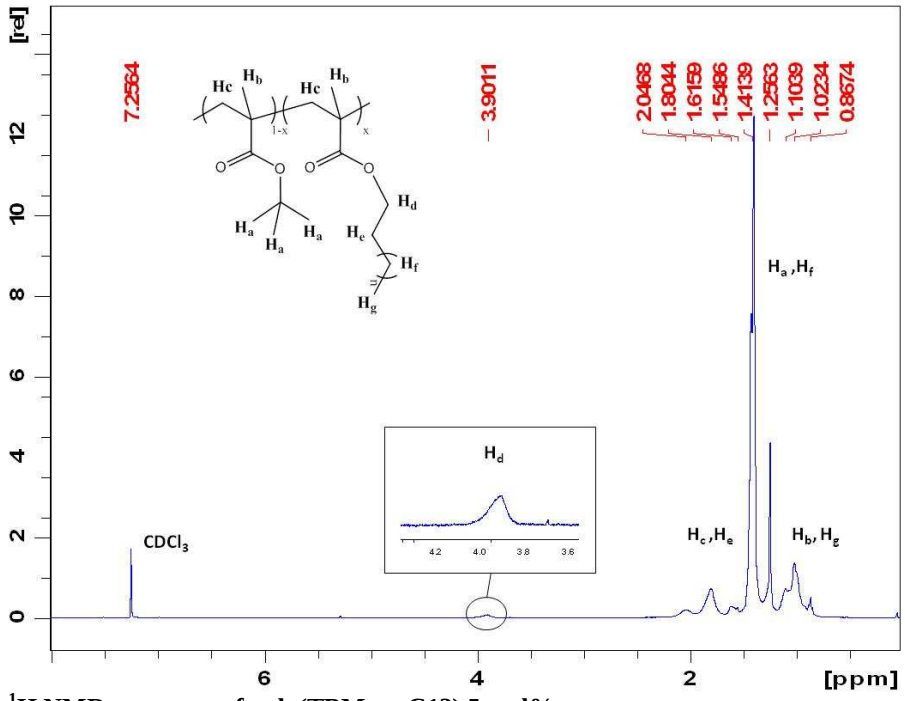

Figure 5. 2. ^{1}H NMR spectrum of poly(TBM-*co*-C12) 5 mol%.

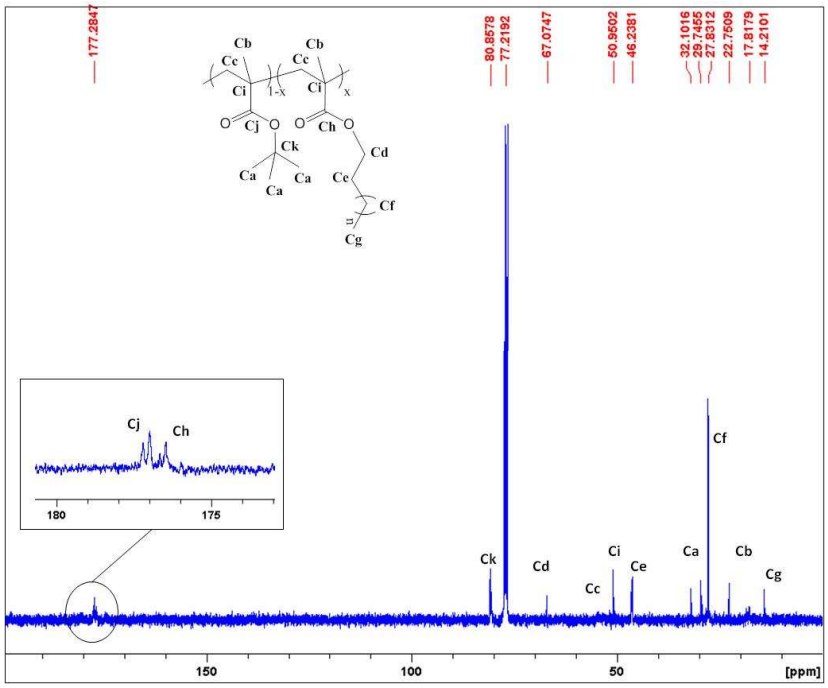

Figure 5. 3. ^{13}C NMR spectrum of poly(TBM-*co*-C12) 5 mol%.

• **by ^{13}C NMR**. The *n*-alkyl proportion was measured by the integrations of the peaks of the quaternary carbon of TBM –C(CH_3) (δ = 80.8 ppm, C_k) and the methyl group of *n*-alkyl

chain (δ = 14.2 ppm, C_g). The differences with the previous the results are due to the uncertainties that are inherent to each method. ^{13}C NMR is less sensitive than ^{1}H NMR, but the largest uncertainty comes from the intensities of the peaks that depend on the relaxation times. Since we compare carbon with different parities, their relaxation times are too different. Therefore ^{13}C NMR to determine the composition of the copolymer was not satisfactory either. (Figure 5.3)

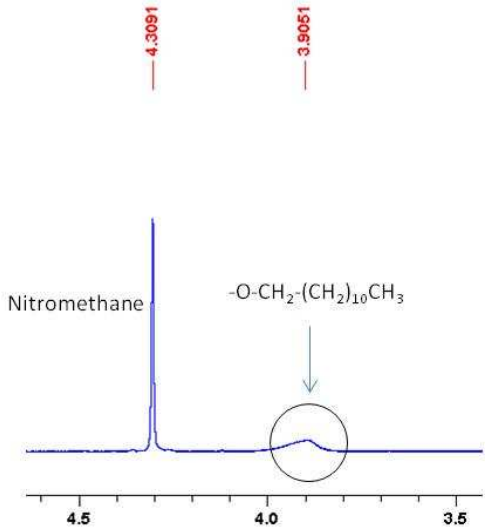

Figure 5. 4. ^{1}H NMR spectrum of poly(TBM-*co*-C12) 5 mol% using nitromethane as standard.

• **by ^{1}H NMR with nitromethane as an internal reference.** The spectra were taken with known amounts of the copolymer and nitromethane. (Figure 5.4). The molar ratio of the comonomers is calculated from the integration ratios of the peak corresponding to $–OCH_2$ (δ = 3.9 ppm, H_d) to the peak of nitromethane (δ = 4,3 ppm). This method proved to be more efficient than the others, because the peak of the nitromethane is not superimposed to any peaks of the polymer.

FTIR is usually more sensitive and could have been an alternative to determine the copolymer composition. But for the synthesized polymers it was not possible because of the signal superposition of both monomers.

The synthesis conditions and the resulting characteristics of the new copolymers are summarized in Table 5. 1.

Table 5. 1. Composition of the copolymers.

Feed ratio of the monomers	Yield (%)	ratio[a] by 1H NMR	ratio[a] by ^{1}H NMR (nitromethane)	ratio[a] by ^{13}C NMR
poly(TBM-*co*-C12)				
99/1	94	5	0.5	2
95/5	87	6	8	6
90/10	84	12	10	14
poly(TBM-*co*-C18)				
99/1	89	1	2	3
95/5	81	5	3	6
90/10	87	10	7	13
poly (TBM-*co*-MBL)				
99/1	73	2	2	1
95/5	76	6	5	6

[a] **ratio of the alkyl chain**

(iii) Characterization of the molecular weights

In order to determine the molecular weight of the polymers, we have analyzed them by SEC coupled with a differential refractometer and a multi angle light scattering (MALS) detectors.

Figure 5.5 shows the superimposed refractive indexes curves of poly(TBM-*co*-C18) with 1, 5 and 10 mol % of alkyl chains. The chromatograms were obtained in THF as eluent. They showed a monomodal distribution. The molar masses of the polymers were first determined from the conventional calibration using poly(methylmethacrylate) (PMMA) as standards. (Table 5.2)

Molar masses were also measured from MALS data. The differential refractive index increment dn/dc was calculated from the data of the refractive index detector at 100 % of mass recovery, and was found equal to 0.077 (mL/g). The resulting weight average (M_w) molecular weights, number average (M_n) molecular weights and polydispersity indices (PDI = M_w/M_n) are tabulated in Table 5.2. Both SEC methods, conventional calibration and SEC-MALS give similar results. MALS gives slightly higher *Mn* and lower PDI values than conventional calibration, which is usually observed since MALS underestimates the lower masses. In this work we take in consideration the values corresponding to MALS. Indeed SEC measures hydrodynamic volumes by comparison to a standard while MALS directly measures the molar mass of the polymer.[230]

Table 5. 2. Physical properties of the copolymers measured by SEC.

Feed ratio of the monomers	SEC					
	Conventional calibration			MALS		
	Mw	***Mn***	**PDI**	***Mw***	***Mn***	**PDI**
poly(TBM-*co*-C12)						
99/1	227 000	115 000	1.98	193 400	119 400	1.65
95/5	199 300	96 000	2.08	247 300	139 100	1.77
90/10	290 000	154 700	1.87	273 000	160 800	1.69
poly(TBM-*co*-C18)						
99/1	143 400	91 600	1.57	148 300	102 600	1.45
95/5	265 400	116 500	1.82	298 700	140 200	1.75
90/10	309 900	109 700	2.36	343 000	178 700	1.92
poly(TBM-*co*-MBL)						
99/1	262 000	165 600	1.58	220 500	166 700	1.32
95/5	208 000	126 000	1.65	237 000	135 900	1.74

The PDI of some sample is amazingly low (1.5) given the unsophisticated polymerization process we used.

In conclusion this technique affords copolymers with higher molecular weight than by controlled radical polymerization and yet with moderate polydispersity (PDI < 2.1).[231 232]

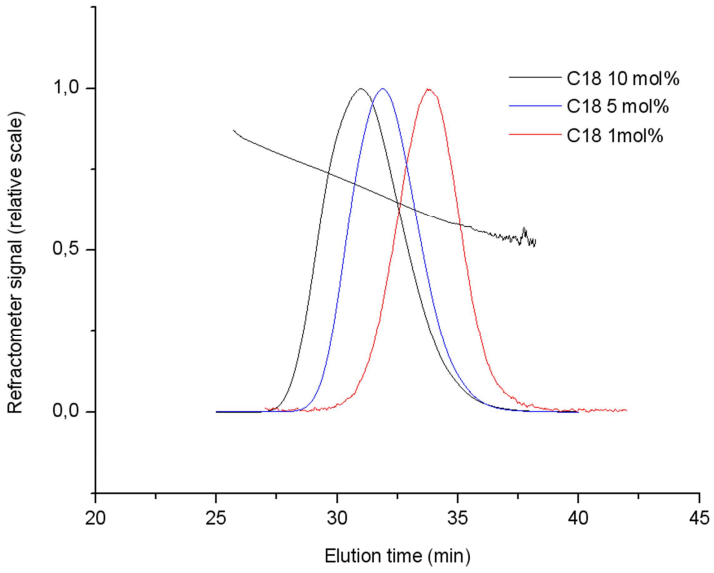

Figure 5. 5. SEC-refractive indexes traces of poly(TBM-*co*-C18).

c) Hydrolysis of tert*-butyl group to obtain poly(MAA-*co*-n-alkyl methacrylate)*

(i) Conditions and chemical characterization

The hydrolysis of *tert*-butyl groups has been widely reported in the literature with 4 M HCL solutions in dioxane,[231, 233] but this method was not successful for our polymers since beside the *tert*-butyl groups, it also hydrolysed part of the *n*-alkyl esters. The effective and selective hydrolysis of the *tert*-butyl groups was achieved with trifluoroacetic acid (TFA) during 18 h in dichloromethane at room temperature. [234, 235] TFA did not hydrolyze the primary esters. This procedure yields the expected poly(MAA-*co*-*n*-alkylmethacrylate) (Scheme 5.6). The yields are higher than 92%.

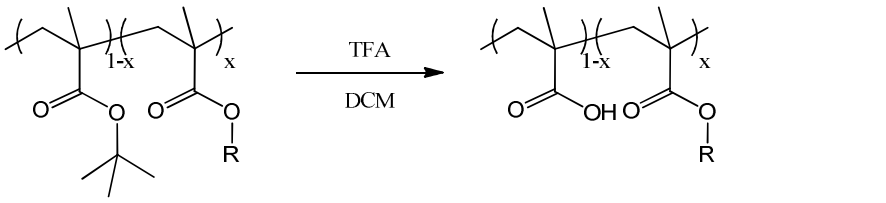

Scheme 5. 6. Hydrolysis of *tert*-butyl groups.

(ii) Characterization of the chemical structure

The analysis by ^{13}C NMR of poly(TBM-*co*-C12) shows the disappearance of the signals of the quaternary carbon and of the methyl in the *tert*-butyl groups (Figure 5.7). The *n*-alkyl esters are not hydrolyzed since the resonance peak of $-(CH_2)_n-$ protons remains at 1.33 ppm in ^1H NMR spectrum. The area of this peak was not diminished by increasing hydrolysis times.

The FTIR also corroborated the hydrolysis of the *tert*-butyl groups. Figure 5.6 shows the spectra of a copolymer before and after hydrolysis. After hydrolysis, it presents all characteristic bands of COOH: 3179 cm^{-1} broad (OH stretching), 2670 cm^{-1} (overtone and combinations) and 1697 cm^{-1} (C=O stretching of H-bonded COOH). The spectrum before hydrolysis shows an unequal intensity doublet at 1392 and 1366 cm^{-1}, the lower frequency band being more intense.

This pattern is typical of the CH_3 symmetrical bending modes in the *tert*-butyl groups. The product after hydrolysis shows that the band at 1366 cm^{-1} strongly decreases. The band at 1392 cm^{-1} decreases less because it overlaps the CH_3 symmetric bending of the *n*-alkyl chains.

Although the band at 1366 cm^{-1} has strongly decreased, it can still be detected. It represents less than 2 % of the initial amount. Therefore, from the FTIR, the hydrolysis of the *tert*-butyl groups cannot be considered rigourously complete, although the NMR showed no trace of them.

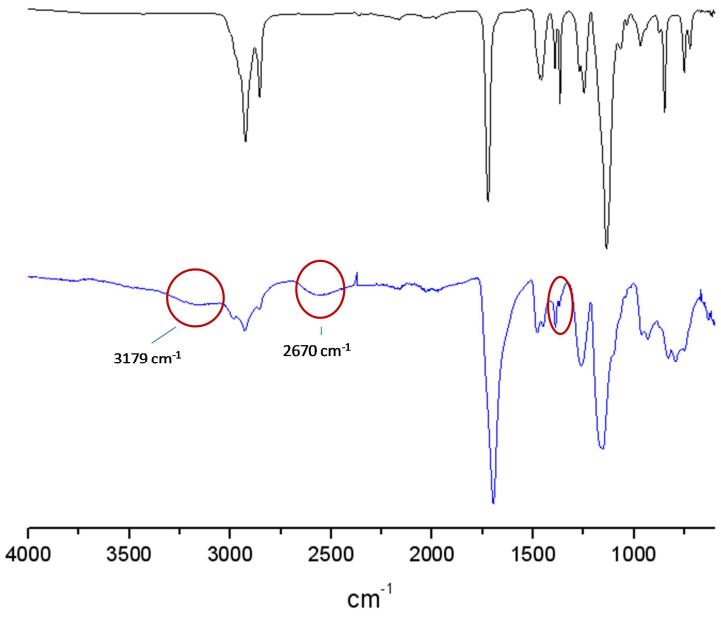

Figure 5. 6. FTIR spectrum of poly(TBM-*co*-C18)(-) and poly(MAA-*co*-C18)(-).

The proportion of the remaining *n*-alkyl chains after the hydrolysis was measured by ^1H NMR with an internal reference (nitromethane). It is calculated from the integration ratios of the signal corresponding to $–OCH_2$ (δ = 3.8 ppm, H_d) with the peak of the nitromethane at (δ = 4,3 ppm). The results are summarized in Table 5.3.

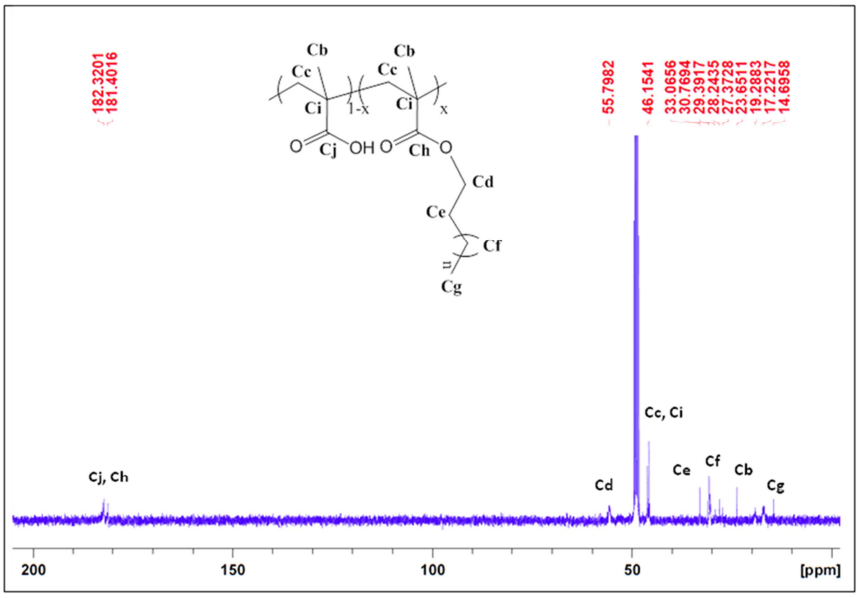

Figure 5. 7. ^{13}C spectrum of poly(MAA-*co*-C18).

(iii) Characterization by size exclusion chromatography (SEC)

The measure of the molecular weight of water soluble copolymers is often difficult, due to their physical properties (polarity, hydrogen bonding, partially hydrophobic character). In the case of amphiphilic copolymers, the difficulties are even worse since it is very hard to select a solvent that solubilizes both the hydrophilic and hydrophobic parts. As a result, the polymer is not fully dispersed, and form aggregates or adsorb on the SEC columns. For these reasons, size exclusion chromatography (SEC) is seldom reliable for amphiphilic polymers. In addition there are few references in the literature.

In our case, we have found that water:acetonitrile (80:20) and 0.1 N $NaNO_3$ is a suitable eluent, but only for polymers with 1 mol % of hydrophobic groups. The polymers were analyzed by SEC coupled with MALS. The masses were determined from MALS are tabulated in Table 5.3.

Table 5. 3. Composition and properties of the hydrolyzed copolymers.

		SEC-MALS		
Feed ratio of the monomers	**Ratio[a] by ^{1}H NMR**	***Mw***	***Mn***	**PDI**
		Poly(MAA-*co*-C12)		
99/1	1	162 557	135 171	1.2
95/5	6	-	-	-
90/10	9	-	-	-
		Poly(MAA-co-C18)		
99/1	2	104 761	89 278	1.17
95/5	5	-	-	-
90/10	8	-	-	-
		Poly(MAA-co-MBL)		
99/1	1	176 380	156 671	1.13
95/5	6	-	-	-

[a] ratio of the alkyl chain with nitromethane

For the three considered copolymers, the molecular weights and PDI before and after hydrolysis are similar. It shows that the polymers are not degraded or cleaved during this step. In the case of poly(TBM-*co*-C12) *Mn* slightly increases after hydrolysis (137 000 vs 119 000) but *Mw* decreases (193 000 vs 162 000). These slight variations are less than the decrease of 25 % expected from the loss of the *tert*-butyl groups. The measured masses might have been overestimated. It is calculated with a dn/dc value that is estimated from the integration of the refractive index. This estimation supposes that the compound was entirely eluted. However, probably part of the compound was adsorbed on the column which can lead to an erroneous value of dn/dc and hence of the mass.

In conclusion, the amphiphilic polymers were obtained by free radical copolymerization of *tert*-butyl methacrylate and *n*-alkyl methacrylate. This very simple method afforded copolymer with weights higher than 100 000 and a PDI < 2, sometimes less than 1.5 which is better than expected. The PDI decreases with the modification percentage decrease. The modification percentage was found to be equivalent to the feed ratio and the hydrolysis step was proven to proceed without cleavage of polymer chains.

The only structural feature that was impossible to explore was the microstructure, especially, it was not possible to check whether the polymers have a random sequence distribution.

5.2 Gel formation and influence of the copolymer structure on the rheological properties

5.2.1 Solubility and gel formation

We have tested the ability of the polymers to form gels in aqueous solutions. They were neutralized and mixed with water at different concentrations and the formation of gels was estimated by visual inspection. The samples were considered gels when they could no longer flow even when the tubes were turned upside down. According to this rough criterion, we were able to determine a gel concentration (Table 5.4).

Table 5. 4. Composition and concentration of gels.

Copolymer	Hydrophobic content (mol%)	Gel concentration (wt.%)
MAA-*co*-C12	5	6%
	10	not soluble
MAA-*co*-C18	1	gels+solution
	5	4%
	10	not soluble
MAA-*co*-MBL	1	viscous solution up to 6%
	5	6%

Poly(MAA-*co*-C12) with 1 mol % hydrophobic rate does not form gels and poly(MAA-*co*-C18) with 1 mol % form heterogeneous mixtures of gels particles and solution. Poly(MAA-*co*-MBL) is a viscous liquid at concentration up to 6 %. Copolymers with 10 mol % were insoluble in all cases at concentrations as low as 1 %.

The main results is that the synthesized polymers are able to form gels when the grafting ratio is 5 mol % and with polymer concentrations higher than 4 wt. %. The gel concentrations seem to depend on the length of the alkyl chains: the copolymers with C_{18} forms gels at lower concentrations than with C_{12}. However those first tests are preliminary and only rheological measurements can quantify this trend.

During these tests we have experienced severe difficulties to form homogeneous gels because of their high viscosity. Indeed, when the polymer is partially dissolved the viscosity is already high enough to hinder the agitation or homogenization of the medium. This issue has strongly influenced our rheological studies.

5.2.2 Rheological properties of the gels

The rheological measurements were performed in a rotational rheometer Haake Mars III with a cone-plate geometry. We have carried out flow, creep-recovery and oscillatory experiments. The experimental setup and the principle of those experiments are described in detail in chapter 6. The measurements were performed at 25 °C.

We have tried to perform flow experiments to measure the viscosity as a function of the shear rate. But those experiments yielded non reproducible results, because of the inhomogeneity of the samples and because the viscosities depend on the history of the samples. The viscosities of some gels resulted in their ejection out of the measurement plate, even at low shears. We have therefore studied these gels by other measurements.

a) Viscosity-time relationship

We have applied a constant stress on the gels and we have measured the viscosity as a function of time. The measurements were done on the 3 polymers (C12, C18 and MBL) at 5 mol % modification and at a concentration of 4 wt. % and 6 wt. %. The viscosity was measured with a stress of 20 Pa for the different samples, for some very viscous samples higher stresses were applied.

All the curves show a sharp viscosity increase during the first minutes (Figure 5.8). The less viscous reach a plateau rapidly, but for the more viscous one the plateau is reached only after 20 min. It shows that those systems are slow to reach equilibrium. The values of the plateaus are reported Table 5.5. As expected the gels at 6 wt.% have much higher viscosities than at 4 wt.%.

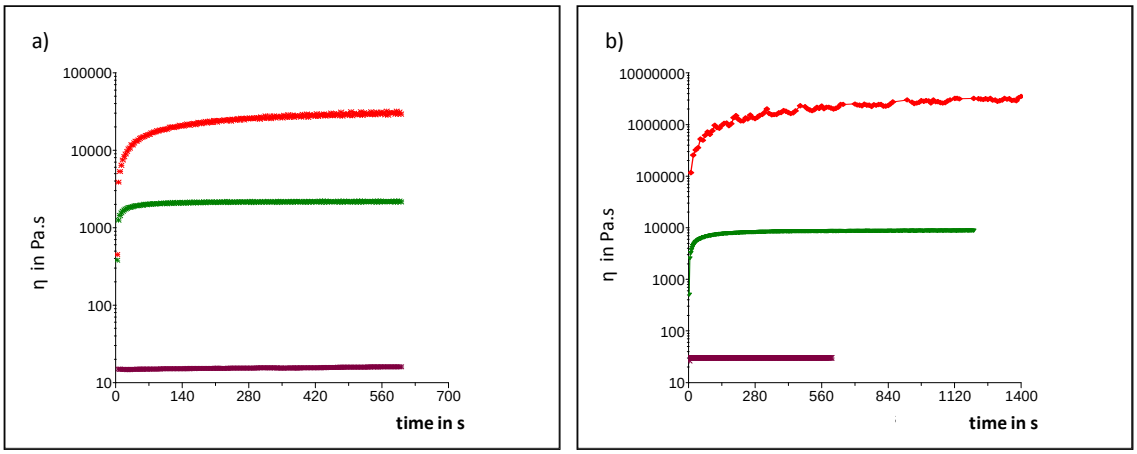

Figure 5. 8. Viscosity-time curve of gels at two concentrations fro copolymers with a hydrophobic content of 5 mol% (a) 4 wt. % (b) 6 wt. % (-) C18; (-) C12; (-) MBL.

C18 gels have a higher viscosity than C12 gels (Table 5.5 and Figure 5.8). For instance, for gels at 4 wt.%, the viscosity of C18 (8500 Pa.s) is 4 times higher than that of C12 (2100 Pa.s). These results are due to length of the alkyl chain: C18 induces stronger hydrophobic interactions than C12. This behavior has been well described in literature (see chapter 4) including by Zhuang et al.[205] on similar polymers.

Table 5. 5. Viscosity from flow and Creep measurements for different copolymers in aqueous solution.

Copolymer with 5 mol %[a]	Gel concentration (wt. %)	η (Pa.s) Flow	η (Pa.s) Creep
MAA-*co*-C12	4	2100	2400
	6	8500	8000
MAA-*co*-C18	4	22 000	36 300
	6	1 615 000	248 000
MAA-*co*-MBL	4	15	18
	6	2300	4800

[a] **Hydrophobic rate in mol%**

MBL gels have weaker viscosities. In the MBL monomer, the hydrophobic tail is composed of an alkyl chain in C_{12} and a hydrophobic spacer in C_4. The ester group itself is not hydrophilic, so the total chains equivalent to a C_{16} chain. One expected a higher viscosity than gels of MAA-*co*-C12. But the low viscosity of the MBL containing copolymers show that the hydrophobic interactions are less or weaker than in the other polymers. This behavior is not well

understood yet. One has to suppose that the ester moieties tend to hinder the interaction between chains either by steric or electronic factors. Another factor can be a non-random distribution of the alkyl chains in the copolymer, leading to weaker hydrophobic interactions.

b) Creep-Recovery

Since flow experiments were not possible, the visco elasticity of the gels was studied by creep-recovery experiments. These measurements are conducted in two steps. In the first step a constant shear stress is steadily applied and the resulting deformation is monitored as a function of the time. In a second step, called recovery phase, the stress is removed, and the deformation is measured while the sample reaches its new equilibrium. Figure 5.9 presents the results for C18 and MBL 5 mol % at 4 wt.%.

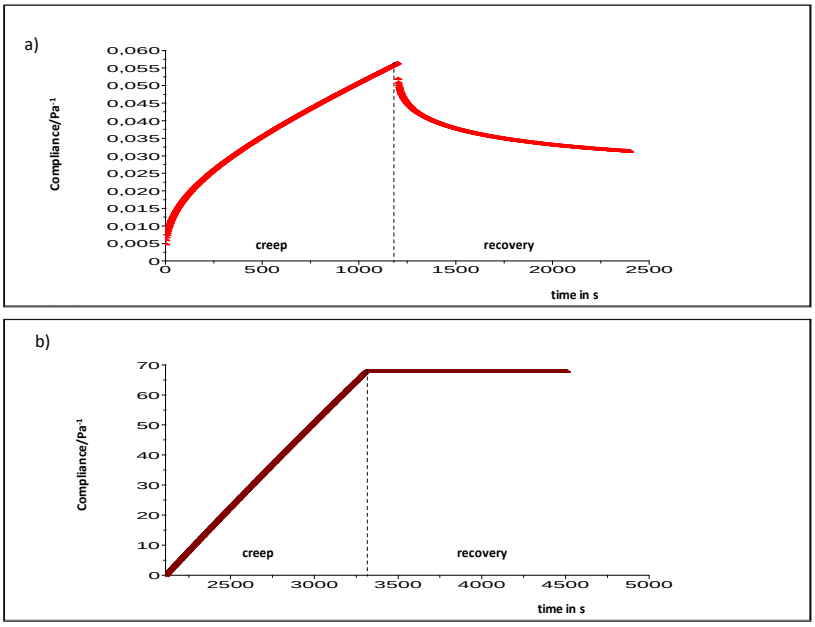

Figure 5. 9. Creep-recovery curves in aqueous solution. a) (-) C18; b) (-) MBL.(at 4 wt.%, applied stress = 20 Pa).

The compliance, $J = \gamma/\sigma$, is plotted against time. For C18 a sample in Figure 5.9 (a), in the first phase, a stress of 20 Pa was applied. The curve shows a sudden increase of the strain that corresponds to the elastic deformation. It is followed by a continuously increase of strain corresponding to the creep phase. In the second phase, the stress is removed. One observes a sudden decrease of the strain that correspond to a partial reformation of the fluid owing its

important elastic behavior (recovery phase). For the same conditions of stress, the behavior of MBL, Figure 5. 9 (b), is very different: under stress, the creep curve is linear and after removing the stress there is no reformation, the fluid is at the equilibrium. This result proves that this fluid has no elasticity. From those compliance-time curves the values of the viscosity can be derived easily: it is the inverse of the slope of the linear regime of J (see annex 1). They can be compared with the values obtained from the viscosity-time experiments. They give similar values except for C18 6%, probably because the gels of C18 are not homogeneous. In those experiments, we have encountered problems of heterogeneities of the gels that had lead to dispersions in the values, especially gels containing C_{18} that are highly viscous: 1 615 000 Pa.s from viscosity-time measurements and 248 000 Pa.s from creep-recovery measurements (Table 5. 5). Other quantities can be calculated: relaxation time, and plateau modulus. The measurements for the gels are summarized in the annex 4.

c) Oscillatory experiments, determination of G' and G''

The visco-elastic behavior has been furthers characterized the measurement of the storage modulus (G') and loss modulus (G'') by oscillatory experiments. The measurements were made in the linear regime for frequencies in the range of 0.001-10Hz. These experiments complete the values obtained by the creep-recovery tests.

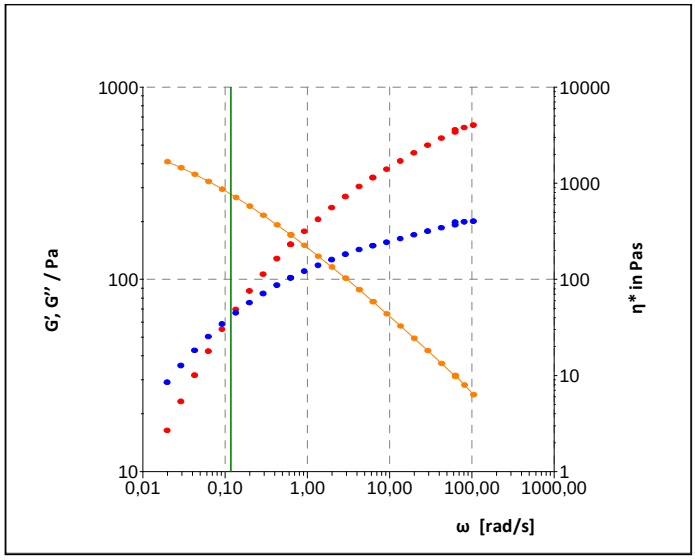

Figure 5. 10. Oscillatory frequency sweep on C12 5 mol% at 4 wt.%.

In Figure 5.10 shows the measurements for MAA-C12-5 mol % at 4 wt. %. At low frequencies the viscous component G'' is higher than the elastic component G'. For frequencies higher than 0.1 Hz, G' is higher G'', which means that the fluid is more elastic than viscous.

The coordinates of the crossing point of G' and G'' curves are noted G_x and ω_x. These values are characteristic of the gels. For a Maxwellian fluid, Gx = $G_0/2$ where G_0 is the plateau modulus and $\omega_x = 1/\tau$, where τ is the relaxation time. Our systems are more complex than Maxwell fluids that have a single relaxation time and so these equations cannot be applied strictly. However, the position of the cross point indicates qualitatively the differences between the gels.

The measurements corresponding to the copolymers of C18 and MBL 5mol % at 4% wt. are displayed in Figure 5.11.

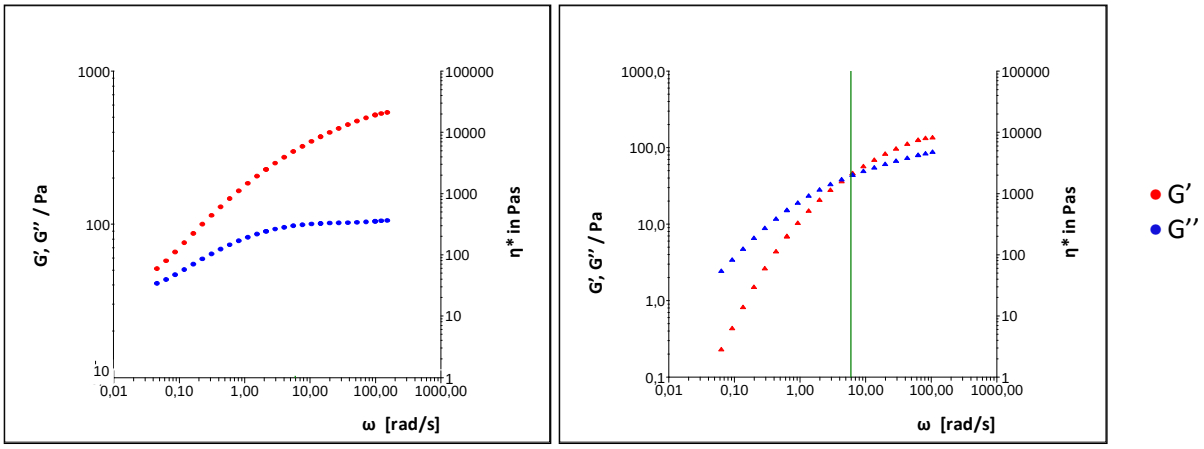

Figure 5. 11. Oscillatory frequency sweep on 4 wt. % of the gels. a) C18 5 mol %; b) MBL 5 mol %.

The Table 5.6 summarizes the results of oscillatory experiments for the gels of C12, C18 and MBL at 4 and 6 wt.%.

Table 5. 6. Results of oscillatory frequency sweep

Copolymer with 5 mol%[a]	Gel concentration (wt.%)	G_x (G'= G'') (Pa)	ω_x (rad/s)	τ_x(s)
MAA-*co*-C12	4	64	0.12	8
	6	115	0.06	17
MAA-*co*-C18	4	-	< 0.001	> 1000
	6	-	-	-
MAA-*co*-MBL	4	42	8	0.13
	6	168	0.1	10

τ_x = relaxation time.

For C18 gels the value of G' is higher than G'' in the full ranges of frequencies, which shows that the fluid have predominant elastic response. The crossover frequency and the terminal behavior cannot be observed because of the experimentally limited accessible frequency range. The cross over frequency is less than 0.001 s^{-1}, which corresponds to relaxation times much higher than MBL.

MBL at 4 wt. % shows a cross point at much lower G values and much higher frequencies than C12 gels. In addition the values for G' and G'' are lower than for C18, which is coherent with a weaker elastic response. At a concentration of 6 wt.%, MBL displays the same characteristics as the gels of C12 at 4 wt.%. From the oscillatory experiments one can also derive the complex viscosity, $\eta^* = (G'^2 + G''^2)^{1/2}/\omega$. (Figure 2.12). Extrapolation at zero frequency gives values that are close to the ones found with from the viscosity-time curves.

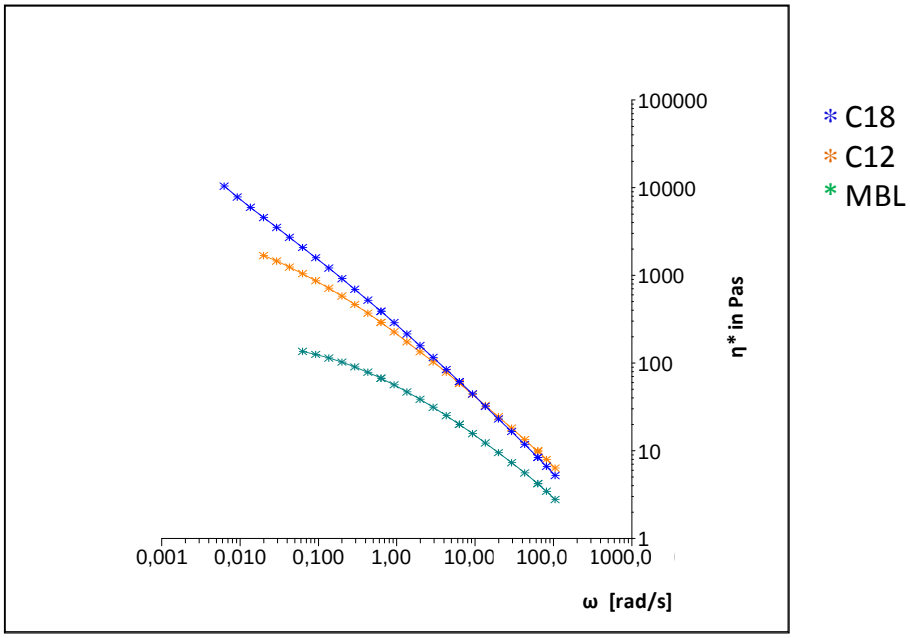

Figure 5. 12. Complex viscosity on 4 wt. % of the gels. (*) C18 5 mol %; (*) C12 5 mol%; (*) MBL 5 mol %.

Conclusion

The rheological analyses of these three fluids were carried out by different methods giving convergent results. The viscosity of the gels, the elastic moduli and the relaxation time of the gels increase in the order MBL < C12 < C18. The comparison between C12 and C18 can be explained easily by the length of the hydrophobic part. The behavior of MBL is peculiar. This

last polymer at low concentration gives flowing liquids while LMA forms a gel at the same concentrations. The role of the middle ester group in MBL chain is not understood.

5.3 Gel degradation

5.3.1 In vitro assays

The gels were incubated with a hydrolytic enzyme during 2 days at 37 °C. The enzyme chosen for this experiment is the lipase from *Burkholderia cepacia* produced by Amano (Amano PS, Sigma Aldrich (≥ 30 000 U/g)).

The gels selected to study the enzymatic degradation were poly(MAA-*co*-C12) and poly(MAA-*co*-MBL) 5 mol%. They were prepared in physiological buffers at pH 7.4 and the concentrations of the tested gels were 4 wt. %. For each measurement we run a blank, consisting in the same gel, prepared in the same conditions but containing no enzyme.

The gel degradation was followed by visual inspection. The C12 sample with the enzyme flows faster than the blank after 30 h, suggesting the loss of hydrophobic interactions in the gel. In order to quantify this behavior rheological measurement were performed on the enzyme containing gels and the blanks. Figure 5.13 describes the viscosity-time relationship of C12 gels. In agreement with the visual observations the viscosity of the enzyme is 3 times lower than the blanks. Oscillatory measurements on these gels were also performed on both gels (Figure 5.14).

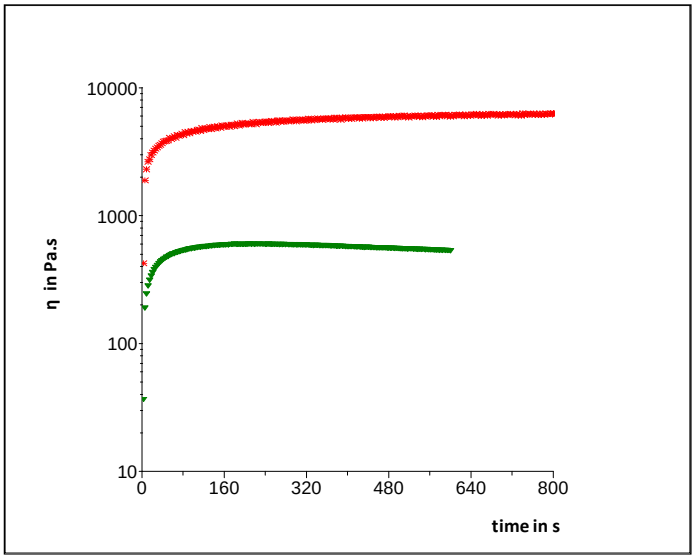

Figure 5. 13 Viscosity-time relationship of gels (poly(MAA-*co*-C12) 5 mol %) at 6 wt.%. (-) blank; (-) enzyme.

The measurements display a strong decrease of both G' and G" after the gel is treated by the enzyme. As a consequence, the complex viscosity (η*) also decreases.

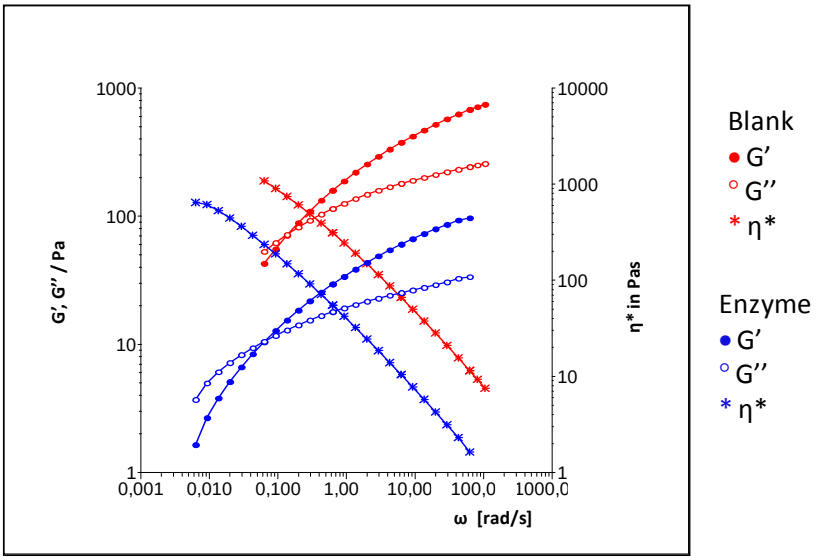

Figure 5. 14. Oscillatory frequency sweep on poly(MAA-*co*-C12) 5 mol% gels at 6 wt.% (stress =20 Pa), in the presence of enzyme (1 mg/mL), and without enzyme (blank).

It is clear that the enzyme acts on the gel by decreasing its viscosity. This can be interpreted by the cleavage of ester moieties by the enzyme, decreasing the number of hydrophobic interchain connections. The values are summarized in Table 5.7.

Using the same methods and conditions as above, we now study the poly(MAA-*co*-MBL) 5 mol % gels. The viscosity-time relationship between the blank and the enzyme are illustrated Figure 5.15. Surprisingly, the curve show a slightly increase of the viscosity for the enzyme treated sample. This result can be explained by the action of the enzyme that liberates dodecanoic acid in the medium that can act as a surfactant. It has been proved that surfactant at low concentration can increase the viscosity of associating polymers. [236,237] The enzyme itself may also interfere since it is an amphiphile polymers that can interact with the hydrophobic parts of the polymers. The Table 5.7 gives the cross point G_x (G' = G'') and relaxation times $\tau_x = 1/\omega_x$ of both samples. The values are almost the same. The viscosities calculated from creep-recovery experiments are also the same for both samples. It suggests that almost no change occurs on the gel in contact with the enzyme.

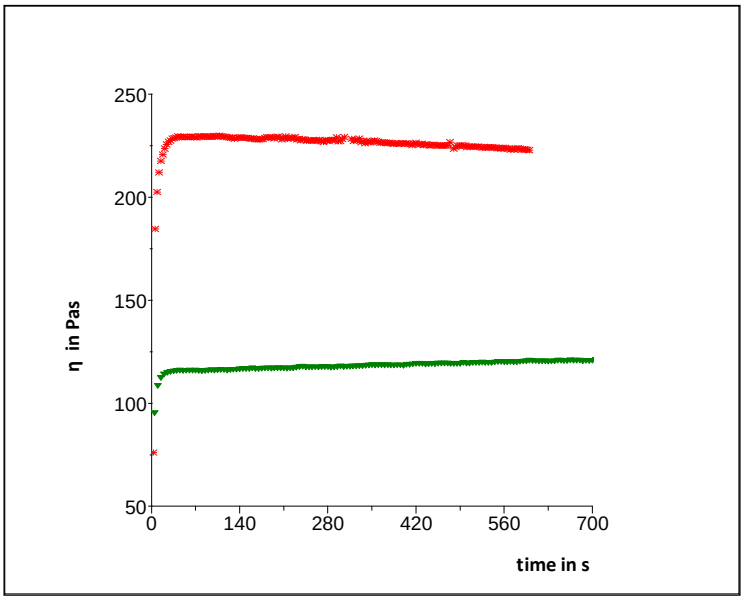

Figure 5. 15. Viscosity-time relationship of gels (poly(MAA-*co*-MBL) 5 mol%) at 6 wt.%. (-) blank; (-) enzyme.

Table 5. 7. Rheological results under Amano Lipase (A.L) during 2 days at 37 °C.

	η (Pa.s) flow	Oscillation			η (Pa.s) Creep
		(G'= G'') (Pa)	ωx (rad/s)	τx(s)	
Gel of MAA-co-C12[a] 5mol% with A.L (1 mg/mL) 2 days 37 °C					
Blank	1856	73	0.14	7	2983
Enzyme	630	11	0.06	15	730
Gel of MAA-co-MBL[a] 5mol% with A.L (1 mg/mL) 2days 37 °C					
Blank	116	57	0.8	1.2	204
Enzyme	231	52	0.9	1.1	241

[a] The gels were prepared at 6 wt.% and diluted to a 4 wt.% under buffer and enzyme+buffer.

In conclusion, the enzymatic degradation of the gels was determined by rheological analysis. The viscosity of samples of C12 decreases in the presence of the enzyme. It may be interpreted by the loss of hydrophobic groups by enzymatic hydrolysis. The MBL samples do not undergo such a decrease in viscosity, in the contrary the viscosity slightly increases.

The difference between both gels shows that the C12 esters is a better substrate for the enzyme than the MBL esters, which is the opposite of that we had surmised. Intercalation of a spacer between the hydrophilic chain and the ester and a longer chain did not improve lability. The viscosity increases observed for the MBL containing polymers suggests that the released chain and may be the enzyme itself interfere with the hydrophobic interactions.

5.3.2 In vivo assays

Tests in vitro on an enzyme may be deceiving, since the lipase produced by the bacteria may be different and inactive toward the substrate. But the main issue is that the bacterium must produce and excrete the lipase in the extracellular medium, which depends on the culture conditions. For these reasons the studies must be completed by assays in vivo. These biological tests were done in collaboration with the biologists of the Department of Bacterial membrane transport (Ecole de Biotechnologie de Strasbourg). The gels of poly(MAA-*co*-C12) 5 mol % at 6 wt.% have been incubated in culture media with *Pseudomonas aeruginosa* of strain PAO1 during one week.

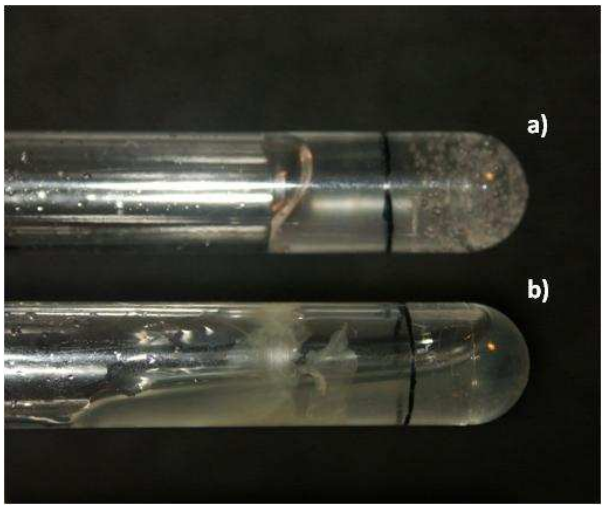

Figure 5. 16. Poly(MAA-*co*-C12) 5 mol % gels at 6 wt.% in the presence of *Pseudomonas aeruginosa* on strain of PAO1. a) Blank; b) Gel + bacteria.

The viscosity of the gels in presence or absence of the bacteria was followed by mere visual inspection after 7 days of incubation. In Figure 5.16 the two samples can be seen: (a) is the gel with the sterile minimal medium as the blank and (b) is the gel in contact with the bacteria in minimal medium. The latter shows a lower viscosity. These behavior shows that the bacteria were able to release enzymes to the hydrolysis of ester moieties. The hydrolysis of the gels was longer than under enzymatic conditions, giving an advantage to be used for biomedical applications as drug delivery by a sustained release.

5.4 Conclusion

The synthesis of the targeted copolymers was successfully achieved by radical polymerization, with molecular weights in the order of 10^5 g/mol and PDI < 2. The copolymers were synthesized with grafting ratios of 1, 5 and 10 mol%. These associating copolymers gels in aqueous solutions for grafting ratios of 5 mol% (C12, C18 and MBL). The gels are formed for concentration of the copolymer above 4 wt.%.

The behaviors of the gels has been studied by rheology experiments . The viscosity of the gels, the elastic moduli and the relaxation of the gels increase in the order MBL < C12 < C18.

The gels of C12 and MBL 5 mol% at 6 wt.% were selected to study their degradation by an enzyme (amino lipase 1 mg/mL). Rheological measurements prove that after 2 days the viscosity

of gels with C12 decreases in the presence of the enzyme (Table 5.7). In contrast the enzyme does not change the properties of MBL gels. C12 gels have proved to be degraded in the presence of *Pseudomonas aeruginosa* during one week. A more detailed characterization of C12 gels after their treatment with the bacteria would be necessary.

The viscosity increase of MBL in the presence of the enzyme is not understood and some more rheological experiments are necessary to understand the influence of the protein or the released hydrophobic tails. They actually can behave as surfactants and influence the rheological properties.

We have proved that hydrophobic moieties can be released. However, the kinetic rates are rather low. The design of hydrophobic moieties can still be improved to be cleaved more efficiently. The natural substrates are triglycerides, that bear 3 alkyl chains and the hydrophobic chains could be designed to mimick more closely those structures. Alternatively, other hydrolases can be targeted, like cholestesterase, or even exoproteases. For the last type of enzymes, one has to choose short hydrophobic peptides that are substrates of these proteases. They can be easily grafted on PMA or PAA as shown in the chapter 3 on the PEM.

CHAPTER 6:

Materials and Methods

6.1 Materials

6.1.1 Solvents and chemical reagents

Organic solvents were purchased at the highest commercial quality from, Aldrich, Fluka, Acros, Riedel-de-Haën. Dry solvents and monomers were distilled under inert atmosphere. Water was deionized by using a milli-gradient system (Millipore, Molsheim, France).

The following chemicals were purchased from the listed suppliers and used as is without further purification : N-hydroxysuccinimidobiotin (NHS-biotin, Iris Biotech GMBH), N-Ethyl-N'-(3-dimethylaminopropyl)carbodiimide hydrochloride (EDCI, Iris biotech GMBH, 99%), 1-hydroxybenzotriazole hydrate (HOBt, Fluka, ≥ 99,0%), tetra(ethylene glycol) (Aldrich, 99%), *N*-(2-Aminoethyl)maleimide trifluoroacetate salt (Fluka, ≥ 98%), *N*-Hydroxysulfosuccinimide sodium salt (NHS, Aldrich, ≥ 98.5%), di-*tert*-butyl dicarbonate (Boc_2O, Fluka, ≥ 99%), triethylamine (TEA, Acros, 99%), tetrabutylammonium iodide (TBAI, Aldrich, ≥ 99,0%), sodium azide (NaN_3, Alfa Aesar, 99%), sodium azide (Alfa Aesar, 99%), triphenylphosphine (PPh_3, Acros, 99%), p-Toluenesulfonyl chloride (p-TsCl, Acros, 98%), O-(2-Aminoethyl)-*O'*-[2-(Boc-amino)ethyl]octaethylene glycol (Aldrich, ≥ 90%), *O,O'*-Bis(2-aminoethyl)octa-decaethylene glycol (Fluka, ≥ 95%), azobisisobutyronitrile (AIBN, Fluka, ≥98%), lauryl methacrylate (LMA, Aldrich, contains 500 ppm MEHQ as inhibitor, 96%), stearyl methacrylate (SMA, Aldrich, contains 500 ppm MEHQ as inhibitor, 97%), poly(acrylic acid) (PAA, Aldrich, 35 wt.% in water, Mw 100 000), poly(allyl amine hydrochloride) (PAH, Aldrich, Mw 15 000), poly(sodium-4-styrenesulfonate) (PSS, Aldrich , Mw 70 000), poly(ethyleneimine) (PEI, Fluka, 50% (w/v) in water, Mw 750 000).

6.1.2 Biomolecules- Enzymes, Proteins, Serum and Polyelectrolytes

6.1.2.1 Lipases

The lipase used for gel degradation was Amano Lipase PS, from *Burkholderia cepacia* (≥30 000 U/g, provide from Sigma-Aldrich).

(See annexes for complementary information)

6.1.2.2 Streptavidin

The streptavidin was prepared in a solution of 0.1 mg/mL TRIS buffer (20 mM, tris: Trizma® base and HCl, 2-amino-2-(hydroxymethyl)-1,3-propanediol, Sigma-Aldrich). The solution have been stored at -20 °C until use.

(See annexes for complementary information)

6.1.2.3 Serum

Fetal bovine serum was purchased from Gibco. It was split into aliquots of 1 mL and frozen; it was thawed and diluted with buffer solution short before each experiment in order to prevent degradation. The serum solutions up to 10 % of serum content (4.4 mg proteins per mL) were filtered.

(See annexes for complementary information)

6.1.3 Polyelectrolytes

The polyelectrolytes used for the construction of polyelectrolyte multilayer films are summarized in Table 6.1 and Table 6.2.

Table 6. 1. Polycations used for the construction of polyelectrolyte multilayer films

Polyelectrolyte	Structure	Mw (g/mol)	pKa	Supplier	Unit mass (g/mol)
Poly(ethylene imine) (PEI)	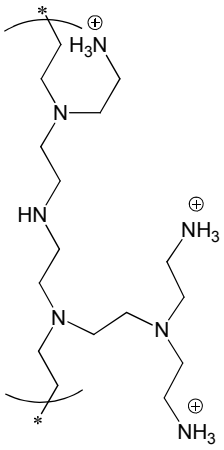	700 000	-	Sigma-Aldrich	332.35
Poly(allylamine hydrochloride) (PAH)	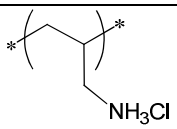	70 000	10	Sigma-Aldrich	93.15

Table 6. 2. Polyanions used for the construction of polyelectrolyte multilayer films

Polyelectrolyte	Structure	Mw (g/mol)	pKa	Supplier	Unit mass (g/mol)
Poly(styrene sulfonate) (PSS)	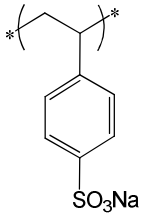	70 000	1	Sigma-Aldrich	206
Poly(acrylic acid) (PAA)	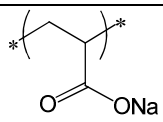	100 000	4	Sigma-Aldrich	72

6.2 Analytical methods and instruments

6.2.1 Chromatographic methods

Reactions were monitored by thin layer chromatography (TLC) on Merck silica gel aluminum plates (60 F_{254}). The spots were revealed by UV light as visualizing agent and *p*-anisaldehyde or 10% ethanolic phosphomolybdic acid. Preparative flash column chromatography were performed using silica gel (Geduran silica gel 60, 40-60 µm, from Merck) or automated flash chromatography purification system (puriFlash^{TM} 430evo from Interchim with 15/35µm silica cartridhges). Some of the polymers were purified by dialysis with cellulose membrane (ZelluTrans, ROTH, with a cut-off of 12000-14 000).

6.2.2 Nuclear Magnetic Resonance (NMR)

NMR spectra were recorded on a Bruker Advance 400 spectrometer operating at 400 MHz for ^{1}H and 100 MHz for ^{13}C. The spectra were calibrated by using residual undeuterated solvent as an internal reference. The multiplicities of the peaks were described by the following convention : singlet (s), doublet (d), triplet (t), quartet (q), multiplet (m) and broad (br). The degree of substitution (DS) was determined from the ratios of integrals of ^{1}H. When NMR spectra were done in D_2O *tert*-butanol was added to the sample and the singlet at 1.24 ppm was used as internal reference.

6.2.3 FTIR spectrometer

The FTIR spectra were recorded on a Bruker Vertex 70 spectrometer by ATR on a diamond plate from Smith. The DS of the associating polyelectrolytes were sometimes determined in CD_2Cl_2.

6.2.4 Size exclusion chromatography (SEC):

Molecular weights and molecular weight distributions were determined using a SEC system equipped with a Shimatzu SPD M20A refractive index detector and a multiangle light scattering detector (miniDAWN Treo from Wyatt). The sample was injected on five PLgel 10 µ

Mixed-B columns. The mobile phase was THF with a flow rate of 1 $mL \cdot min^{-1}$. Toluene was used as internal reference. The PMMA was used as a standard for calibration.

6.2.5 MALDI-TOF MS

The mass spectrometry was recorded in a Bruker Autoflex spectrometer for detection of molecular masses from 1 MDa with a N_2-Laser, 337 nm.

6.2.6 Elemental analysis

The elemental analysis was performed by the Service de Microanalyse, Institut Charles Sadron (ICS).

6.3 Gels formation

The copolymer powder was added in basic solution of NaOH (0.9 eq. with respect to the acidic units in the copolymer) and the solution was completed with NaH_2PO_4 buffer (40 mM) at pH 7.4. The mixture was vigourously stirred at room temperature during 3 days to ensure the complete dissolution. After this period, the gel was mechanically stirred and centrifuged for 45 min at 4000 rpm to eliminate the air bubbles trapped in the gels. No phase separation occurs during centrifugation.

6.4 Rheology

The studies were carried out using a rotational rheometer Haake Mars III with a cone-plate geometry (diameter 35 mm, angle 2°). To prevent water evaporation, the measuring system was surrounded with a solvent trap or, for long-time measurements, low-viscosity silicon oil was added to the edges of the cone.

The linear viscosity was measured at stress of 20 Pa for curves with viscosity-time relationship. For creep-recovery analysis result in compliance-time curves recorded in the regime of the linear response, the values of the steady-state viscosity, relaxation time, and plateau

modulus could be calculated with software supplied by the manufacturer (RheoWin 4 Data Manager).

The oscillatory measurements have been done for the study of the visco-elasctic behavior of the gels. The measurements were done under stress of 20 Pa in the linear response for frequencies in the range of 0.001-10Hz.

6.5 Buildup of polyelectrolyte multilayer films

The polyelectrolytes used for the construction of the mutilayers were dissolved in the following TRIS buffer solution: A solution of 20 mM Trizma® base (2-amino-2-(hydroxymehyl)-1,3-propanediol from Sigma Aldrich) and 150 mM NaCl was prepared with ultrapure water (18.2 MΩ.cm Milli-Q plus system, Millipore) and its pH was adjusted at 7.4 with aqueous HCl.

Poly(ethylene imine) PEI, poly(allylamine hydrochloride) PAH and poly(styrene sulfonate) PSS were used at a concentration of 1 mg/mL. PAA and modified PAA were used at a concentration of 0.5 mg/mL.

The construction of polyelectrolyte multilayer films was achieved by deposition of the polyelectrolyte solutions on quartz substrates by contact. Each deposition step of polyelectrolytes was followed by rinsing with buffer (TRIS).

6.6 Quartz crystal microbalance (QCM)

Measurements data

The results for the construction of the films were obtained from QCM-D301 (Q-Sense). The crystals for the measurements are the type QSX 303 (Q-Sense): they are SiO_2 crystals recovered by gold electrodes. The crystals have a ground frequency of 5. This frequency as well as three first odd overtones at 15, 25 and 35 MHz are used for the detection, but only the three overtones are considered for the data treatment, due to instabilities of the ground frequency. The crystal was rinsed with Hellmanex (2%) solution for 15 min, followed by HCl (0.1 M) and finally with ultrapure water and treated during 15 min with UV/O_3 prior to use.

The polyelectrolyte multilayer films were constructed *in situ* on the gold electrode of the crystal at 25°C. The solution of polyelectrolytes were injected (600 µL) into the cell and let adsorb during the time necessary to reach the stabilization of the frequency. After each adsorption the cell was rinsed with buffer solution during 4 min to eliminate the excess of the prior solution. The frequencies evolutions and the dissipations values were monitored during experiments with the software Qsoft 401.

6.7 Biological assays

6.7.1 *In vitro* assays

1 g of the gels were prepared as described above at a concentration of 6 wt. %. in phosphate buffer (NaH_2PO_4 at 40 mM, pH 7.4). A solution of lipase (0.5 mL, 1mg/mL) in the same buffer was added. The gel was stirred at room temperature during 3 days to ensure the complete dissolution. After this period, the gel was mechanically stirred and centrifuged for 45 min at 4000 rpm to eliminate the air bubbles trapped in the gels. The final concentration of the polymer in the gel was 4 wt. %.

Blank samples were prepared the same way but the enzyme solution was replaced by mere buffer. The gels were incubated for 48 hrs at 37°C.

6.7.2 *In vivo* assays

A stock solution of minimal medium (x10) is prepared by mixing K_2HPO_4 340 mM, KH_2PO_4 220 mM, $(NH_4)_2SO_4$ 75 mM, $MgSO_4$ 8 mM, succinic acid 34 mM and adjusting pH to 7 with NaOH. The solution is sterilized. The concentration of this stock solution is 10 fold the one of the final culture medium.

The polymer (70 mg) is mixed with NaOH (0.95 equiv. per mol of methacrylic acid) and water (630 µL) in a sterile culture tube. The tube is vortexed 1 hr and 70 µL of the 10 x medium solution is added under sterile conditions. The culture tube is agitated for 96 h. In the test tube *Ps. aeruginosa* is introduced as a suspension in the same culture medium (200 µL) under sterile conditions. In the blank, only culture medium is added. The gels are let incubated for 24 hrs, and the bacteria suspension (resp: the culture medium) is removed from test tube (resp; from the

blank), and replaced by a fresh suspension of bacteria (resp: medium culture). The procedure is repeated during 7 days.

6.8 Syntheses

6.8.1 Monomers for associating copolymers

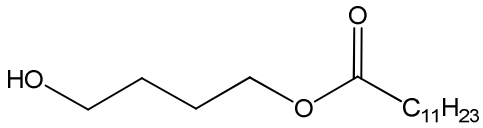

1

4-hydroxybutyl dodecanoate: a solution of 1,4–butanediol (80 mg, 0.88 mmol), triethylamine (TEA, 150 µl, 1.06 mmol, 1.2 eq.) in dry THF (2 ml) was cooled and stirred at 0 °C. dodecanoyl chloride (240 µl, 1.06 mmol, 1.2 eq.) was added dropwise. The reaction mixture was warmed at room temperature and stirred for 4 h. The THF was evaporated under reduced pressure, the residual solid was dissolved in CH_2Cl_2 (20 mL) and washed with H_2O (3 x 5 ml). The organic layer was dried over $MgSO_4$ and evaporated under reduced pressure. The crude was purified by silica gel chromatography (EtOAc:cyclohexane 1:2) to yield **1** as a white solid (203 mg, 85%). **^{1}H NMR** $CDCl_3$, 400 MHz, δ ppm): 4.10 (t, ^3J = 6.3 Hz, 2 H), 3.68 (t, ^3J = 6.3 Hz, 2 H), 2.29 (t, ^3J = 7.5 Hz, 2 H), 1.72-1.63 (m, 6 H), 1.26 (m, 16 H), 0.88 (t, ^3J = 6.5 Hz, 3 H). **^{13}C NMR** ($CDCl_3$, 100 MHz, δ ppm): 64.1, 62.1, 34.3, 31.8, 29.4, 29.3, 29.2, 29.1, 29.0, 25.1, 25.0, 22.6, 14.1.

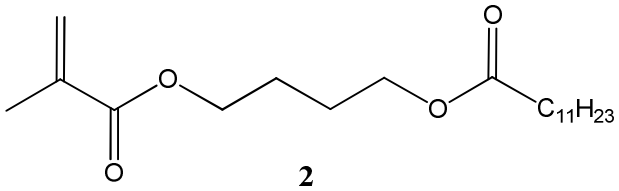

2

Methacrolyxybutyl laurate (MBL): compound **1** (200 mg, 660 µmol, 1 eq.) and triethylamine (TEA, 140 µl, 0.99 mmol, 1.5 eq.) were dissolved in dry THF (5 ml). The mixture was cooled at 0 °C and methacryloyl chloride (100 µl, 0.99 mmol, 1.5 eq.) was added dropwise. The reaction

was warmed at room temperature and stirred for 2 h. The solid residue was dissolved in CH_2Cl_2 (20 ml), washed with H_2O (3 x 5 ml) and dried over $MgSO_4$. The solvent was removed under reduced pressure and the crude was purified by silica gel chromatography (EtOAc:cyclohexane 1:9) to afford **2** as a colorless oil (107 mg, 40%). For its storage, a polymerization inhibitor, 4-methoxyphenol (MEHQ), was added to the compound. **^{1}H NMR** ($CDCl_3$, 400 MHz, δ ppm): 6.05 (s, 1H), 5.55 (m, 1 H), 4.17 (t, ^3J = 6.0 Hz, 2 H), 4.10 (t, ^3J = 6.5 Hz, 2 H), 2.28 (t, ^3J = 7.5 Hz, 2 H), 1.94 (s, 3 H), 1.75 (m, 4 H), 1.61 (q, ^3J = 7.2 Hz, 2 H), 1.25 (m, 16 H), 0.88 (t, ^3J = 6.8 Hz, 3 H). **^{13}C NMR** ($CDCl_3$, 100 MHz, δ ppm): 174.1, 167.6, 136.6, 125.6, 64.4, 63.9, 34.6, 32.1, 30.4, 29.8, 29.7, 29.6, 29.5, 29.4, 25.7, 25.6, 25.2, 22.9, 18.5, 14.3.

6.8.2 Copolymerization reactions

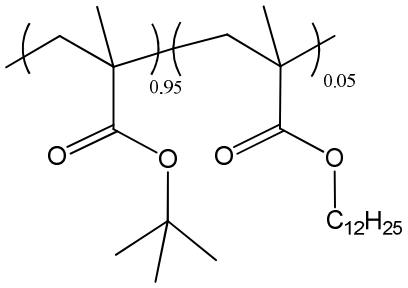

3

Poly(*tert*-butyl methacrylate-*co*-lauryl methacrylate) (poly(TBM-*co*-C12)): *tert*-butyl methacrylate (2 mL, 12.3 mmol, 0.95 eq.), lauryl methacrylate (140 µL, 647 µmol, 0.05 eq.) were dissolved in dry dioxane (6 mL) in a Schlenk flask, degassed and purged with argon. AIBN (21 mg, 129 µmol, 0.01 eq.) was added under argon and the solution was stirred at 60 °C for 24h. The reaction was stopped by cooling to room temperature and the mixture was precipitated in 100 mL of methanol. The precipitate was washed 3 times with methanol and dried to afford **3** (166 mg , 87 % yield). *Mn* = 247 300 g.mol^{-1}; *Mw/Mn* =1.77. **^{1}H NMR** ($CDCl_3$, 400 MHz, δ ppm): 3.94 (br s, 2 H), 2.06-1.83 (m, 4 H), 1.63 (br s, 2 H), 1.44 (br s, 9 H), 1.28 (br s, 16 H), 1.05 (m, 2 H), 0.94 (t, ^3J =6.7 Hz, 9 H).**^{13}C NMR** ($CDCl_3$, 100 MHz, δ ppm): 177.2, 177, 80.8,

67.0, 54.6, 50.9, 46.2, 32.1, 29.7, 29.2, 27.8, 22.5, 17.8, 14.2. **FTIR** (neat): 2975 (υ_{as} CH_3), 2928 (υ_{as} CH_2), 2856 (υ_s CH_2), 1719 (υ C=O), 1391 (δ_{as} CH_3), 1365 (δ_{as} CH_2), 1248, 1131, 847 cm^{-1}. **Anal.** Found C, 68.28; H, 10.15. Calcd for 95 % $C_8H_{14}O_2$ – 5 % $C_{16}H_{30}O_2$: C, 68.26; H, 10.09.

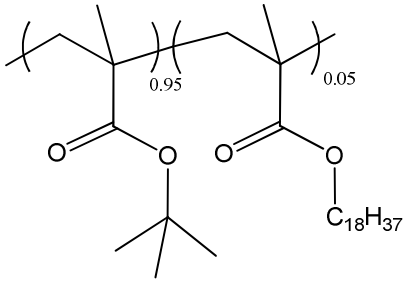

4

Poly(*tert*-butyl methacrylate-*co*-stearyl methacrylate) (poly(TBM-*co*-C18)): this compound was synthesized as described above for **3**, with *tert*-butyl methacrylate (2 mL, 12.3 mmol, 0.95 eq.), stearyl methacrylate (260 µL, 647 µmol, 0.05 eq.), AIBN (21 mg, 129 µmol, 0.01 eq.). Poly (TBM-*co*-SMA) **4** was obtained as a white powder (354 mg, 81% yield), (*Mn* = 298 746 $g.mol^{-1}$; *Mw/Mn* =1.75). **^{1}H NMR** ($CDCl_3$, 400 MHz, δ ppm): 3.96 (br s, 2 H), 2.04-1.82 (m, 4 H), 1.65 (br s, 2 H), 1.43 (br s, 9 H), 1.28 (br s, 16 H), 1.04 (m, 2 H), 0.93 (t, ^3J =6.7 Hz, 9 H). **^{13}C NMR** ($CDCl_3$, 100 MHz, δ ppm): 177.2, 177, 80.8, 67.0, 54.6, 50.9, 46.2, 32.1, 29.7, 29.2, 29.2, 27.8, 22.5, 17.8,17.5, 14.3. ATR-**FTIR** (neat): 2977 (υ_{as} CH_3), 2929 (υ_{as} CH_2), 2866 (υ_{as} CH_3), 1720 (υ C=O), 1393 (δ_s CH_3), 1367 (δ_s CH_2), 1249, 1132 , 848 cm^{-1}. **Anal.** Found C, 68.65; H, 10.21. Calcd for 95 % $C_8H_{14}O_2$ – 5 % $C_{20}H_{38}O_2$: C, 68.58; H, 10.17.

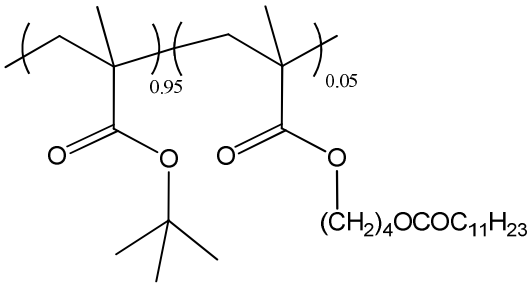

5

Poly(*tert*-butyl methacrylate-*co*-methacrylate butyl laurate) (poly(TBM-*co*-MBL): this compound was synthesized as described above for **4**, with *tert*-butyl metahcrylate (3 mL, 18.5 mmol, 0.95 eq.), methacrylate butyl laurate (331 mg, 974 µmol, 0.05 eq.), AIBN (31.9 mg, 194

µmol, 0.01 eq.). Poly (TBM-*co*-MBL) **5** was obtained as a white powder (115 mg, 76% yield), (*Mn* = 237 176 g.mol^{-1}; *Mw/Mn* =1.74). **^{1}H NMR** ($CDCl_3$, 400 MHz, δ ppm): 4.07 (br s, 2 H), 3.95 (br s, 2 H), 2.27 (m, 2 H), 2.04 (br s, 4 H), 1.81 (m, 6 H), 1.40-1.25 (m, 25 H), 1.02-0.88 (m, 9 H). **^{13}C NMR** ($CDCl_3$, 100 MHz, δ ppm): 177.2, 176.7, 80.8, 46.5, 46.3, 34.3, 31.9, 29.6, 29,5, 29.3, 29.2, 27.7, 24.9, 22.7, 18,5, 17.2, 14.1. ATR-**FTIR** (neat): 2976 (υ_{as} CH_3), 2932 (υ_{as} CH_2), 2852 (υ_s CH_2), 1719 (υ C=O), 1392 and 1366 (δ_s CH_2), 1248, 1131, 847 cm^{-1}.

6.8.3 Hydrolysis of tert-butyl groups

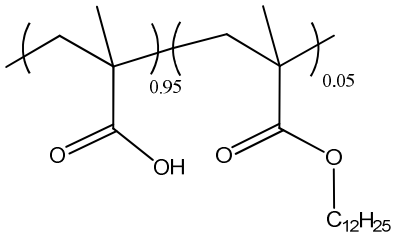

6

Poly(methacrylic acid-*co*-lauryl methacrylate) (poly(MAA-*co*-C12)): poly(TBM-*co*-C12) **3** (200 mg, 2 mmol) was dissolved in 1 mL of CH_2Cl_2, followed by the addition of TFA (0.76 mL, 10 mmol). The reaction was stirred at room temperature for 2 h. The solvent was evaporated under evaporator. Diethyl ether (15 mL) was added to the polymer and the residue was filtrated, this operation was repeated twice. The residue was dried under vacuum for 12 hrs to yield a white powder **6** (193 mg, 96% yield). **^{1}H NMR** (CD_3OD, 400 MHz, δ ppm): 3.91 (br s, 2 H, COO-CH_2), 1.97-1.88 (m, 4 H, CH_2-C-CH_2-C), 1.65 (br s, 2 H, COO-CH_2-CH_2), 1.32 (br s, 16 H, COO-CH_2-CH_2-$(CH_2)_8$-CH_2-CH_3), 1.08 (m, 6 H,C(CH_3)-CH_2-C(CH_3)), 0.95(brs, 3 H, COO-CH_2-CH_2-$(CH_2)_8$-CH_2-CH_3). **^{13}C NMR** (CD_3OD, 100 MHz, δ ppm): 182.3, 181.4, 55.8, 46.2, 33.0, 30.7, 29.4, 28.2, 27.3, 23.6, 19.3, 17.2, 14.7. ATR-**FTIR** (neat): 3179 (υ OH), 2985 (υ_{as} CH_3), 2929 (υ_{as} CH_2), 2857 (υ_s CH_2), 2553 (comb. and overtone COOH), 1697 (υ C=O), 1392 (δ_s CH_3), 1370 (δ_s CH_3), 1248, 1149, 813 cm^{-1}. **Anal. Found** C, 54.08; H, 7.35. **Calcd**. for 95 % $C_4H_6O_2$ - 5 % $C_{16}H_{30}O_2$ – 40 % H_2O: C, 54.32; H, 7.93.

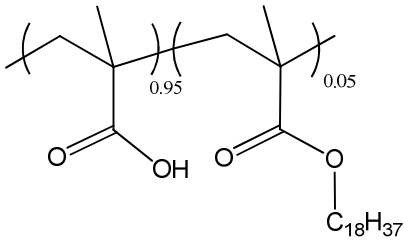

7

Poly(methacrylic acid-*co*-stearyl methacrylate) (poly(MAA-*co*-C18)): this compound was synthesized as described above for **6** from Poly(TBM-*co*-C18) **4** (200 mg, 1.92 mmol) with TFA (735 µL, 9.60 mmol). **7** was obtained as a white powder (187 mg, 93 %yield). **^{1}H NMR** (CD_3OD, 400 MHz, δ ppm): 3.96 (br s, 2 H, COO-C**H**$_2$), 1.99-1.87 (m, 4 H, C**H**$_2$-C-C**H**$_2$-C), 1.67 (br s, 2 H, COO-CH_2-C**H**$_2$), 1.33 (br s, 16 H, COO-CH_2-CH_2-(C**H**$_2$)$_8$-CH_2-CH_3), 1.08 (m, 2 H, C(C**H**$_3$)-CH_2-C(C**H**$_3$)), 0.94 (br s, 9 H, COO-CH_2-CH_2-$(CH_2)_8$-CH_2-C**H**$_3$). **^{13}C NMR** (CD_3OD, 100 MHz, δ ppm): 182.3, 181.3, 55.8, 46.2, 33.0, 30.6, 29.4, 28.2, 27.3, 23.5, 19.3, 17.2, 14.8. ATR-**FTIR** (neat): 3182 (υ OH), 2982 (υ_{as} CH_3), 2930 (υ_{as} CH_2), 2853 (υ_{as} CH_2), 2560 (comb. and overtone COOH), 1695 (υ C=O), 1392 and 1371 (δ_s CH_3), 1246, 1148, 812 cm^{-1}. **Anal. Found** C, 50.81; H, 7.14. **Calcd.** for 99 % $C_4H_6O_2$ - 1 % $C_{20}H_{38}O_2$ – 52 % H_2O: C, 51.14; H, 7.59.

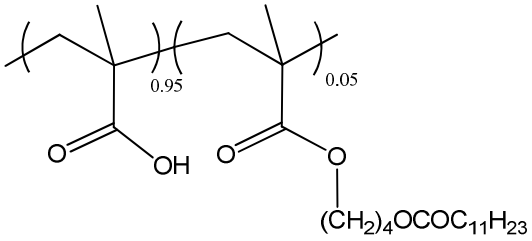

8

Poly(methacrylic acid-*co*-methacrylate butyl laurate) (poly(MAA-*co*-MBL): this compound was synthesized as described above for **7** with Poly(TBM-MBL) **5** (200 mg, 1.87 mmol), TFA (715 µL, 9.35 mmol). **8** was obtained as a white powder (188 mg, 94 % yield). **^{1}H NMR** (CD_3OD, 400 MHz, δ ppm): 3.96 (br s, 2 H, COO-CH_2), 1.99-1.87 (m, 4 H, CH_2-C-CH_2-C), 1.67 (br s, 2 H, COO-CH_2-CH_2), 1.33 (br s, 16 H, COO-CH_2-CH_2-$(CH_2)_8$-CH_2-CH_3), 1.08 (m, 2 H, C(CH_3)-CH_2-C(CH_3)), 0.94(br s, 9 H, COO-CH_2-CH_2-$(CH_2)_8$-CH_2-CH_3). **^{13}C NMR** (CD_3OD, 100 MHz, δ ppm): 185.2, 184.2, 58.5, 51.8, 49.2, 48.8, 36.1, 33.4, 29.1, 27.3, 22.0, 20.3, 20.0, 17.2, 15.3. **FTIR** (neat): 3172 (υ_sOH), 2993 (υ_{as} CH_3), 2931 (υ_{as} CH_2), 2856 (υ_{as}

CH_2), 2570 (comb. and overtone COOH), 1695 (υ C=O), 1392 (δ_s CH_3), 1372 (δ_s CH_2), 1331, 1159, 704 cm^{-1}.

6.8.4 Modification of PAA

Other compounds (**1**, **2**, **3**, **4**, **5**, **6**, **PAA-Maleimide** and **PAA-RGD**) are reported in the supporting information of chapter 3

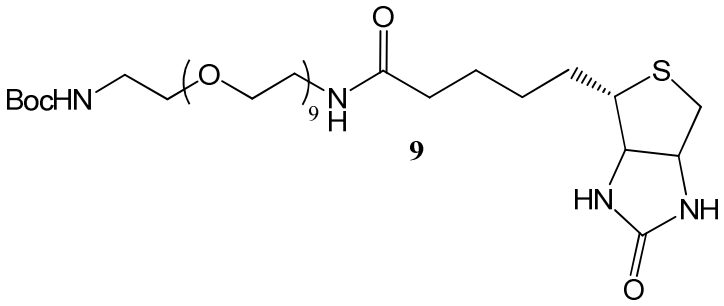

9

6.8.4.1 Compounds for the modification of PAA

***N*-Boc-*N'*-biotinyl-3,6,9,12,15,18,21,24,27-nonaoxanoneicosan-1,30-diamine, (BocNH(EO)$_9$Biotin) 9:** O-(2-Aminoethyl)-*O'*-[2-(Boc-amino)ethyl]octaethylene glycol (100 mg, 179 µmol, provided from Sigma-Aldrich company), and triethylamine (20 µL, 680 µmol, 1 eq.) were dissolved in DMF (2.5 mL). The solution was stirred for 30 min at 25 °C, and *N*-hydroxsuccinimidobiotin (281 mg, 880 µmol, 1.2 eq.) was added. The reaction mixture was stirred for 12 h at room temperature and then concentrated in vacuum. The residue was purified by silica gel column chromatography (acetone:methanol 9:1 as eluent) to afford **9** as a white powder (314 mg, 89 % yield). **^{1}H NMR** (CD_3OD, 400 MHz, δ ppm) 4.48 (ddd, $^3J_{trans}$ = 8.0 Hz, $^3J_{trans}$ = 5.5 Hz, $^3J_{cis}$ = 1.0 Hz, 1 H), 4.3 (dd, $^3J_{trans}$ = 8.0 Hz, $^3J_{trans}$ = 5.5 Hz, 1 H), 3.64 (m, 28 H), 3.55 (t,t, ^3J = 5.6 Hz, 4 H), 3.36 (t, ^3J = 5.4 Hz, 2 H), 3.2 (m, 2H), 2.95 (dd, ^2J = 13.0 Hz, $^3J_{trans}$ = 5.1 Hz, 1 H), 2.73 (d, ^2J = 13.0 Hz, 1 H), 2.20 (t, ^3J= 7.3 Hz, 2 H), 1.67 (m, 6 H), 1.44 (s, 9H). **^{13}C NMR** (CD_3OD, 100 MHz, δ ppm): 176.3, 174.6, 165.8, 71.6, 71.53, 71.28, 71.14, 70.8, 70.6, 63.3, 61.6, 57.0, 51.8, 41.0, 40.4, 36.8, 29.8, 29.5, 26.8, 26.5; **Anal. Calcd**. for $C_{35}H_{66}N_4O_{13}S$: C, 53.69; H, 8.50; N, 7.16; S, 4.10; found C, 53.15; H, 8.17; N, 6.98; S, 4.03.

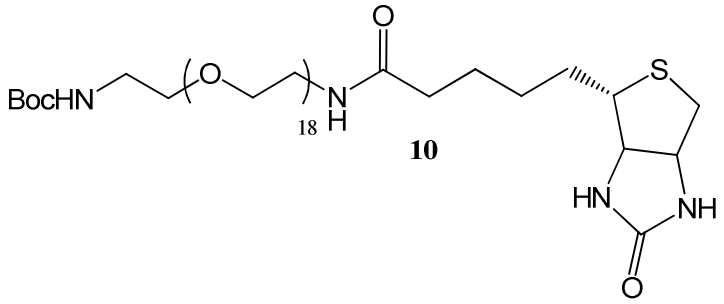

10

O-(2-(N-biotinyl)aminoethyl),O'-(2-(N-tert-butyloxycarbonyl)aminoethyl octadecaethylene glycol (BocNH(EO)$_{18}$Biotin) 10 : a solution of *O,O'*-Bis(2-aminoethyl)octadecaethylene glycol (86 mg, 96 µmol, purchased from Sigma-Aldrich) in 1.5 mL of THF was cooled at 0 °C and BOC_2O (21 mg, 96 µmol, 1 eq.) was added. The reaction was stirred at room temperature for 5 h and the solvent was removed by rotary evaporator. The solid product was dissolved in DMF (1.5 mL) with *N*-hydroxsuccinimidobiotin (35.4 mg, 101 µmol, 1.2 eq.) and triethylamine (20 µL, 680 µmol, 1 eq.) and the solution was stirred at room temperature for 12 hrs. The DMF was removed by vacuum and the residue was purified by silica gel column chromatography (acetone:methanol 9:1) to afford **10** as a white powder (260 mg, 45% yield). **^{1}H NMR** (CD_3OD, 400 MHz, δ ppm) 4.51 (ddd, $^3J_{trans}$ = 8.0 Hz, $^3J_{trans}$ = 5.5 Hz, $^3J_{cis}$ = 1.0 Hz, 1H), 4.3 (dd, $^3J_{trans}$ = 8.0 Hz, $^3J_{trans}$ = 5.5 Hz, 1 H), 3.64 (m, 70 H), 3.54 (t,t, ^3J = 5.6 Hz, 4 H), 3.4 (t, ^3J = 5.4 Hz, 2 H), 3.35 (t, ^3J = 5.4 Hz, 2 H) 3.22 (m, 4 H), 2.93 (dd, ^3J = 12.8 Hz, ^2J = 5.1 Hz, 1 H), 2.70 (d, ^3J = 12.8 Hz, 1 H), 2.22 (t, ^3J = 7.3 Hz, 2 H), 1.66 (m, 6H), 1.43 (s, 9H). **^{13}C NMR** (CD_3OD, 100 MHz, δ ppm): 176.2, 174.8, 166.4, 71.4, 71.1, 70.9, 70.4, 63.2, 61.4, 56.8, 41.1, 40.8, 40.2, 36.5, 29.6, 29.3, 28.6, 26.7, 26.2. **MS** (**MALDI-TOF**): 1223.659 (M^-, calcd for $C_{55}H_{106}N_4O_{23}S$ 1222.697).

6.8.4.2 Coupling Reactions

The procedure for the coupling of side chains to the polymers is exemplified here by the synthesis of PAA(EO)$_9$Biotin and PAA(EO)$_{18}$Biotin at 5 mol%. The others coupling reactions leading to PAA-Biotin and PAA(EO)$_3$Biotin are described chapter 4 in the supplementary information of the article.

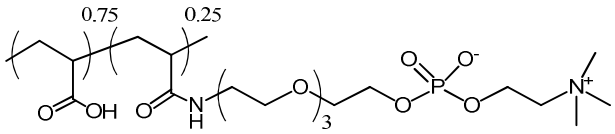

PAA(EO)$_3$PC 25%. The synthesis of this modified PAA is described by Reisch et *al*.[97]

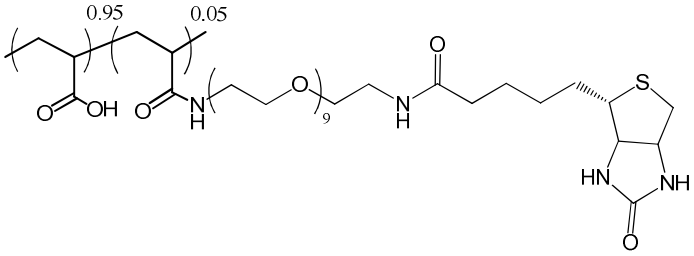

PAA(EO)$_9$Biotin 5%: BOCNH(EO)$_9$Biotin (35 mg, 550 µmol, 0.05 eq.) was mixed with aq. HCl (1 ml, 2.5M) and stirred at room temperature for 2 hours and the mixture was dried under vacuum. The residue and poly(acrylic acid) (PAA, Mw 100 000, 35% in water, from Sigma-Aldrich, 100 mg, 902 µmol. of acrylic acid units, 1 eq.) were dissolved in water (4 mL) and HOBt (60.8 mg, 450 µmol, 0.5 eq.) was added to the mixture followed by the minimal amount of NEt_3 to allow the dissolution of HOBt. The pH was adjusted to 5 with aqueous HCl (0.1 M) and EDCI (126 mg, 812 µmol, 0.9 eq.) was added at 0°C. The reaction mixture was stirred at room temperature for 18 h. The solution was dialyzed with a cellulose ester membrane (MWCO 12000-14000) against a 1 M NaCl solution for one day and against pure water for 5 days. Lyophilization of the solution afforded PAA(EO)$_9$Biotin as a white solid (86% yield). **^{1}H NMR** (D_2O, 400 MHz, δ ppm) 2.72 (d, SCH_2, 1H) comparison with the signal at 2.26 (all CHα of PAA) give a 6 % of degree of modification; 4.62 (q, ^3J =4.8 Hz), 4.43 (q, ^3J = 4.8 Hz), 3.78 (br s), 3.64 (br t ^3J = 5.5 Hz), 3.4 (t, ^3J =5.2 Hz), 3.33 (br m), 2.99 (dd, ^3J = 13 Hz, ^2J = 5.2 Hz), 2.78 (d, ^3J = 13 Hz), 2.27 (br m), 1.65 (m). **^{13}C NMR** (D_2O, 100 MHz, δ ppm): 175.9, 165.2, 69.7, 69.5, 68.9, 62.1, 60.2, 55.2, 39.8, 38.9, 35.5, 28.2, 27.8, 25.3. **FTIR** (neat)**:** ν_{max}: 3370 cm^{-1} (ν NH and ν OH), 2932 cm^{-1} (ν_{as} CH_2), 2875 (ν_{as} CH_2 ethylenoxide), 1699 (ν CO and urea amide I), 1649 (amide I), 1560 (ν_{as} COO^-), 1478 (amide II and δ_s CH_2), 1449, 1403 (ν_s COO^-), 1227, 1084 and 1052 cm^{-1} (ν_{as} CH_2-O-CH_2), 954 cm^{-1}.

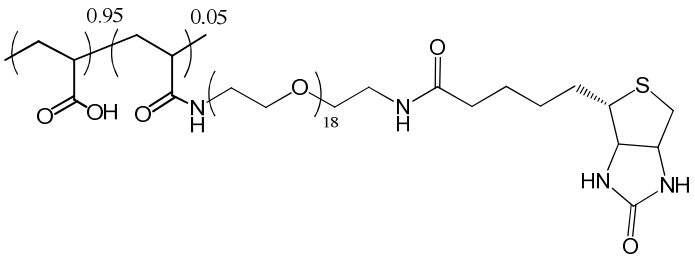

PAA(EO)$_{18}$Biotin 5%. BOCNH(EO)$_{18}$Biotin **10** (65 mg, 53 µmol, 0.05 eq.) was mixed with aq. HCl (1 ml, 2.5M) and stirred at room temperature for 2 hours and the mixture was dried under vacuum. PAA (Mw 100 000, 35% in water, provided from Sigma-Aldrich company) was freeze dried. Solid PAA (15.3 mg, 212 µmol. of acrylic acid units, 1 eq.) was dissolved in 5 mL of DMF then, BOP (5.6 mg, 12.7 µmol) was added and the reaction mixture was stirred for 10 min. **10** and TEA (0.03 mL, 212 µmol) were added. After 5 hour under stirring, the solvent was evaporated under reduced pressure. The residue was dissolved into aqueous solution of NaOH (1 mL; 2 N) and evaporated under reduced pressure again. The solution was dialyzed with a cellulose ester membrane (MWCO 12000-14000) against a 1 M NaCl solution for one day and against pure water for 5 days. Lyophilization of the solution afforded. PAA(EO)$_{18}$Biotin as a white powder. **^{1}H NMR** (D_2O, 400 MHz, δ ppm): 2.72 (d, SCH_2, 1H) 4.62 (q, ^{3}J =4.8 Hz), 4.43 (q, ^{3}J = 4.8 Hz), 3.78 (br s), 3.64 (br t ^{3}J = 5.5 Hz), 3.4 (t, ^{3}J =5.2 Hz), 3.33 (br m), 2.99 (dd, ^{3}J = 13 Hz, ^{2}J = 5.2 Hz), 2.78 (d, ^{3}J = 13 Hz), 2.27 (br m), 1.65 (m). **^{13}C NMR** (D_2O, 100 MHz, δ ppm): 176.6, 165.2, 69.7, 69.5, 68.9, 62.1, 60.2, 55.4, 39.8, 38.9, 35.5, 28.0, 27.8, 25.3. **FTIR** ν_{max}: 3370 (ν NH and ν OH), 2925 (ν_{as} CH_2), 2874 (ν_{as} CH_2 ethylenoxide), 1704 (ν CO acid and urea amide I), 1665 (amide I) 1557 (amide II and ν_{as} COO^-), 1478 (δ_s CH_2), 1449, 1403 (ν_s COO^-), 1222, 1082-1052 (ν_{as} CH_2-O- CH_2), 955 cm^{-1}. Comparing the signal at 4.62 ppm with the signal at 2.26 ppm (all CHα of PAA) give a 6 % of degree of modification.

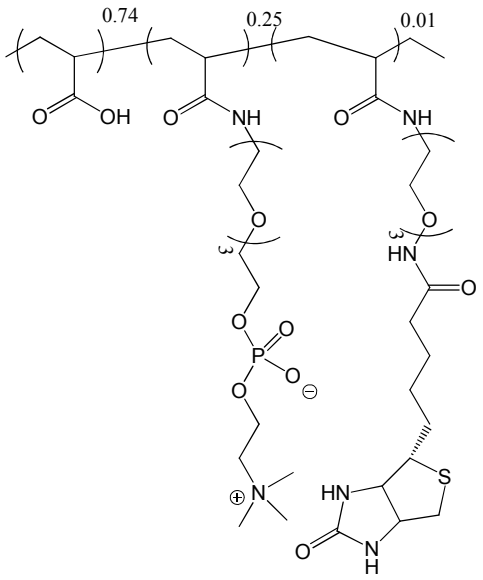

PAA(EO)$_3$PC-Biotin (25-1)%. Biotin hydrazide (3.09 mg, 120 µmol, 0.01 eq.) was mixed with aq. HCl (0.5 ml, 2.5M) and stirred at room temperature for 2 hours and the mixture was dried under vacuum. The residue and PAA(EO)$_3$PC (86 mg, 1.19 mmol. of acrylic acid units, 1 eq.) were dissolved in water (3 ml). HOBt (80.4 mg, 0.59 mmol, 0.5 eq.) was added followed to by the minimal amount of NEt_3 to allow the dissolution of HOBt. The pH was adjusted to 5 with HCl (0.1 M), and EDCI (166 mg, 1.07 mmol, 0.9 eq.) was added at 0°C. The reaction mixture was stirred at room temperature for 18 h. The solution was dialyzed with a cellulose ester membrane (MWCO 12000-14000) against 1 M NaCl solution for one day and against pure water for 5 days. Lyophilization of the solution afforded PAA(EO)$_3$PC-Biotin as a white solid (82% yield). **^{1}H NMR** (D_2O, 400 MHz, δ ppm): 4.61, 4.45, 4.33, 4.04, 3.73, 3.69, 3.61, 3.39, 3.20, 3.05, 2.90, 2.81, 2.79, 2.38, 1.87, 1.69.

PAA(EO)$_3$PC-(EO)$_3$Biotin (25-1)%: this compound was synthesized as described above for PAA(EO)$_3$PC-Biotin with PAA(EO)$_3$PC (90 mg, 1.25 mmol. of acrylic acid units, 1 eq.) and BocNH(EO)$_3$Biotin **7** (6.5 mg, 130 µmol, 0.01 eq.). PAA(EO)$_3$PC-(EO)$_3$Biotin was obtained as a white powder (86% yield). **^{1}H NMR** (D_2O, 400 MHz, δ ppm): 4.63, 4.44, 4.35, 4.06, 3.75, 3.70, 3.64, 3.40, 3.25, 3.07, 3.00, 2.83, 2.80, 2.25, 1.78, 1.59.

PAA(EO)$_3$PC25%/(EO)$_9$Biotin1%: this compound was synthesized as described above for PAA(EO)$_3$PC-(EO)$_3$Biotin with PAA(EO)$_3$PC (60 mg, 0.83 mmol. of acrylic acid units, 1 eq.) and BocNH(EO)$_9$Biotin **9** (6.5 mg, 80 µmol, 0.01 eq.). PAA(EO)$_3$PC-(EO)$_9$Biotin was

obtained as a white powder (82% yield). **^{1}H NMR** (D_2O, 400 MHz, δ ppm): 4.62, 4.44, 4.34, 4.04, 3.72, 3.63, 3.39, 3.25, 3.06, 3.00, 2.81, 2.79, 2.29, 1.84, 1.63.

PAA(EO)$_3$PC25%-(EO)$_{18}$Biotin1%: this compound was synthesized as described above for PAA(EO)$_3$PC-(EO)$_9$Biotin with PAA(EO)$_3$PC (98 mg, 1.36 mmol. of acrylic acid units, 1 eq.) and BocNH(EO)$_{18}$Biotin **11** (16.5 mg, 14 µmol, 0.01 eq.). PAA(EO)$_3$PC-(EO)$_{18}$Biotin was obtained as a white powder (76% yield). **^{1}H NMR** (D_2O, 400 MHz, δ ppm): 4.58, 4.41, 4.31, 4.03, 3.71, 3.61, 3.39, 3.22, 3.05, 2.79, 2.77, 2.29, 1.82, 1.61.

Conclusions and Perspectives

Addressing fundamental challenges that biomedical applications face nowadays in the fields of drug delivery and tissue engineering, we have designed and characterized PAA and PMA modified with various groups. We have been able to link these polyelectrolytes with alkyl chains, peptides, phosphorylcholine or biotin, with well-controlled modification rates. The chemistry of polyelectrolytes and their purification often sounds tedious and deterring. But these polymers can be easily modified with the coupling reagents coming from peptide chemistry and that operate in water. They can be linked to any biological species, even if the latter are water-soluble and sometimes fragile. The purification can always be done by dialysis, which warranties high purity levels in a single step.

We were able to prepare a whole library of polyelectrolytes where we have varied the nature of the side chains, their length and their grafting ratio. These polymers provided sound material to carry out the following studies.

First, we have used them to elaborate surfaces with controlled and selective adsorption properties. We have searched for surfaces able to bind selectively and specifically one protein and prevent the physisorption of all other proteins. PEM films were capped with with PAA-$(EO)_n$Biotin (n = 0, 3, 9 and 18) and the adsorption and the specific binding of these films were studied by QCM. As expected, these films can bind specifically streptavidin. But when the spacers are long enough, they also impede non-specific adhesion. In a less extent, long spacers also hinder specific binding. So the spacers have an optimal length (n=9) providing the highest ratio of mass of adsorbed streptavidin over the mass of adsorbed serum proteins. This ratio defines the selectivity of the films

A better selectivity could be reached with PAA bearing simultaneously PC and biotins. This double functionalization is possible with the same chemistry used for mono functionalization. It yields an interesting polymer since the deposition of a single layer suffices to endow the film with the desired selectivity.

The interplay between specific binding and non-adhesive properties was exploited to create a device that prevents specific and non specific adsorption of proteins when it is not stretched and induces the specific adsorption of proteins and cell adhesion when it is stretched. It consists of films PEM films containing PAA$(EO)_n$Biotin and PAA-PC, assembled on silicon substrates. This system is one of the few mechano-responsive ones known in the literature.

This work will be pursued along two directions. First, the selective binding surface will be used as biosensors. A complete immuno-assay will be carried out with streptavidin and a biotin-labeled antibody. The selectivity of the surface should allow exclusively the binding of the desired material. The non-specific adsorption should be considerably diminished and therefore increase the signal/noise ratio.

The study of the PEMs will be completed by the measurements of the thicknesses and densities of the layers, and the neat mass of deposited polymers, to deduce the water content and the number of side groups $(EO)_n$biotin and PC per unit surface. This work can be done by optical wave guide spectroscopy (OWLS).

In a second part, we have synthesized associating polymers in two steps by classical free radical polymerization. These polymers are PMA modified with different alkyl chains (C12, C18 and MBL) and grafting ratio GR = 1, 5 and 10 %. The main chain and the hydrophobic alkyl chain were connected through ester functions. These polymers were able to form hydrogels at concentrations of 4 wt. % with a GR of 5 %. The aim of these macromolecules was to study the cleavage of the ester moieties *in vitro* by the action of an enzyme (Amano Lipase) and *in vivo* by a *Pseudomonas aeruginosa*. The ultimate goal of this work is to obtain a responsive hydrogels that can release drugs.

The gel viscosity and the change of viscosity in the presence of bacterial enzymes were studied by rheology using a cone-plane rheometer. The rheological analysis showed that the viscosity of the gels increase in the order MBL< C12 < C18. The samples of C18 exhibit some dispersion in the values of the viscosity due to the heterogeneities of the gel.

The effect of the enzyme on the gels was studied after 2 days at 37 °C (incubation in vitro). The viscosity of the gels with C12 alkyl chains decreased, which showed a slight hydrolysis of the hydrophobic chains. MBL gels did not reveal any changes in their properties. The gels were incubated during 7 days for C12 in the presence of *Pseudomonas aeruginosa*. The results confirm the effective hydrolysis of the gels, which indicates a degradation of the hydrophobic associating parts.

The work will be continued by the optimization of the formation of the gels to avoid the heterogeneities we had observed and gain better reproducibility in rheological experiments. The group will graft other side chains to increase their cleavage rate by the bacteria. One may seek chains that have a structure closer to the one of the natural lipase substrates. Alternatively, we

will also modify PAA with peptides bearing alkyl chains, to frame proteases. The test *in vitro* can be further study with a deactivation of the enzyme at 80 °C, to check whether the enzyme modify the properties also by physical interaction with the polymers. The collaborating biologists are also developing high throughput tests and plan to use antibiotic resistant strains.

Annexes

Annexe 1.

Rheology

The rheology is the study of flow and deformation of matter under stress. The flow behavior of the polymers determines the nature and their properties and in this case their viscosity.

Under idealised conditions, ideal solids are subjected to shear stresses between two parallel walls. A force applied to an area, leads to a flow in the liquid layer A in contact with the liquid underneath as represented in Figure A1.1.

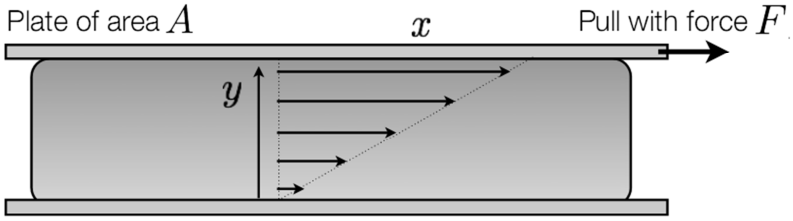

Figure A1. 1. Flow between two parallel plates

The velocity of flow that can be maintained for a given force is controlled by the internal resistance of the liquid, e.g by it is viscosity.

The shear stress is equal to:

$$\sigma = \frac{F(force)}{A(area)} = \frac{N}{\mathrm{m}^2} = \mathrm{Pa(Pascal)}$$

The shear stress σ causes the liquid to flow in a special pattern. The between two parallel plates, one is moving a constant speed while the other one is stationary. Where the different layers speed correspond to the shear rate:

$$\dot{\gamma} = \frac{dv}{dy} = \frac{1}{s} = (s^{-1})$$

There is possible to describe the basic law of viscosity for ideal liquid:

$$\eta = \frac{\sigma}{\dot{\gamma}} = \frac{N}{m^2}.s = Pas$$

The correlation between shear stress and shear rate defining the flow behavior of a liquid.

The viscosity (η) is the physical property of a liquid to resist at the influence of flow. The viscosity can be influenced by several parameters, as the temperature (T), shear rate ($\dot{\gamma}$), time (t), between others.

The rheometry can measure materials that exhibit a combination of elastic and viscous characteristics, property called visco-elasticity. There are two techniques that allows the measure of this properties, one is creep-recovery and the second is by oscillatory regime.

- Visco-elastic measurements

The visco-elastic measure by creep and recovery allows one to differentiate well between the viscous and the elastic responses of a fluid. This measurement is a response-time to the stress-dependency of both the viscous and elastic behavior, displayed in Figure A1.2.

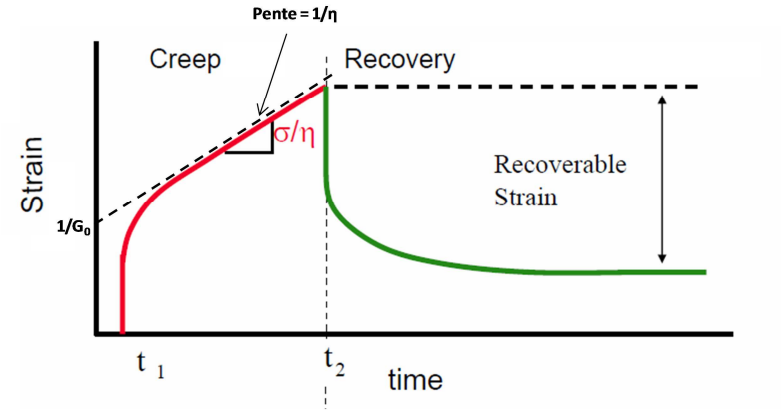

Figure A1. 2. Creep-recovery responses.

The first step is the creep by a constant applied stress leads to a proportional strain response with the time, interrelated by:

$$\gamma(t) = J(t).\sigma$$

This equation introduces the new term of the time-related compliance J(t) describe as

$$J(t) = \frac{\gamma(t)}{\sigma} = \frac{1}{Pa}$$

The recovery allows to determine the elastic response of the fluid, and is obtained by removing the stress the strain drops immediately to a new-time constant level.

Maxwell model principle

A viscoelastic material behaves as a Maxwell liquid (Figure A1.3). Their mechanical properties can be describes as for mechanical model, which combines a dashpot and a spring in series.

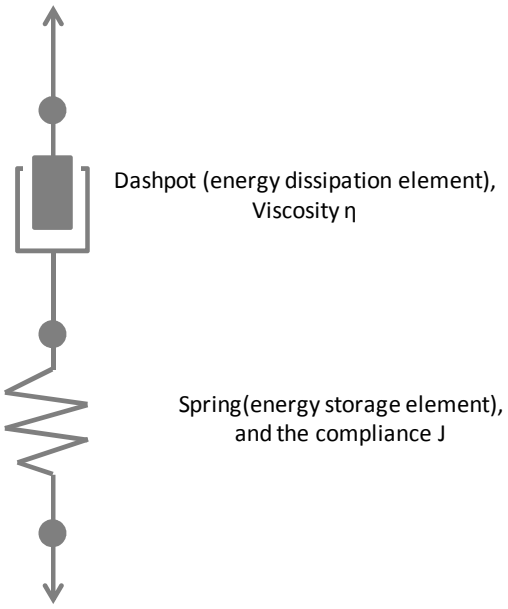

Figure A1. 3. Schematic representation of Maxwell model

In a dynamic test of a Maxwell fluid the modules are

$$G' = Go.\frac{\omega^2\tau^2}{1 + \omega^2\tau^2}$$

$$G'' = Go.\frac{\omega\,\tau}{1 + \omega^2\tau^2}$$

Where,

G_0 is the plateau modulus (Pa),

ω is the angular velocity (rad.s^{-1}),

τ is relaxation time (s).

When ω < 1/τ, G' and G'' are proportional to ω, the moduli are

$$G' \sim Go\ \omega^2\tau^2$$

$$G'' \sim Go\ \omega\tau$$

Figure A1.4 represents the variation of G' and G'' as a function of time for a Maxwell fluid and the complex viscosity η*

$$\eta * = \frac{\sqrt{G'^2 + G''^2}}{\omega}$$

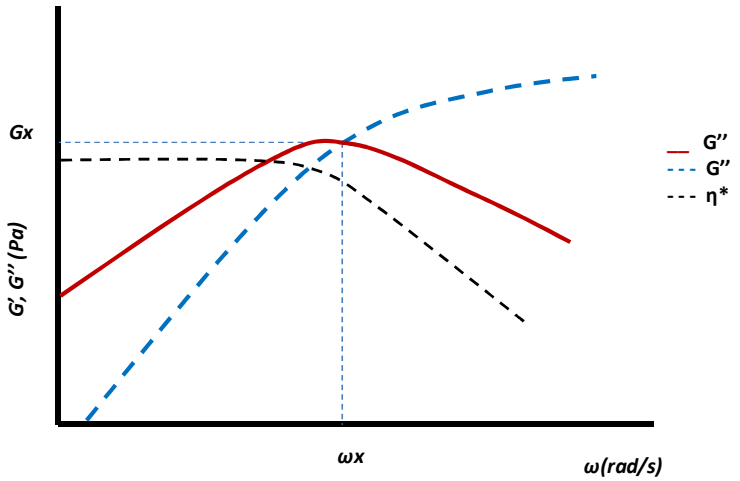

Figure A1. 4. Oscillatory moduli G' and G''- ω relationship for a Maxwell fluid

This model allows to determine the theoretical values of relaxation time (τ_x) and the plateau module (G_o).

The cross point when G' = G''when ($\omega_x.\tau$= 1)

$$\omega_x = \frac{1}{\tau}$$

$$G_x = G_o/2$$

Annexe 2.

Quartz crystal microbalance

The quartz crystal microbalance (QCM) is an ultra-sensitive weighing device that utilizes the mechanical resonance of piezoelectric crystalline quartz. The measurement is done from the changes of the frequency of resonance which is proportional to the mass deposited on the quartz crystal (Figure A2.5). This technique allows following the adsorption of thin films on the surface of the device.

We have used a QCM-D to following the multilayer build-up and adsorption of proteins. QCM-D has a sensitivity of up to 1 ng/cm^2.

The core of QCM is a thin disk made of single crystal piezoelectric quartz that is brought to oscillation by an electric potential provided by an external driving oscillator circuit. The electrodes are of thin gold layers coating each side of the crystal surface. During the experiments the frequencies are recorded the ground frequency and the 3rd, 5th and 7th harmonic. The values of those frequencies are 5, 15, 25 and 35 MHz respectively.

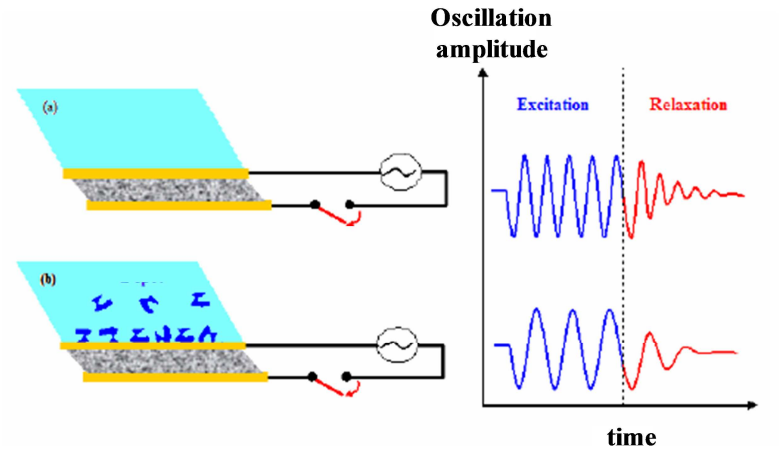

Figure A2. 1. Principle of QCM by the frequency and dissipation change in QCM experiments upon adsorption of molecules on the sensor surface.-Theory

The bottom side is fixed on a still stand. Under an oscillating electric potential, the upper side undergoes an horizontal oscillatory translational motion. As a first approximation, the whole

system is equivalent to a harmonic oscillator. The harmonic is characterized by its resonant frequency (f_r):

$$f_r = \frac{1}{2\pi}\sqrt{\frac{k}{M}}$$

Where M is the mass of the crystal and k is stiffness constant. The mass deposition of a material ($m << M$) on the crystal, the total mass is equal to $M + m$, giving the following expresion for resonant frequency:

$$f_r = \frac{1}{2\pi}\sqrt{\frac{k}{M+m}} \approx f_r\left(1 - \frac{m}{2M}\right)$$

The mass deposition of a material produce the change of the resonance frequency (Δf) describe as:

$$\Delta f = f - f_r = \frac{-mf_r}{2M} = \frac{m}{C}$$

Where C is the constant that depends only on the thickness and the properties of the quartz crystal. C is called the constant of Sauerbrey:

$$C = \frac{2M}{f_r}$$

e.g for the crystals we have C = 17.7 ng/cm^2.

From the previous equations, one can derive the mass adsorbed on the electrodes (m) as a function of the frequency variations. It can be generalized to all the harmonic frenquencies in the the Sauerbrey relation:

$$m = -C\frac{\Delta f_v}{v}$$

Where f_v is the fundamental resonance frequency and their odd harmonics. This relation permits the determination of mass deposition. This relation permits the determination of mass deposition. For this work the crystal surface is in contact with a liquid and the liquid exerts a shear stress on the adsorbed layer, which leads to a change of the resonance frequency and to viscous dissipation For these reason the measurements have been done in a QCM-D, were D stands for dissipation.

Annexe 3.

Biomolecules

Lipases

Lipases are water soluble enzymes that hydrolyze ester bonds of water-insoluble substrates such as triglycerides, phospholipids, and cholesteryl esters. Usually lipases are a "hydrolytic enzyme cocktail" elaborated by an organism. There have been found in organism from the microbial, plant, and animal kingdom. Commercially available lipases are usually derived from microorganism. The activity of the lipases increase in the presence of aggregates, emulsion or micellar solutions. The common architecture for the lipases is α/ß hydrolase fold, composed of lid or flat α helices and *ß* strands peptide sequence consisting serine, histidine and aspartic acid/glutamic acid. The activation of the enzyme consists of a mobile element at the surface a lid, which covers the active site. The lid is opening at a hydrophobic interface, making the active site accessible for substrates and enhancing the activity of the lipase.[238]

The 3D structure of Aeruginosa has been determined at a 2.54 Å resolution by crystallography.[239] It is an α /β protein, with alternate ß sheet and alpha helix. This structure is shared by all lipases.

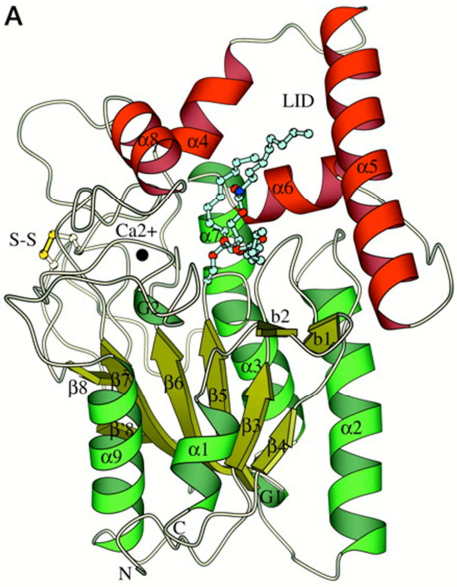

Figure A3. 1. 3D structure of Ps. aeruginosa Lipase.[239]

Streptavidin

Streptavidin is obtained from cultures of the bacterium *Streptomyces avidinii*.[240] It is a tetramer of four identical subunits that are built up of 159 amino acids. The tetramer has an approximately spherical shape with a diameter of about 5.5 nm and overall molecular weight of 60 kDa. The isoelectric point of streptavidin lies between 5 and 6. Strepatavidin can bind four equivalents of biotin. The interaction between streptavidin and biotin are, with a binding constant of the order of 10^{15} M^{-1}, among the strongest non-covalent interactions known. It was used in our for the specific adsorption of biotin, detailed in chapter 3 and 4.

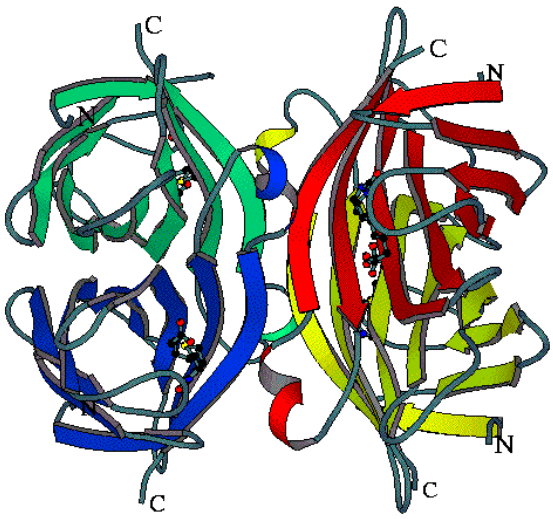

Figure A3. 2. Tetrameric molecular structure of Streptavidin

Serum

Fetal bovine serum was used to test the adsorption of proteins. Serum is the liquid fraction of the blood that is obtained after removal of the cells and of the blood clot by centrifugation. It is a “cocktail” of various proteins, growth factors, ion, lipids and other molecules. A more detail list of its constituents is given in Table A3.1.

Table A3. 1. Ingredients of Fetal bovine serum.

	Function	Concentration
Proteins		30-50 mg/mL
albumin	Osmotic pressure regulation	20 mg/mL
α, β, γ-globulins	Various; immune reponse	1-15 mg/mL
fibronectin vitronectin laminin	Attachment factors	1-100 µg/mL
Growth factors		
EGF, PDGF, IGF, FGF, insulin	Control of cell behavior	1-100 ng/mL
Lipids		
Chlolesterol, linoleic acid		0.1-10 µM
Trace elements		
Fe, Zn, Se etc.		Of the order of µM

Albumin and globulins are the major constituents. Fibronectin, vitronectin and laminin are minor constituents but have the strongest tendency to adsorb on surfaces and promote cell adhesion.

FBS is also used as a complement for cell culture medium in adhesion assays. Their importance for culture lies in the presence of growth factors, transferring, anti-proteases and lipids, which are vital for cells.

Annexe 4.

Rheological results

Creep-recovery

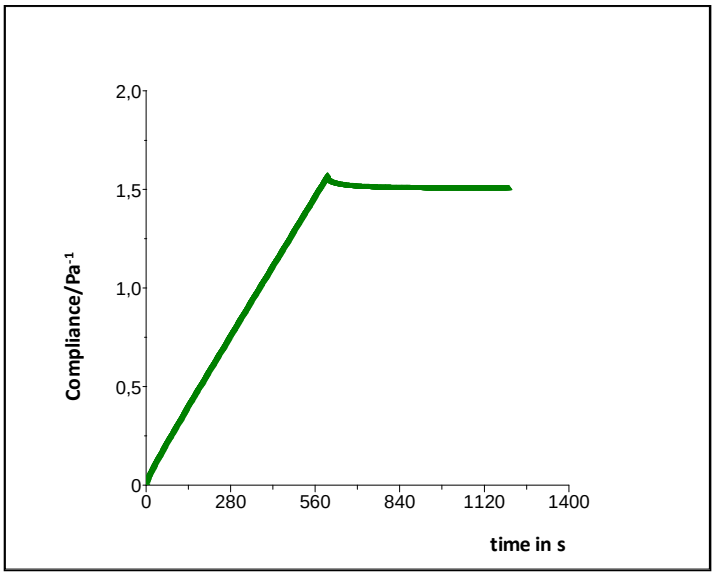

Figure A4. 1. Creep-recovery curve of C12 at 4 wt.%, applied stress = 20 Pa

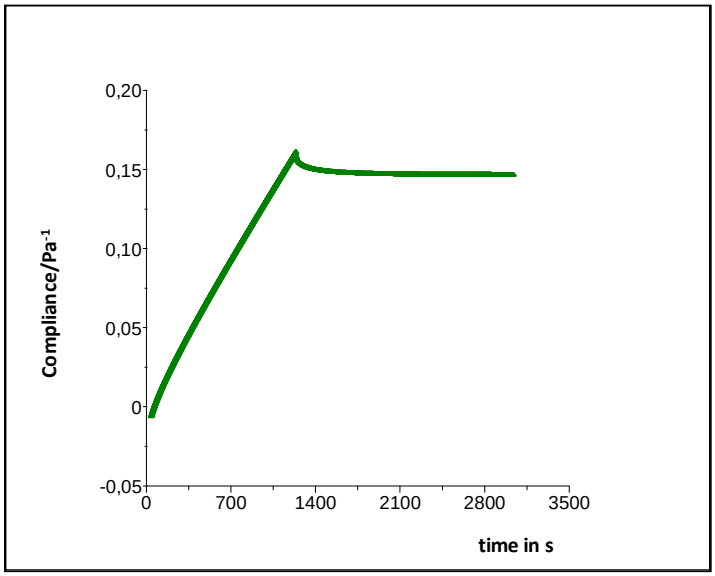

Figure A4. 2. Creep-recovery curve of C18 at 6 wt.%, applied stress = 20 Pa

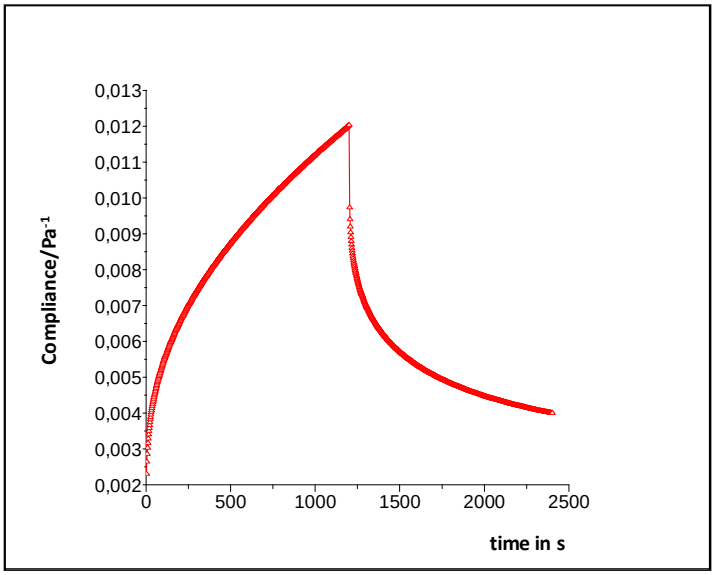

Figure A4. 3. Creep-recovery curve of C18 at 6 wt.%, applied stress = 20 Pa.

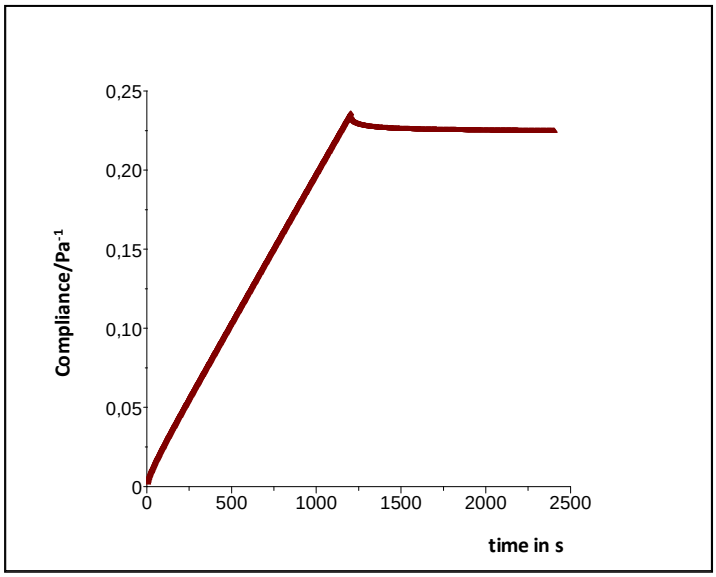

Figure A4. 4. Creep-recovery curve of MBL at 6 wt.%, applied stress = 20 Pa

Oscillatory measurements

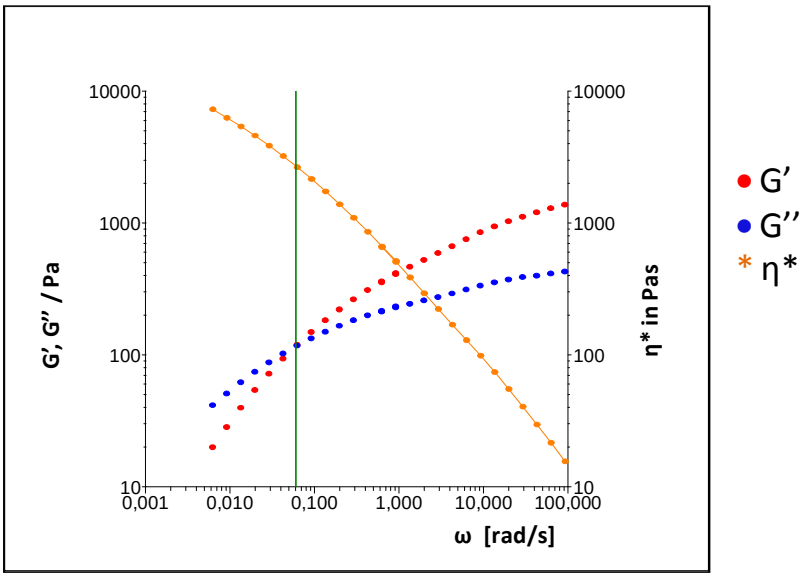

Figure A4. 5. Oscillatory frequency sweep on C12L 5 mol % at 6wt.%

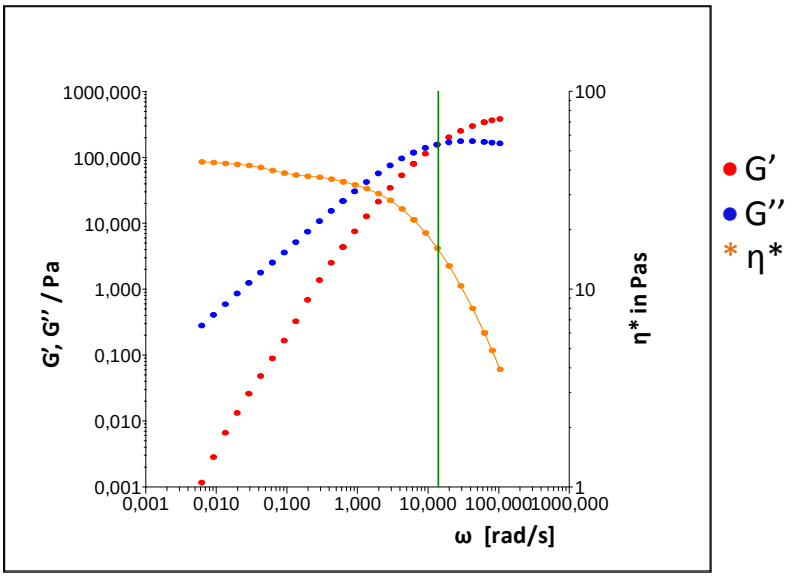

Figure A4. 6. Oscillatory frequency sweep on MBL 5 mol % at 6 wt.%

References

1. Liu, S.; Maheshwari, R.; Kiick, K. L. *Macromolecules* **2009**, *42*, (1), 3-13.
2. Duncan, R. *Nat. Rev. Cancer.* **2006**, *6*, (9), 688-701.
3. Vicent, M. J.; Duncan, R. *Trends in biotechnology* **2006**, *24*, (1), 39-47.
4. Thanou, M.; Duncan, R. *Curr. Opin. Investig. Drugs* **2003**, *4*, (6), 701-9.
5. Duncan, R. *Nat. Rev. Drug. Discov.* **2003**, *2*, (5), 347-60.
6. Duncan, R. *Anti-cancer drugs* **1992**, *3*, (3), 175-210.
7. Duncan, R. *Curr. Opin. Biotechnol.* **2011**, *22*, (4), 492-501.
8. Jacob, S.; Panaich, S. S.; Maheshwari, R.; Haddad, J. W.; Padanilam, B. J.; John, S. K. *Europace* **2011**, 13, (9), 1222-1230.
9. Abraham, S.; Narine, S. S. *J. Nanosci. Nanotechnol.* **2011**, *11*, (8), 7027-7032.
10. John, S. K.; Rangan, Y.; Block, C. A.; Koff, M. D. *American Journal of Emergency Medicine* **2011**, *29*, (9).
11. Kato, N.; Oishi, A.; Takahashi, F. *Mater. Sci. Eng.: C* **1998**, *6*, (4), 291-296.
12. Tartaj, P.; Morales, M. P.; Veintemillas-Verdaguer, S.; González-Carreno, T.; Serna, C. J. *J. Phys. D: Appl. Phys.* **2003**, *36*, R182-R182.
13. Blodgett, K. B. *J. Am. Chem. Soc.* **1934**, *56*, (2), 495-495.
14. Blodgett, K. B.; Langmuir, I. *Phys. Rev.* **1937**, *51*, (11), 964-982.
15. Netzer, L.; Sagiv, J. *J. Am. Chem. Soc.* **1983**, *105*, (3), 674-676.
16. Guang, C.; Hong, H. G.; Mallouk, T. E. *Acc. Chem. Res.* **1992**, *25*, (9), 420-427.
17. R.K, I. *J.f Colloid Interface Sci.* **1966**, *21*, (6), 569-594.
18. Gölander, C. G.; Arwin, H.; Eriksson, J. C.; Lundstrom, I.; Larsson, R. *Colloids Surf.* **1982**, *5*, (1), 1-16.
19. Gaines, G. L. *Thin Solid Films* **1983**, *99*, (1-3), 243-248.
20. Decher, G. *Science* **1997**, *277*, (5330), 1232-1237.
21. Lvov, Y.; Decher, G.; Sukhorukov, G. *Macromolecules* **1993**, *26*, (20), 5396-5399.
22. Kotov, N. A. *Nanostruct. Mater.* **1999**, *12*, (5-8), 789-796.
23. Hao, E. C.; Lian, T. Q. *Chem. Mater.* **2000**, *12*, (11), 3392-3396.
24. Brynda, E.; Houska, M. *J. Colloid Interface Sci.* **1996**, *183*, (1), 18-25.
25. Caruso, F.; Donath, E.; Mohwald, H. *J. Phys. Chem. B* **1998**, *102*, (11), 2011-2016.
26. Lvov, Y.; Ariga, K.; Onda, M.; Ichinose, I.; Kunitake, T. *Colloids Surf a-Physicochem. Eng. Aspects* **1999**, *146*, (1-3), 337-346.
27. Decher, G.; Schmitt, J., Fine-Tuning of the film thickness of ultrathin multilayer films composed of consecutively alternating layers of anionic and cationic polyelectrolytes. In *Trends in Colloid and Interface Science VI*, Steinkopff: Darmstadt, Vol. 89, pp 160-164.
28. Schlenoff, J. B.; Dubas, S. T.; Farhat, T. *Langmuir* **2000**, *16*, (26), 9968-9969.
29. Porcel, C. H.; Izquierdo, A.; Ball, V.; Decher, G.; Voegel, J. C.; Schaaf, P. *Langmuir* **2005**, *21*, (2), 800-802.
30. Kolasinska, M.; Krastev, R.; Gutberlet, T.; Warszynski, P. *Langmuir* **2009**, *25*, (2), 1224-1232.
31. Lefort, M.; Boulmedais, F.; Jierry, L.; Gonthier, E.; Voegel, J. C.; Hemmerle, J.; Lavalle, P.; Ponche, A.; Schaaf, P. *Langmuir* **2011**, *27*, (8), 4653-4660.

32. Cho, J.; Char, K.; Hong, J. D.; Lee, B. *Adv. Mater.* **2001,** *13*, (14), 1076-1078.
33. Chiarelli, P. A.; Johal, M. S.; Casson, J. L.; Roberts, J. B.; Robinson, J. M.; Wang, H. L. *Adv. Mater.* **2001**, *13*, (15), 1167-1171.
34. Lavalle, P.; Gergely, C.; Cuisinier, F. J. G.; Decher, G.; Schaaf, P.; Voegel, J. C.; Picart, C. *Macromolecules* **2002**, *35*, (11), 4458-4465.
35. Shiratori, S. S.; Rubner, M. F. *Macromolecules* **2000**, *33*, (11), 4213-4219.
36. Dubas, S. T.; Schlenoff, J. B. *Macromolecules* **1999**, *32*, (24), 8153-8160.
37. Picart, C.; Lavalle, P.; Hubert, P.; Cuisinier, F. J. G.; Decher, G.; Schaaf, P.; Voegel, J. C. *Langmuir* **2001**, *17*, (23), 7414-7424.
38. Lvov, Y.; Ariga, K.; Onda, M.; Ichinose, I.; Kunitake, T. *Langmuir* **1997**, *13*, (23), 6195-6203.
39. Vautier, D.; Hemmerle, J.; Vodouhe, C.; Koenig, G.; Richert, L.; Picart, C.; Voegel, J. C.; Debry, C.; Chluba, J.; Ogier, J. *Cell Motility and the Cytoskeleton* **2003**, *56*, (3), 147-158.
40. Dubas, S. T.; Schlenoff, J. B. *Macromolecules* **2001**, *34*, (11), 3736-3740.
41. Green, A. E. S.; Sadrameli, S. M. *J. Anal. Appl. Pyrol.* **2004**, *72*, (2), 329-335.
42. Puskas, J. E.; Chen, Y. *Biomacromolecules* **2004**, *5*, (4), 1141-1154.
43. Ai, H.; Meng, H.; Ichinose, I.; Jones, S. A.; Mills, D. K.; Lvov, Y. M.; Qiao, X. *J. Neurosci. Methods* **2003,** *128*, (1-2), 1-8.
44. Forry, S. P.; Reyes, D. R.; Gaitan, M.; Locascio, L. E. *Langmuir* **2006**, *22*, (13), 5770-5775.
45. Nolte, A. J.; Rubner, M. F.; Cohen, R. E. *Macromolecules* **2005**, *38*, (13), 5367-5370.
46. Nolte, A. J.; Cohen, R. E.; Rubner, M. F. *Macromolecules* **2006**, *39*, (14), 4841-4847.
47. Izumrudov, V. A.; Kharlampieva, E.; Sukhishvili, S. A. *Biomacromolecules* **2005**, *6*, (3), 1782-1788.
48. Quinn, J. F.; Caruso, F. *Macromolecules* **2005**, *38*, (8), 3414-3419.
49. Angelatos, A. S.; Radt, B.; Caruso, F. *J. Phys Chem. B.* **2005**, *109*, (7), 3071-3076.
50. Russell, T. P. *Science* **2002**, *297*, (5583), 964-967.
51. Genzer, J.; Efimenko, K. *Science* **2000**, *290*, (5499), 2130-2133.
52. Hemmerlé, J.; Roucoules, V.; Fleith, G.; Nardin, M.; Ball, V.; Lavalle, P.; Marie, P.; Voegel, J. C.; Schaaf, P. *Langmuir* **2005**, *21*, (23), 10328-10331.
53. Fruh, J.; Kohler, R.; Mohwald, H.; Krastev, R. *Langmuir* **2010**, *26*, (19), 15516-15522.
54. Vogel, V.; Sheetz, M. *Nat. Rev. Mol. Cell. Biol.* **2006**, *7*, (4), 265-275.
55. Smith, M. L.; Gourdon, D.; Little, W. C.; Kubow, K. E.; Eguiluz, R. A.; Luna-Morris, S.; Vogel, V. *Plos Biology* **2007**, *5*, (10), 2243-2254.
56. Mertz, D.; Vogt, C.; Hemmerle, J.; Mutterer, J.; Ball, V.; Voegel, J. C.; Schaaf, P.; Lavalle, P. *Nat. Mater* **2009**, *8*, (9), 731-735.
57. Ladam, G.; Schaad, P.; Voegel, J. C.; Schaaf, P.; Decher, G.; Cuisinier, F. *Langmuir* **2000**, *16*, (3), 1249-1255.
58. Muller, M.; Rieser, T.; Dubin, P. L.; Lunkwitz, K. *Macromol. Rapid Commun.* **2001**, *22*, (6), 390-395.
59. Cassier, T.; Lowack, K.; Decher, G. *Supramol. Sci.* **1998**, *5*, (3-4), 309-315.
60. Ladam, G.; Schaaf, P.; Cuisinier, F. J. G.; Decher, G.; Voegel, J. C. *Langmuir.* **2001**, *17*, (3), 878-882.
61. Cheng, Y. L.; Darst, S. A.; Robertson, C. R. *J. Colloid. Interface Sci.* **1987**, *118*, (1), 212-223.

62. Lee, J. H.; Kopeckova, P.; Kopecek, J.; Andrade, J. D. *Biomaterials* **1990**, *11*, (7), 455-464.
63. Kenausis, G. L.; Voros, J.; Elbert, D. L.; Huang, N. P.; Hofer, R.; Ruiz-Taylor, L.; Textor, M.; Hubbell, J. A.; Spencer, N. D. *J. Phys. Chem. B* **2000**, *104*, (14), 3298-3309.
64. Huang, N. P.; Michel, R.; Voros, J.; Textor, M.; Hofer, R.; Rossi, A.; Elbert, D. L.; Hubbell, J. A.; Spencer, N. D. *Langmuir* **2001**, *17*, (2), 489-498.
65. Boulmedais, F.; Frisch, B.; Etienne, O.; Lavalle, P.; Picart, C.; Ogier, J.; Voegel, J. C.; Schaaf, P.; Egles, C. *Biomaterials* **2004**, *25*, (11), 2003-2011.
66. Zhang, Z.; Chao, T.; Chen, S. F.; Jiang, S. Y. *Langmuir* **2006**, *22*, (24), 10072-10077.
67. Hall, B.; Bird, R. L.; Kojima, M.; Chapman, D. *Biomaterials* **1989**, *10*, (4), 219-224.
68. Reisch, A.; Voegel, J. C.; Gonthier, E.; Decher, G.; Senger, B.; Schaaf, P.; Mesini, P. J. *Langmuir* **2009**, *25*, (6), 3610-3617.
69. Reisch, A.; Hemmerle, J.; Voegel, J-C.; Gonthier, E.; Decher, G.; Benkirane-Jessel, N.; Chassepot, A.; Mertz, D.; Lavalle, P.; Mesini, P.; Schaaf, P. *J. Mater. Chem.* **2008**, *18*, (36), 4242-4245.
70. Brusatori, M. A.; Van Tassel, P. R. *Biosensors and Bioelectronics* **2003**, *18*, (10), 1269-1277.
71. Decher, G.; Lehr, B.; Lowack, K.; Lvov, Y.; Schmitt, J. *Biosensors and Bioelectronics* **1994**, *9*, (9-10), 677-684.
72. Tang, Z. Y.; Wang, Y.; Podsiadlo, P.; Kotov, N. A. *Adv. Mat.* **2006**, *18*, (24), 3203-3224.
73. Hersel, U.; Dahmen, C.; Kessler, H. *Biomaterials* **2003**, *24*, (24), 4385-4415.
74. Berg, M. C.; Yang, S. Y.; Hammond, P. T.; Rubner, M. F. *Langmuir* **2004**, *20*, (4), 1362-1368.
75. Kinnane, C. R.; Wark, K.; Such, G. K.; Johnston, A. P. R.; Caruso, F. *Small* **2009**, *5*, (4), 444-448.
76. VandeVondele, S.; Voros, J.; Hubbell, J. A. *Biotechnol. Bioeng.* **2003**, *82*, (7), 784-790.
77. Clark Jr, L. C.; Lyons, C. *Annals of the New York Academy of Sciences* **1962**, *102*, (1), 29-45.
78. Kafi, A. K. M.; Lee, D.-Y.; Park, S.-H.; Kwon, Y.-S. *J. Nanosci. Nanotechnol.* **2006**, *6*, (11), 3539-3542.
79. Sirkar, K.; Revzin, A.; Pishko, M. V. *Anal. Chem.* **2000**, *72*, (13), 2930-2936.
80. Lvov, Y.; Ariga, K.; Ichinose, I.; Kunitake, T. *J. Am. Chem. Soc.* **1995**, *117*, (22), 6117-6123.
81. Holmberg, A.; Blomstergren, A.; Nord, O.; Lukacs, M.; Lundeberg, J.; Uhlen, M. *Electrophoresis* **2005**, *26*, (3), 501-510.
82. Decher, G.; Essler, F.; Hong, J. D.; Lowack, K.; Schmitt, J.; Lvov, Y. *Abstr. Pap. Am. Chem. Soc.* **1993**, *205*, 334-POLY.
83. Decher, G.; Essler, F.; Hong, J. D.; Lowack, K.; Schmitt, J.; Lvov, Y. *Abstr. Pap. Am. Chem. Soc.* **1993**, *205*, 334-POLY.
84. Geissler, A.; Vallat, M. F.; Fioux, P.; Thomann, J. S.; Frisch, B.; Voegel, J. C.; Hemmerle, J.; Schaaf, P.; Roucoules, V. *Plasma. Proc. Polym.* **2010**, *7*, (1), 64-77.
85. Caruso, F.; Niikura, K.; Furlong, D. N.; Okahata, Y. *Langmuir* **1997**, *13*, (13), 3427-3433.
86. Wang, M. J.; Wang, L. Y.; Yuan, H.; Ji, X. H.; Sun, C. Y.; Ma, L.; Bai, Y. B.; Li, T. J.; Li, J. H. *Electroanalysis* **2004**, *16*, (9), 757-764.

87. Huang, N.-P.; Vörös, J.; De Paul, S. M.; Textor, M.; Spencer, N. D. *Langmuir* **2001**, *18*, (1), 220-230.
88. Harris, J. M., *Poly(ethylene glycol) chemistry: biotechnical and biomedical applications*. Springer: New York, **1992**.
89. Svedhem, S.; Hollander, C.-Ã. k.; Shi, J.; Konradsson, P.; Liedberg, B.; Svensson, S. C. T. *J. Org. Chem.* **2001**, *66*, (13), 4494-4503.
90. Zalipsky, S. *Bioconjugate Chem.* **1995**, *6*, (2), 150-165.
91. Patel, K.; Angelos, S.; Dichtel, W. R.; Coskun, A.; Yang, Y.-W.; Zink, J. I.; Stoddart, J. F. *J. Am. Chem. Soc.* **2008**, *130*, (8), 2382-2383.
92. Dix, A. V.; Fischer, L.; Sarrazin, S.; Redgate, C. P. H.; Esko, J. D.; Tor, Y. *Chembiochem* **2010,** *11*, (16), 2302-2310.
93. Martin, O. M.; Mecozzi, S. *Tetrahedron* **2007**, *63*, (25), 5539-5547.
94. Ning, X.; Guo, J.; Wolfert, M. A.; Boons, G. J. *Angew. Chem., Int. Ed. Engl.* **2008**, *47*, (12), 2253-2255.
95. McReynolds, K. D.; Bhat, A.; Conboy, J. C.; Saavedra, S. S.; Gervay-Hague, J. *Bioorganic & Medicinal Chemistry* **2002**, *10*, (3), 625-637.
96. Brockerhoff, H.; Ayengar, N. *Lipids* **1979**, *14*, (1), 88-89.
97. Reisch, A.; Voegel, J. C.; Decher, G.; Schaaf, P.; Mesini, P. J. *Macromol. Rapid Commun.* **2007**, *28*, (23), 2217-2223.
98. Nallicheri, R. A.; Rubner, M. F. *Macromolecules* **1991**, *24*, (2), 517-525.
99. Davis, D. A.; Hamilton, A.; Yang, J. L.; Cremar, L. D.; Van Gough, D.; Potisek, S. L.; Ong, M. T.; Braun, P. V.; Martinez, T. J.; White, S. R.; Moore, J. S.; Sottos, N. R. *Nature* **2009**, 459, (7243), *68*-72.
100. John, S.; Fernando, R.; Loftus, R. *Crit. Care Med.* **2010**, *3*8, (12), U302-U302.
101. Nayak, K. S.; Sinoj, K. A.; Subhramanyam, S. V.; Mary, B.; Rao, N. V. V. *Peritoneal Dialysis International* **2007**, *27*, S27-S31.
102. Abraham, S.; Ha, C. S.; Batt, C. A.; Kim, I. *J. Polym. Sci., Part A: Polym. Chem.* **2007**, *45*, (16), 3570-3579.
103. Li, H.; Abraham, S.; Yan, W.; Ha, C. S.; Kim, I. *Macromol. Rapid Commun.* **2007**, *28*, (15), 1534-1539.
104. Abraham, S.; Choi, J. H.; Ha, C. S.; Kim, I. *J. Polym. Sci., Part A: Polym. Chem.* **2007**, *45*, (23), 5559-5572.
105. John, S.; Loftus, R.; Dewhirst, W.; Surgenor, S.; Koff, M. *Crit. Care Med.* **2010**, *38*, (12), U277-U277.
106. Abraham, S.; Choi, J. H.; Lee, J. K.; Ha, C. S.; Kim, I. *Macromol. Res.* **2007**, *15*, (4), 324-329.
107. Abraham, S.; Unsworth, L. D. *J. Polym. Sci., Part A: Polym. Chem.* **2011**, *49*, (5), 1051-1060.
108. John, S.; Corwin, H.; Robison, C.; Houston, D.; Surgenor, S. *Crit. Care Med.* **2010**, *38*, (12), U173-U173.
109. Hicks, R.; Satti, A. K.; Leach, G. D. H.; Naylor, I. L. *J. Appl. Toxicol.* **1989**, *9*, (3), 191-198.
110. Becker, J. M.; Dayton, M. T.; Fazio, V. W.; Beck, D. E.; Stryker, S. J.; Wexner, S. D.; Wolff, B. G.; Roberts, P. L.; Smith, L. E.; Sweeney, S. A.; Moore, M. *Journal of the American College of Surgeons* **1996**, *183*, (4), 297-306.

111. Sikkink, C. J.; Postma, V. A.; Reijnen, M. M.; De Man, B.; Bleichrodt, R. P.; Van Goor, H. *Eur. Surg. Res.* **2004**, *36*, (2), 123-8.
112. Becker, J. M.; Dayton, M. T.; Fazio, V. W.; Beck, D. E.; Stryker, S. J.; Wexner, S. D.; Wolff, B. G.; Roberts, P. L.; Smith, L. E.; Sweeney, S. A.; Moore, M. *J Am Coll Surg* **1996**, *183*, 297-306.
113. Falk, K.; Lindman, B.; Bengmark, S.; Larsson, K.; Holmdahl, L. *Biomaterials* **2001**, *22*, (16), 2185-2190.
114. Lindenschmidt, R. C.; Stone, L. C.; Seymour, J. L.; Anderson, R. L.; Forshey, P. A.; Winrow, M. J. *Toxicol. Sci.* **1991**, *17*, (1), 128-135.
115. CIR. *Int. J. Toxicol.* **2002**, *21*, (3 suppl), 1-50.
116. Bernkop-Schnürch, A., Mucoadhesive Polymers. In *Polymeric Biomaterials*, 2nd ed.; Dumitriu, S., Ed. Dekker: New-York, **2001**; pp 147-165.
117. Yang, X.; Robinson, J. R., Bioadhesion in mucosal drug delivery. In *Biorelated Polymers and Gels, Controlled Release Applications in Biomedicine*, Okano, T., Ed. Academic Press: San Diego, **1998**; pp 135-192.
118. Lee, J. H.; Kim, J. J.; Park, K., Glucose-Sensitive Hydogel Membranes. In *Polymeric Biomaterials*, 2nd ed.; Dumitriu, S., Ed. Dekker: New-York, 2001; pp 739-752.
119. Strauss, U. P.; Jackson, E. G. *J. Polym. Sci.* **1951**, *6*, (5), 649-659.
120. Noda, T.; Hashidzume, A.; Morishima, Y. *Macromolecules* **2001**, *34*, (5), 1308-1317.
121. Yang, Y.; Schulz, D.; Steiner, C. A. *Langmuir* **1999,** *15*, (13), 4335-4343.
122. Tam, K. C.; Jenkins, R. D.; Winnik, M. A.; Bassett, D. R. *Macromolecules* **1998**, *31*, (13), 4149-4159.
123. Xu, B.; Yekta, A.; Li, L.; Masoumi, Z.; Winnik, M. A. *Colloids Surf., A. Physicochem. Eng. Aspects.* **1996**, *112*, (2-3), 239-250.
124. Vorobyova, O.; Lau, W.; Winnik, M. A. *Langmuir* **2001**, *17*, (5), 1357-1366.
125. Beaudoin, E.; Hiorns, R. C.; Borisov, O.; François, J. *Langmuir* **2003**, *19*, (6), 2058-2066.
126. Fusco, S.; Borzacchiello, A.; Netti, P. A. *Journal of Bioactive and Compatible Polymers* **2006**, *21*, (2), 149-164.
127. Mocanu, G.; Carpov, A.; Chapelle, S.; Merle, L.; Muller, G. *Canadian Journal Chemistry* **1995,** *73*, 1933-1940.
128. Rouzes, C.; Durand, A.; Leonard, M.; Dellacherie, E. *J. Colloid Interface Sci.* **2002**, *253*, (1), 217-223.
129. Picton, L. Propriétés en solution aqueuse d'éthers cellulosiques associatifs. Influence des cosolutés et de la température : conséquences rhéologiques. Université de Rouen, Rouen, France, **1996**.
130. Tarng, M. R.; Kaczmarski, J. P.; Lundberg, D. J.; Glass, J. E., Comparative flow properties of model associative thickener aqueous solutions. In *Hydrophilic Polymers: Performance with Environmental Acceptability*, Glass, J. E., Ed. American Chemical Society: Washington, DC, 1996; Vol. 248, pp 305-341.
131. Svanholm, T.; Molenaar, F.; Toussaint, A. *Progress in Organic Coatings* **1997,** *30*, (3), 159-165.
132. Kaczmarski, J. P.; Tarng, M. R.; Ma, Z. Y.; Glass, J. E. *Colloids Surf., A. Physicochem. Eng. Aspects* **1999,** *147*, (1-2), 39-53.
133. Nishikawa, K.; Yekta, A.; Pham, H. H.; Winnik, M. A.; Sau, A. C. *Langmuir* **1998,** *14*, (25), 7119-7129.

134. Panmai, S.; Prudhomme, R. K.; Peiffer, D. G. *Colloids Surf., A. Physicochem. Eng. Aspects* **1999**, *147*, (1-2), 3-15.
135. Picton, L.; Merle, L.; Muller, G. *Int. J. Polym. Anal. Charact.* **1996**, *2*, 103-113.
136. Picton, L.; Muller, G. *Progress in Colloid and Polymer Science* **1996**, *102*, 26-31.
137. Kästner, U.; Hoffmann, H.; Dönges, R.; Ehrler, R. *Colloids Surfaces, Part A* **1996**, *112*, (2-3), 209-225.
138. Kumar, V.; Steiner, C. A. *Colloids Surf., A. Physicochem. Eng. Aspects* **1999**, *147*, (1-2), 27-38.
139. Hoffmann, H.; Kästner, U.; Dönges, R.; Ehrler, R. *Polymers Gels and Networks* **1996**, *4*, (5-6), 509-526.
140. Panmai, S.; Prud'homme, R. K.; Peiffer, D. G.; Jockusch, S.; Turro, N. J. *langmuir* **2002**, *18*, (10), 3860-3864.
141. Bourges, X.; Weiss, P.; Coudreuse, A.; Daculsi, G.; Legeay, G. *Biopolymers* **2002**, *63*, (4), 232-238.
142. Joabsson, F.; Lindman, B. *Progress. Colloid. Polym. Sci.* **2000**, *116*, 74-78.
143. Zou, S.; Zhang, W.; Zhang, X.; Jiang, B. *Langmuir* **2001**, *17*, (16), 4799-4808.
144. Tsianou, M.; Thuresson, T.; Piculell, L. *Colloid. Polym Sci.* **2001**, *279*, (4), 340-347.
145. Joabsson, F.; Thuresson, K.; Blomberg, E. *Langmuir* **2001**, *17*, (5), 1506-1510.
146. Kjoniksen, A.-L.; Nilsson, S.; Thuresson, K.; Lindman, B.; Nystroem, B. *Macromolecules* **2000**, *33*, (3), 877-886.
147. Badiger, M. V.; Lutz, A.; Wolf, B. A. *Polymer* **1999**, *41*, (4), 1377-1384.
148. Karlson, L.; Joabsson, F.; Thuresson, K. *Carbohyd Polym* **2000**, *41*, (1), 25-35.
149. Thuresson, K.; Nilsson, S.; Lindman, B. *Langmuir* **1996**, *12*, (10), 2412-2417.
150. Thuresson, K.; Joabsson, F. *Colloids Surf., A. Physicochem. Eng. Aspects* **1999**, *151*, (3), 513-523.
151. Thuresson, K.; Lindman, B. *J. Phys. Chem. B* **1997**, *101*, (33), 6460-6468.
152. Thuresson, K.; Lindman, B.; Nyström, B. *J. Phys. Chem. B* **1997**, *101*, (33), 6450-6459.
153. Thuresson, K.; Södermann, O.; Hansson, P.; Wang, G. *J. Phys. Chem.* **1996**, *100*, (12), 4909-4918.
154. Landoll, L. M. *J. Polymer Science, Polymer Chemistry Edition* **1982**, *20*, 443-455.
155. Winnik, F. M., Fluorescence studies of cellulose ethers.(Synthesis, Characterization, and spectroscopic properties of labeled polymers). In *Hydrophilic Polymers: Performance with Environmental Acceptability*, Glass, J. E., Ed. American Chemical Society: Washington, DC, **1996**; Vol. 248, pp 409-423.
156. Caritey, J.-P. Relation entre la modification chimique de précurseurs hydrophiles d'origine naturelle et leurs propriétés en solution diluée et semi-diluée. Thèse, Université de Rouen, Rouen, France, **1994**.
157. Sinquin, A. Alginates associatifs : synthèse et étude physico-chimique en milieu aqueux. Thèse, Institut National Polytechnique de Lorraine, Nancy, Nancy, France, 1995.
158. Sinquin, A.; Hubert, P.; Dellacherie, E. *Langmuir* **1993**, *9*, (12), 3334-3337.
159. Sinquin, A.; Hubert, P.; Dellacherie, E. *Polymer* **1994**, *35*, 3557-3560.
160. Sinquin, A.; Hubert, P.; Marchal, P.; Choplin, L.; Dellacherie, E. *Colloids Surf., A. Physicochem. Eng. Aspects* **1996**, *112*, 193-200.
161. Pelletier, S.; Hubert, P.; Lapicque, F.; Payan, E.; Dellacherie, E. *Carbohydrate Polymers* **2000,** 43, (4), 343-349.

162. Pelletier, S.; Hubert, P.; Payan, E.; Marchal, P.; Choplin, L.; Dellacherie, E. *Journal of Biomedical Materials Research* **2000**, *54*, (1), 102-108.
163. Desbrieres, J.; Rinaudo, M., Solution properties of some amphiphilic polysaccharide derivatives. In *Biopolymers from Polysaccharides and Agroproteins*, **2001**; Vol. 786, pp 72-85.
164. Philippova, O. E.; Volkov, E. V.; Sitnikova, N. L.; Khokhlov, A. R.; Desbrieres, J.; Rinaudo, M. *Biomacromolecules* **2001**, *2*, (2), 483-490.
165. Charpentier, D.; Mocanu, G.; Carpov, A.; Chapelle, S.; Merle, L.; Muller, G. *Carbohydrate Polymers* **1997**, *33*, 177-186.
166. Bataille, I.; Huguet, J.; Muller, G.; Mocanu, G.; A., C. *International Journal of Biological Macromolecules* **1997**, *20*, 179-191.
167. Fischer, A.; Houzelle, M. C.; Hubert, P.; Axelos, M. A. V.; Geoffroy-Chapotot, C.; Carré, M. C.; Viriot, M. L.; Dellacherie, E. *Langmuir* **1998**, *14*, 4482-4488.
168. Miralles-Houzelle, M. C.; Hubert, P.; Dellacherie, E. *Langmuir* **2001,** *17*, (5), 1384-1391.
169. Amis, E. J.; Hu, N.; Seery, T. A. P.; Hogen-Esch, T. E.; Yassini, M.; Hwang, F., Associating polymers containing fluorocarbon hydrophobic units. In *Hydrophilic Polymers: Performance with Environmental Acceptability*, Glass, J. E., Ed. American Chemical Society: Washington, DC, 1996; Vol. 248, pp 279-302.
170. Raynaud, J.; Choquenet, B.; Marie, E.; Dellacherie, E.; Nouvel, C.; Six, J. L.; Durand, A. *Biomacromolecules* **2008**, *9*, (3), 1014-21.
171. Nouvel, C.; Raynaud, J.; Marie, E.; Dellacherie, E.; Six, J. L.; Durand, A. *J. Colloid Interface Sci.* **2009**, *330*, (2), 337-43.
172. Candau, F.; Selb, J. *Adv. Colloid Interface Sci.* **1999**, *79*, 149-172.
173. Guillaumont, L.; Bokias, G.; Iliopoulos, I. *Macromol. Chem. Phys* **2000**, *201*, (2), 251-260.
174. Vasiliadis, I.; Bokias, G.; Mylonas, Y.; Staikos, G. *polymer* **2001**, *42*, (21), 8911-8914.
175. Chen, J.; Du, L. B.; Zhang, Y. X.; Hogen-Esch, T. E.; Jiang, M. *Polymer International* **2001**, 50, (1), 148-156.
176. Shi, X.; Li, J.; Sun, C.; Wu, S. *Colloids Surf., A. Physicochem. Eng. Aspects* **2000**, *175*, (1-2), 41-49.
177. Poncet-Legrand, C.; Winnik, F. M. *Polymer Journal* **2001**, *33*, (3), 277-283.
178. Kujawa, P.; Ester Goh, C. C.; Winnik, F. M. *Macromolecules* **2001**, *34*, (18), 6387-6395.
179. Ezzell, S. A.; McCormick, C. L. *Polymer Preprints (ACS, Polymer Chemistry)* **1989**, *30*, (2), 340-341.
180. Ezzell, S. A.; McCormick, C. L., Synthesis and solution characterization of pyrene-labeled polyacrylamides. In *Water-Soluble Polymers: Synthesis, Solution Properties and Applications*, Shalaby, S. W.; McCormick, C. L.; Butler, G. B., Eds. American Chemical Society: Washington, DC, 1991; Vol. 467, pp 130-150.
181. Ezzell, S. A.; Hoyle, C. E.; Creed, D.; McCormick, C. L. *Macromolecules* **1992**, *25*, (7), 1887-1895.
182. Meyer, V. Synthèse et caractérisation de polymères associatifs porteurs de groupes siloxanes. Thèse, Université Louis Pasteur, Strasbourg, Strasbourg, France, 1999.
183. Volpert, E.; Selb, J.; Candau, F. o. *Macromolecules* **1996**, *29*, (5), 1452-1463.
184. Dirk, S. *Adv. Drug Deliv. Rev.* **2006**, *58*, (15), 1655-1670.
185. Brazel, C. S.; Peppas, N. A. *J. Controlled Release* **1996,** *39*, (1), 57-64.
186. Zhang, J.; Peppas, N. A. *Macromolecules* **1999**, *33*, (1), 102-107.

187. Yin, X.; Hoffman, A. S.; Stayton, P. S. *Biomacromolecules* **2006**, *7*, (5), 1381-1385.
188. Gohon, Y.; Giusti, F.; Prata, C.; Charvolin, D.; Timmins, P.; Ebel, C.; Tribet, C.; Popot, J.-L. *Langmuir* **2006**, *22*, (3), 1281-1290.
189. Wang, K. T.; Iliopoulos, I.; Audebert, R. *Polym. Bull.* **1988**, *20*.577-582.
190. Zhang, Y. X.; Da, A. H.; Butler, G. B.; Hogen-Esch, T. E. *J. Polym. Sci. A* **1992**, *30*, (7), 1383-1391.
191. Yang, D.; Tong, L.; Li, Y.; Hu, J.; Zhang, S.; Huang, X. *Polymer* 51, (8), 1752-1760.
192. StÃ¤hler, K.; Selb, J.; Candau, F. o. *Langmuir* **1999**, *15*, (22), 7565-7576.
193. Ma, Y.; Cao, T.; Webber, S. E. *Macromolecules* **1998**, *31*, (6), 1773-1778.
194. Ezzell, S. A.; McCormick, C. L. *Macromolecules* **1992**, *25*, (7), 1881-1886.
195. Xie, X.; Hogen-Esch, T. E. *Macromolecules* **1996**, *29*, (5), 1734-1745.
196. Lim, H. J.; Cho, E. C.; Kim, J.; Chang, I.-S. *Colloids Surf., A. Physicochem. Eng. Aspects* **2007**, *294*, (1-3), 71-79.
197. Cho, E. C.; Lim, H. J.; Kim, H. J.; Son, E. D.; Choi, H. J.; Park, J. H.; Kim, J.-W.; Kim, J. *Mater. Sci. Eng.: C* **2009**, *29*, (3), 774-778.
198. Cho, E. C.; Lim, H. J.; Shim, J.; Park, J. Y.; Dan, N.; Kim, J.; Chang, I.-S. *J. Colloid Interface Sci.* **2007**, *311*, (1), 243-252.
199. Bromberg, L. *Ind. Eng. Chem. Res.* **1998**, 37, (11), 4267-4274.
200. Bromberg, L.; Temchenko, M.; Alakhov, V.; Hatton, T. A. *Inter. J. Pharm.* **2004**, *282*, (1-2), 45-60.
201. Le Bourlais, C. A.; Treupel-Acar, L.; Rhodes, C. T.; Sado, P. A.; Leverge, R. *Drug Development and Industrial Pharmacy* **1995**, *21*, 19-59.
202. Bromberg, L. *Industrial & Eng. Chem. Res.* **1998**, *37*, (11), 4267-4274.
203. Guo, X.; Abdala, A. A.; May, B. L.; Lincoln, S. F.; Khan, S. A.; Prud'homme, R. K. *Polymer* **2006**, *47*, (9), 2976-2983.
204. Aubry, T. *J.Rheology* **1994**, *38*, (6), 1681-1681.
205. Zhuang, D. q.; Ai-hua Da, J. C.; Zhang, Y. x.; Dieing, R.; Ma, L.; Haeussling, L. *Polym. Adv. Technol.* **2001**, *12*, (11-12), 616-625.
206. Philippova, O. E.; Hourdet, D.; Audebert, R.; Khokhlov, A. R. *Macromolecules* **1997**, *30, (26), 8278-8285.*
207. Philippova, O. E.; Hourdet, D.; Audebert, R.; Khokhlov, A. R. *Macromolecules* **1996**, *29*, (8), 2822-2830.
208. Nakamura, K.; Murray, R. J.; Joseph, J. I.; Peppas, N. A.; Morishita, M.; Lowman, A. M. *J. Controlled Release* **2004**, *95*, (3), 589-599.
209. Hourdet, D.; Gadgil, J.; Podhajecka, K.; Badiger, M. V.; BrÃ»let, A.; Wadgaonkar, P. P. *Macromolecules* **2005**, *38*, (20), 8512-8521.
210. Zhuang, D. Q.; Cao, Y.; Zhang, H. D.; Yang, Y. L.; Zhang, Y. X. *Polymer* **2002**, *43*, (7), 2075-2084.
211. Magny, B.; Iliopoulos, I.; Zana, R.; Audebert, R. *Langmuir* **1994**, *10*, (9), 3180-3187.
212. Winnik, M. A.; Yekta, A. *Curr. Opin. Colloid Interface Sci.* **1997**, *2*, (4), 424-436.
213. Pollack, M. *Rev.infectious diseases* **1984**, *6* Suppl 3, S617-26.
214. König, B.; Jaeger, K. E.; Sage, A. E.; Vasil, M. L.; König, W. *Infect.Imm.* **1996**, *64*, (8), 3252-8.
215. Nishio, T.; Chkano, T.; Kamimura, M. *Agric. Biol. Chem.* **1987**, *51*, (9), 2525-2529.

216. Amada, K.; Haruki, M.; Imanaka, T.; Morikawa, M.; Kanaya, S. *Biochimica et Biophysica Acta (BBA) - Protein Structure and Molecular Enzymology* **2000**, *1478*, (2), 201-210.
217. An, S.-Y.; Kim, S.-W.; Choi, Y.-L.; Cho, Y.-S.; Joo, W.-H.; Lee, Y.-C. *J. Microbioloy* **2003**, *41*, (2), 95-101.
218. Zune, C.; Archambeau, C.; Dubois, P.; Jeröme, R. *J. Polym. Sci., Part A: Polym. Chem.* **2001**, *39*, (10), 1774-1785.
219. Mather, B. D.; Viswanathan, K.; Miller, K. M.; Long, T. E. *Progress in Polymer Science* **2006**, *31*, (5), 487-531.
220. Matyjaszewski, K.; Xia, J. *Chem. Rev.* **2001**, *101*, (9), 2921-2990.
221. Kim, J.; Tirrell, D. A. *Macromolecules* **1999**, *32*, (3), 945-948.
222. Qin, S. H.; Qiu, K. Y. *J. Polym. Sci., Part A: Polym. Chem.* **2001**, *39*, (9), 1450-1455.
223. Cao, B.; Yan, S.; Zhang, K.; Song, Z.; Cao, T.; Chen, X.; Cui, L.; Yin, J. *Macromol. Biosci. 11*, (7), 970-977.
224. Adams, N.; Schubert, U. S. *Adv. Drug Deliv. Rev.* **2007**, *59*, (15), 1504-1520.
225. Morihara, K. *Methods Enzymol.* **1995**, 248, 242-253.
226. Buback, M.; Junkers, T. *Macromol. Chem. Phys.* **2006**, *207*, (18), 1640-1650.
227. Krishnan, R.; Srinivasan, K. S. V. *Eur. Polym. J.* **2004**, *40*, (10), 2269-2276.
228. Ruzette, A. V. G.; Banerjee, P.; Mayes, A. M.; Pollard, M.; Russell, T. P.; Jerome, R.; Slawecki, T.; Hjelm, R.; Thiyagarajan, P. *Macromolecules* **1998**, *31*, (24), 8509-8516.
229. Katime, I.; Novoa, R.; Zuluaga, F. *Eur. Polym. J.* **2001**, *37*, (7), 1465-1471.
230. Hill, A.; Candau, F.; Selb, J. *Macromolecules* **1993**, *26*, (17), 4521-4532.
231. Choi, W.-J.; Kim, Y.-B.; Kwon, S.-K.; Lim, K.-T.; Choi, S.-K. *J. Polym. Sci., Part A: Polym. Chem.* **1992**, *30*, (10), 2143-2148.
232. Yoshioka, M.; Otsu, T. *Macromolecules* **1992**, *25*, (10), 2599-2602.
233. Ramireddy, C.; Tuzar, Z.; Prochazka, K.; Webber, S. E.; Munk, P. *Macromolecules* **1992**, *25*, (9), 2541-2545.
234. Abraham, S.; Ha, C. S.; Kim, I. *J. Polym. Sci., Part A: Polym. Chem.* **2005**, *43*, (24), 6367-6378.
235. Ramakrishnan, A.; Dhamodharan, R. *Macromolecules* **2003**, *36*, (4), 1039-1046.
236. Kujawa, P.; Audibert-Hayet, A.; Selb, J.; Candau, F. *J. Polym. Sci., Part A: Polym. Chem.* **2003**, *41*, (21), 3261-3274.
237. Hansson, P.; Lindman, B. *Curr. Opin. Colloid Interface Sci.* **1996**, 1, (5), 604-613.
238. van Tilbeurgh, H.; Egloff, M.-P.; Martinez, C.; Rugani, N.; Verger, R.; Cambillau, C. *Nature* **1993**, *362*, (6423), 814-820.
239. Nardini, M.; Lang, D. A.; Liebeton, K.; Jaeger, K.-E.; Dijkstra, B. W. *J. Biol. Chem.* **2000**, *275*, (40), 31219-31225.
240. Waldrop, G. L., *Biotin*. Encyclopedia of Life Science: **2001**.